R. & M. No. 2704
A.R.C. Monograph

MINISTRY OF SUPPLY

AERONAUTICAL RESEARCH COUNCIL
REPORTS AND MEMORANDA

Four Studies in the Theory of Stress Concentration

By

H. L. Cox, M.A., F.R.Ae.S., A.M.I.Mech.E.,
of the Engineering Division, N.P.L.

LONDON: HER MAJESTY'S STATIONERY OFFICE
1953
PRICE £1 0s 0d NET

MINISTRY OF SUPPLY

AERONAUTICAL RESEARCH COUNCIL
REPORTS AND MEMORANDA

Four Studies in the Theory of Stress Concentration

By
H. L. Cox, M.A., F.R.Ae.S., A.M.I.Mech.E.,
of the Engineering Division, N.P.L.

PART I
The Effect of Holes on the Strength of Materials under Complex Stress Systems

PART II
Stress Concentration due to Holes and Grooves other than Elliptical in Form

PART III
The Effect of Surface Irregularities on Fatigue Strength

PART IV
Stress Concentration in Twisted Shafts

LONDON: HER MAJESTY'S STATIONERY OFFICE
1953

PRINTED AND PUBLISHED BY HER MAJESTY'S STATIONERY OFFICE

To be purchased from

York House, Kingsway, LONDON, W.C.2 423 Oxford Street, LONDON, W.1

P.O. BOX 569, LONDON, S.E.1

13a Castle Street, EDINBURGH, 2 1 St. Andrew's Crescent, CARDIFF

39 King Street, MANCHESTER, 2 Tower Lane, BRISTOL, 1

2 Edmund Street, BIRMINGHAM, 3 80 Chichester Street, BELFAST

or from any Bookseller

1953

Price £1 0*s* 0*d* net

PRINTED IN GREAT BRITAIN

S.O. Code No. 23–2704

Four Studies in the Theory of Stress Concentration

By

H. L. Cox, M.A., F.R.Ae.S., A.M.I.Mech.E.,

of the Engineering Division, N.P.L.

Reports and Memoranda No. 2704*

January, 1950

General Introduction.—The four papers comprised in this monograph were written over the period 1937 to 1947 and they are printed in chronological order. Each is a study of some of the theoretical aspects of experimental work in progress in the Engineering Division of the National Physical Laboratory during that period. The greater part of the experimental work related to failure of materials by fatigue under alternating stresses and in the theoretical analysis chief attention is paid to this mode of failure. At the same time in some respects the theory is capable of wider application, and the bearing of the analysis on other modes of failure is therefore considered.

A change or discontinuity of section in a stressed component always results in a concentration of stress in its neighbourhood, and failure, particularly failure by fatigue, usually originates by a crack starting from such a region. In so far as such changes of section and discontinuities are unavoidable in actual machine parts, information as to their quantitative effect in reducing the strength of components is urgently needed by the designer. Since materials differ in their susceptibility to stress concentration effects, and since even one material may vary in susceptibility according to the absolute size of the component, the technical data needed can be acquired only by exhaustive tests.

If the factors which govern failure were better understood, the experimental programme could be curtailed, and for this reason alone every effort should be made to analyse the experimental results and to correlate them with theory. Analysis by the theory of elasticity need not, however, be restricted to stress raisers, such as oil-holes and fillets, which are technically important, because it is capable also of affording information as to the effect of surface irregularities and internal faults of microscopic or even submicroscopic size, provided only that this size is still large by comparison with the atomic structure of the material itself.

Parts II and IV of this monograph deal primarily with the development of means to compute the stress distribution in the neighbourhood of holes, grooves and fillets of diverse forms. In respect of direct stresses the results obtained relate only to holes or grooves in infinite or semi-infinite blocks under plane stress or plane strain transverse to the axis of the hole or groove. In this field theory is no more than supplementary to analogical methods, particularly photo-elasticity, which is applicable to pieces of finite size and by the ' frozen stress ' technique to parts other than flat plates of uniform thickness.

* Eng. Div. reports 359/48, 361/48, 360/48, 362/48, 444A/50. Published with the permission of the Director, National Physical Laboratory.

Nevertheless, theoretical analysis has three special merits, (a) that it is better able to show the trend of the variation of the stress distribution as one or more individual factors is varied, (b) that it may be applied to cases, such as very sharp notches or very shallow grooves, of which models cannot readily be made, and (c) that it can be used to establish general principles. In respect of shear and torsion these merits of theoretical analysis are still more marked, and the use of the soap bubble method based on the membrane analogy[10] would appear preferable to the analytical methods only in the few cases for which the computational work becomes too heavy.

One principal conclusion drawn from the analysis in Part II is that the approximate formula for the stress concentration factor under direct stress, $\mu_f = 1 + 2(a/\varrho)^{1/2}$, where a is the depth of the notch or half-depth of the hole and ϱ is the radius at its root, is seldom very much in error, whatever the form of the notch or hole; but that the corresponding formula for the stress concentration factor in shear $\mu_q = 1 + (a/\varrho)^{1/2}$ is much less reliable. If the latter formula is rewritten in the form $\mu_q = 1 + K(a/\varrho)^{1/2}$, the factor K decreases from unity towards about $\frac{1}{2}$ as the groove is widened, and for a ' half-groove ', represented for instance, by the fillet at the root of a spline in a shaft under torsion, the formula $\mu_q = 1 + \frac{1}{2}(a/\varrho)^{1/2}$ appears often to be a good approximation. In both Parts II and IV it is demonstrated conclusively that abrupt changes of curvature in the contour of a section do not in themselves cause any concentration of stress.

Another most useful principle established in Parts II and IV is that when a slight secondary irregularity is superposed on a primary one the two separate stress concentration factors are multiplicative. This conclusion, supplemented by the observation that a low outstanding ridge causes a local reduction of stress virtually opposite to the local concentration which would result from the equivalent shallow groove, is applied to ' correct ' the stress distribution computed for a wavy contour to that appropriate to the similar contour lacking the waviness. By this means a close approach to a prescribed contour can often be obtained on the basis of a representation including only a few terms of a series analogous to a Fourier series.

By contrast with this process of correction for slight superposed irregularities, in Part II the conditions under which the effect of a *sharp* secondary irregularity may not be multiplicative with the effect of a primary stress raiser is examined, and the results are applied to show how a system of small internal flaws may mask the effect of other larger stress raisers.

Part I is concerned mainly with the effect of holes and internal flaws on the behaviour of materials under complex systems of stress. It is there demonstrated that the fatigue resistance of testpieces containing diametral drilled holes, when subjected to combined alternating bending and torsional stresses, conform very closely to the form of relationship predicted by theory; it may be added here that the evidence presented in respect of seven materials (Fig. 2) has since been supplemented by tests on four more and that the agreement with theory is still closer. It is shown further that the behaviour of cast iron in fatigue under the same complex stress system is entirely concordant with the hypothesis that the graphite inclusions act as internal flaws, and the ' typical shape ' of the flaws deduced from the results of fatigue tests is in fair agreement with experiment also in respect of the ratio of the compressive to the tensile strength.

These points are emphasized here because the principal conclusion from Part I is that the behaviour of ductile materials under combined alternating bending and torsion differs radically from that to be expected from any material which contains internal flaws. This conclusion is supported by the analysis in Part II of the effect of flaws in masking other stress concentration effects; although this masking effect accords qualitatively with experimental evidence, to achieve quantitative agreement much larger flaws would be needed than could for other reasons be accounted possible.

In the light of research carried out since these papers were written, the comparison between theory and experiment might now be carried considerably further; this is not attempted here for two reasons. First, experimental data are now being compiled at an increased rate, and, if the task of analysing and correlating all data now available were undertaken, there would be a grave temptation to defer publication month by month in order to include the latest results. Moreover,

correlation of experimental data would necessitate a far wider survey of the theory than is here made, because, as explained above, in respect of technical stress raisers data obtained by analogical processes, such as photoelasticity are often more relevant than those obtained by pure analysis.

For these reasons the four studies in the theory of stress concentration are here presented almost exactly in the forms in which they were first written, and the references made to experimental results should be regarded as illustrations only of the practical sense of the conclusions to be drawn from theory. It is hoped that in the near future a thorough survey of all existing experimental data will be undertaken and that in this survey the present monograph may assist in the task of correlation with theory.

Some of the material available for such a survey and the form which it might take is illustrated by Refs. 15 to 18.

Acknowledgments.—The work described has been carried out as part of the research programme of the National Physical Laboratory.

PART I

The Effect of Holes on the Strength of Materials under Complex Stress Systems

Synopsis.—In a plane test piece pierced by a cylindrical hole the greatest stress is set up at some point in the periphery of the hole. This stress is a principal stress and both the other principal stresses, that normal to the contour of the hole and that parallel to the axis of the hole and normal to the free surface of the test piece, are zero. Therefore, failure of such a test piece under any system of applied loading depends almost entirely on the shape of the hole and on the properties of the material only in respect of a possible difference between its strengths in tension and in compression.

On this basis criteria are developed for the failure of test pieces containing circular and elliptical cylindrical holes under systems of complex stress. The results are applicable to tests on pieces pierced by oil holes drilled either perpendicularly to the axis of the test piece or obliquely. The resulting criterion for circular holes perpendicular to the plane of stress is compared with some experimental results of tests under combined alternating bending and torsion.

Criteria are also developed for elliptical holes oriented at random, and it is shown that these criteria do not in themselves accord with the results of tests on the majority of materials. It is concluded that internal flaws are unlikely to account for the mechanical properties of engineering materials.

I.1. *Introduction.*—In a test piece containing a hole with its axis perpendicular to the plane in which the piece is stressed, the maximum stress or stress range is the circumferential stress at some point in the periphery of the hole. This stress is a principal stress and both the other principal stresses, that normal to the contour of the hole and that normal to the (free) surface of the test piece, are zero. Therefore, if failure of the material is determined by any criterion of stress at a single point, failure of such a test piece occurs always under identical conditions, that is, at one specific value of the one principal stress, which alone differs from zero. As a result the failure of test pieces containing such holes under systems of combined stress may be predicted simply from the geometry of the hole without reference to the precise nature of the criterion which otherwise, under a system of complex stress, might determine failure. Moreover, in consequence, this prediction of behaviour of test pieces containing holes is independent of the nature of the material, except in respect of the magnitude and sign of the failing stress. For instance, the ratio of the limiting stress under shear to that under uniaxial tension applied to the test piece as a whole depends only on the geometry of the hole and on the nature of the material only in respect of a possible difference between the strength of the material under tension and under compression.

If by experiment actual materials were proved not to conform to this principle, it could only be concluded that failure cannot be determined simply by the attainment of a certain limiting stress at a point and that the rate of variation of stress in the neighbourhood of the point of maximum stress must also have a separate influence. That the ' supporting effect ' of under-stressed material adjacent to the region of highest stress may be important is widely recognized; but the investigators, who have examined this possibility, appear to have disregarded the case of the test piece pierced by a hole, by which the possibility should be most readily put to the proof.

The present report establishes the criteria for failure under combined stress systems of test pieces subjected to systems of plane stress and containing elliptical holes with their axes perpendicular to the plane of stress. The results are applied to two cases. The first is that of engineering components pierced by relatively large holes, such as oil holes, and the conclusions for this case are compared with some few experimental results of failure under combined alternating stresses. The second is that of semi-solid materials in which there is a large number

of microscopic holes or flaws roughly all similar in shape but distributed and oriented at random throughout the body of the material. In this case, since the present analysis is restricted to the effect of cylindrical holes all having their axes perpendicular to the plane of stress, comparison with the behaviour of actual materials, in which the flaws would be more general in type and not so preferentially oriented, cannot be finally reliable. Yet the analysis does indicate certain principles, which may be expected to apply more generally regardless of the precise nature of the flaws.

I.2. *Holes of Circular Section.*—As a preliminary example it is convenient to discuss the case of the circular hole, particularly with regard to the practically important case of an oil hole in a shaft subjected to combined flexure and torsion.

The circumferential tensile stress at the periphery of a hole of circular section in an infinite plane test piece under a uniform uniaxial tensile stress f, is $f - 2f\cos 2\theta$, where θ is the angle measured from the diameter parallel to the direction of the stress[1]. The tensile stress due to a shear stress q on planes parallel and perpendicular to this direction is $4q \sin 2\theta$. Thus the stress due to combined tensile stress f and shear stress q, is $f - 2f\cos 2\theta + 4q \sin 2\theta$ and the maximum and minimum values are $f \pm 2(f^2 + 4q^2)^{1/2}$ at $\theta = \frac{1}{2}\tan^{-1}(-2q/f)$ and at right-angles to this radius. The condition for failure is then $f + 2(f^2 + 4q^2)^{1/2} = f_0$, where f_0 is the failing stress of the material under uniaxial tension. This relation may be expressed in the form

$$16q^2 + 3(f + \tfrac{1}{3}f_0)^2 = (\tfrac{4}{3})f_0^2 \qquad .. \quad .. \quad .. \quad .. \quad (1)$$

which is an ellipse, having its centre at $f = -\frac{1}{3}f_0$, $q = 0$ and intercepts on the axes at $f = \frac{1}{3}f_0$ and $-f_0$ and $q = \pm f_0/4$. This ellipse is shown in Fig. 1.

Under static load, if the material itself is more than three times stronger under uniaxial compression than it is under uniaxial tension, the strength of the piece containing a circular hole should be exactly three times greater in compression than in tension. On the other hand if failure actually depends on the maximum shear stress, so that its strength under uniaxial compression is the same as that under uniaxial tension, the sign of the applied direct stress becomes irrelevant and the failure when f is negative is determined by the dotted line in Fig. 1. Comparative tests on pieces containing holes under tension and compression will thus show at once whether failure of the material depends on the maximum tensile stress or on the maximum shear stress; but unfortunately this test is restricted to brittle materials, because plastic deformation alters the shape of the test piece before failure occurs.

When the applied stresses alternate between equal positive and negative values, the signs of f and q are, of course, irrelevant, and in that case failure must be determined by the upper part of the curve shown in Fig. 1. This curve is shown in Fig. 2 together with a number of points representing the results of fatigue tests under combined alternating flexure and torsion made on test pieces containing diametral holes of seven different qualities of steel[2]. It will be seen that the experimental results all conform quite closely to the theoretical curve; the experimental accuracy itself was not better than ± 5 per cent.

I.3. *Holes of Elliptical Section.*—This case is, of course, a generalization of that discussed in Section I.2, but attention is for the present restricted to the instance in which the direct stress f is applied parallel to one of the principal axes of the elliptical cross-section of the hole.

Using elliptic co-ordinates α and β, with the contour of the hole represented by $\alpha = \alpha_0$, the circumferential stress $\bar{\beta}\bar{\beta}$ at β is[1]

$$\frac{(\sinh 2\alpha_0 + e^{2\alpha_0}\cos 2\beta - 1)f - 2e^{2\alpha_0}\sin 2\beta . q}{\cosh 2\alpha_0 - \cos 2\beta} \qquad .. \quad .. \quad .. \quad (2)$$

where f and q are respectively the direct and shear stresses applied.

The maximum and minimum values of $\bar{\beta}\beta$ occur at the values of β defined by

$$A \sin 2\beta + B \cos 2\beta + C = 0 \quad .. \quad .. \quad .. \quad .. \quad (3)$$

where

$$A = (1 - e^{2\alpha_0} \cosh 2\alpha_0 - \sinh 2\alpha_0) f = -4\varrho f/(1-\varrho)^2 (1+\varrho)$$

$$B = -2e^{2\alpha_0} \cosh 2\alpha_0 \, q = -2(1+\varrho^2) q/(1-\varrho)^2$$

$$C = 2e^{2\alpha_0} q = 2(1+\varrho) q/(1-\varrho)$$

and $\varrho = \tanh \alpha_0 =$ ratio of lengths of principal axes of the elliptical hole. The corresponding values of $\cos 2\beta$ are $[-BC \pm A(A^2 + B^2 - C^2)^{1/2}]/[A^2 + B^2]$ and the values of $\sin 2\beta$ are similar with A for B and $-B$ for A. By substitution of these values in formula (2) after some reduction the maximum and minimum stresses can be expressed in the form

$$\bar{\beta}\beta = \frac{\varrho(\varrho^2 + 2\varrho - 1) f (f^2 + q_1^2)^{1/2} \pm (1+\varrho)\{\varrho(1+\varrho) f^2 + (1+\varrho^2) q_1^2\}}{\varrho\{(1+\varrho^2)(f^2 + q_1^2)^{1/2} \pm (\varrho^2 - 1) f\}}$$

where $q_1 = (1+\varrho) q$.

Taking $(f^2 + q_1^2)^{1/2} > 0$, the maximum stress is that given by the two plus signs. If this stress is equated to f_0, the failing stress, the condition for failure under combined direct stress and shear is

$$\varrho\{(\varrho^2 + 2\varrho - 1) f - (1+\varrho^2) f_0\}(f^2 + q_1^2)^{1/2} + (1+\varrho)\{\varrho(1+\varrho) f^2 + \varrho(1-\varrho) f f_0 + (1+\varrho^2) q_1^2\} = 0$$

$$.. \quad .. \quad (4)$$

After rationalizing this relation may be expressed in the form

$$\{4\varrho^2 f^2 + (1+\varrho^2)^2 q_1^2\}\{\varrho(\varrho+2) f^2 + 2\varrho f f_0 + (1+\varrho)^2 q_1^2 - \varrho^2 f_0^2\} = 0 \, . \quad .. \quad .. \quad (5)$$

The first factor is obviously not zero, so that the condition for failure is

$$(1+\varrho)^4 q^2 + \varrho(\varrho+2)\{f + f_0/(\varrho+2)\}^2 = \varrho(\varrho+1)^2 f_0^2/(\varrho+2) \, . \quad .. \quad .. \quad .. \quad (6)$$

This is an ellipse with its centre at $q = 0$ and $f = -f_0/(\varrho+2)$, the lengths of its semi-axes being $(f = \quad)(\varrho+1) f_0/(\varrho+2)$ and $(q = \quad)\{\varrho/(\varrho+2)\}^{1/2} f_0/(\varrho+1)$; the intercepts on the axes are $f = \varrho f_0/(\varrho+2)$ and $-f_0$ and $q = \pm \varrho f_0/(\varrho+1)^2$. When ϱ is very large the ellipse (6) degenerates into an infinitely narrow rectangle $f = \pm f_0$ and $q = \pm f_0/\varrho$, the hole being a narrow crack parallel to the direction of the direct stress applied. When ϱ is very small the ellipse (6) degenerates into the parabola $2(\varrho f_0) f + q^2 = (\varrho f_0)^2$, the hole being then a narrow crack transverse to the direction of the applied direct stress. A series of curves for intermediate values of ϱ is shown in Fig. 3*.

It is tedious to prove mathematically, but on the lines of Section I.2 it may be shown that under static stresses, the whole of each contour in Fig. 3 represents the condition that the maximum *tensile* stress should be f_0. For instance all the contours touch at $f = -f_0$, because when a piece containing an elliptical hole is compressed along either of the principal axes of the ellipse, the greatest tensile stress is numerically equal to the applied stress; this tensile stress occurs at the top and bottom of the hole and in the direction transverse to that of the applied compression†.

When the applied stresses alternate, the signs of f and q become irrelevant and the condition for failure is represented by reflecting the upper portions of the contours in Fig. 3 in the axis of q, as represented by the dotted line in Fig. 1. It is interesting then to note the physical meaning of the cusp on the axis of q. Under pure shear the maximum stress is set up at four points, one in each quadrant of the elliptical contour of the hole. When direct stress is superposed the stress

---

* It is interesting that the curve for $\varrho = \sqrt{2} - 1$ is a true circle and that the curves for both higher and lower values of ϱ grow progressively more elongated, tending eventually to zero width when $\varrho = 0$ or 1.

† In tensile tests on pieces of thin sheet containing large circular holes the existence of transverse compressive stresses above and below the hole is evidenced by buckling of the sheet in these regions.

in two opposite quadrants is increased and that in the other two is correspondingly reduced. Thus the sign of the direct stress applied in relation to the sign of the shear affects the position of the maximum stress. Therefore, if the material round the contour of the hole were differentially hardened, so that in one pair of opposite quadrants it was made stronger than in the other, the relative signs of the direct and shear stresses would be reflected by a difference of strength according to the quadrant in which the greater stress would be developed. Such differential hardening would, therefore, result in a diagram like Fig. 4, even under alternating stresses.

In practice holes of truly elliptical section are not likely to be encountered; but holes of circular section drilled obliquely intersect the axis of a test piece in an ellipse. It is possible that the present analysis is applicable to such cases provided that the obliquity is not very great.

I.4. *Holes of Elliptical Section Oriented at Random.*—If an infinitely large plate pierced by an elliptical hole ($\alpha = \alpha_0$ as before) is subjected to principal stresses f and f' in directions making the angle θ with the principal axes of the ellipse, the stress $\bar{\beta}\bar{\beta}$ at β in the contour of the hole is[1]

$$\bar{\beta}\bar{\beta} = \{(f_1 + f_2)\sinh 2\alpha_0 + (f_1 - f_2)(e^{2\alpha_0}\cos 2\beta - 1) - 2qe^{2\alpha_0}\sin 2\beta\}/(\cosh 2\alpha_0 - \cos 2\beta) \quad .. \quad (7)$$

where

$$f_1 + f_2 = f + f', \quad f_1 - f_2 = (f - f')\cos 2\theta \text{ and } 2q = (f - f')\sin 2\theta.$$

Substituting in terms of f and f' and dropping the suffix 0 from α for convenience, the formula (7) may be expressed in the form

$$\bar{\beta}\bar{\beta} = \{(f + f')\sinh 2\alpha + (f - f')(e^{4\alpha} - 2e^{2\alpha}\cos 2\beta + 1)^{1/2}\cos(2\theta + \varepsilon)\}/(\cosh 2\alpha - \cos 2\beta) \quad (8)$$

where $\tan \varepsilon = e^{2\alpha}\sin 2\beta/(e^{2\alpha}\cos 2\beta - 1)$.

The maximum and minimum values of $\bar{\beta}\bar{\beta}$ are therefore

$$\frac{(f + f')\sinh 2\alpha}{\cosh 2\alpha - \cos 2\beta} \pm (f - f')\left(\frac{2e^2\alpha}{\cosh 2\alpha - \cos 2\beta}\right)^{1/2} \quad .. \quad .. \quad .. \quad .. \quad (9)$$

and this may also be written in the form

$$\left[\left\{\frac{(f + f')\sinh 2\alpha}{\cosh 2\alpha - \cos 2\beta}\right\}^{1/2} \pm \frac{(f - f')}{(f + f')^{1/2}}\left\{\frac{e^{2\alpha}}{2\sinh 2\alpha}\right\}^{1/2}\right]^2 - \frac{(f - f')^2}{(f + f')}\frac{e^{2\alpha}}{2\sinh 2\alpha}. \quad .. \quad .. \quad (10)$$

Without loss of generality we may take $f > f'$. Then if $f + f' > 0$, the greatest tensile stress is found from (9) and it occurs at $\beta = 0$, so that its value is

$$(f + f')\coth \alpha + (f - f')(e^{\alpha}/\sinh \alpha) \quad .. \quad .. \quad .. \quad .. \quad (11)$$

or

$$(f + f')/\varrho + (1 + \varrho)(f - f')/\varrho \quad .. \quad .. \quad .. \quad .. \quad .. \quad (11a)$$

where $\varrho = \tanh \alpha$ is the ratio of the lengths of axes of the ellipse, and in this application

$$0 < \varrho < 1.$$

By equating this stress to the limiting stress f_0 the condition for failure becomes

$$(2 + \varrho)f - \varrho f' = \varrho f_0 \quad .. \quad .. \quad .. \quad .. \quad .. \quad .. \quad (12)$$

When $f+f' < 0$, the greatest tensile stress is from (10) $-\dfrac{(f-f')^2}{(f+f')}\dfrac{e^{2\alpha}}{2\sinh 2\alpha}$, provided that $\dfrac{(f+f')\sinh 2\alpha}{\cosh 2\alpha - \cos 2\beta} = \dfrac{(f-f')^2}{(f+f')}\dfrac{e^{2\alpha}}{2\sinh 2\alpha}$. This formula reduces to

$$(f-f')^2(1+\varrho)^2 + 4\varrho(f+f')f_0 = 0 \qquad \ldots\ldots\ldots\ldots \quad (13)$$

provided that

$$\cosh 2\alpha - \cos 2\beta = \frac{(f+f')^2\, 2\sinh^2 2\alpha}{(f-f')^2\, e^{2\alpha}}.$$

For real values of β, this condition restricts the formula (13) to the range

$$\cosh\alpha > \left|\frac{f+f'}{f-f'}\right| \frac{\sinh 2\alpha}{e^{\alpha}} > \sinh\alpha \qquad \ldots\ldots\ldots\ldots \quad (14)$$

or

$$\frac{1+\varrho}{2\varrho} > \frac{f+f'}{f'-f} > \frac{1+\varrho}{2} \qquad \ldots\ldots\ldots\ldots\ldots\ldots \quad (14a)$$

or

$$(1-\varrho)f' < (1+3\varrho)f \text{ and } < -(3+\varrho)f. \qquad \ldots\ldots\ldots\ldots \quad (14b)$$

Since f' is negative and $\varrho < 1$ the first condition is relevant only when $f < 0$, and similarly the second is relevant only when $f > 0$.

When $|f+f'| \geqslant \frac{1}{2}(1+\varrho)(f-f')$, the maximum tensile stress is defined by formula (9) and it occurs at $\beta = 0$, so that formula (12) applies. When $|f+f'| \leqslant (1+\varrho)(f-f')/2\varrho$, formula (9) again applies but now the maximum tensile stress occurs at $\beta < \pi/2$ and the condition for failure is

$$(f+f')\varrho + (f-f')(1+\varrho) = f_0 \qquad \ldots\ldots\ldots\ldots\ldots \quad (15)$$

or

$$(1+2\varrho)f - f' = f_0 \qquad \ldots\ldots\ldots\ldots\ldots \quad (15a)$$

The complete system of conditions (12), (13) and (15a) is shown in Figs. 5 and 6 for the cases $\varrho = \frac{1}{2}$ and $\varrho \to 0$. In the latter case the limiting stress is of the order $\frac{1}{2}\varrho f_0$ and therefore, in Fig. 6, this value is represented as f_1. In this case also the first condition in (14b) coincides with the line $f = f'$ and the parabola (13) extends over the whole region in which $f' < 1{\cdot}5f_1$.

If the material fails at a specific tensile stress, the ratio of the strength under uniaxial compression of a piece containing a hole to its strength under uniaxial tension is $4(2+\varrho)/(1+\varrho)^2$; this ratio varies from 3 to 8 as ϱ ranges from unity down to zero. On the other hand, if the strength of the parent material is determined by the maximum shear stress, the strength of the piece containing a hole should be the same under compression as under tension. In relation to a solid body containing three-dimensional flaws we may expect the same general principle to apply: that is, if the strength of the parent material depends on the maximum shear stress, the flawed material will be equally strong in tension as in compression; whereas, if the parent material fails always in tension, the flawed material will be considerably stronger under compression than it is under tension. For instance, cast iron under compression is about five times stronger than under tension; this suggests that the material may fail always in tension and that the internal flaws may be equivalent to elliptical cylindrical holes, of which the axes are in the ratio 8 : 3. In this case, of course, the flaws are probably graphite inclusions.

For the special case of pieces subjected to combined direct stress f and shear stress q, the values of the principal stresses are $\frac{1}{2}\{f \pm (f^2 + 4q^2)^{1/2}\}$. Then, so long as f is positive, condition (11a) is applicable and is

$$f + (1 + \varrho)(f^2 + 4q^2)^{1/2} = \varrho f_0 \quad .. \quad .. \quad .. \quad .. \quad .. \quad .. \quad .. \quad .. \quad (16)$$

or

$$\varrho(\varrho + 2)\{f + f_0/(\varrho + 2)\}^2 + 4(1 + \varrho)^2 q^2 = \varrho(\varrho + 1)^2 f_0^2/(\varrho + 2) \text{ (}cf.\text{ formula (6)).} \quad .. \quad (16a)$$

This formula applies also for $f < 0$ so long as $f/(f^2 + 4q^2)^{1/2} < -\frac{1}{2}(1 + \varrho)$ that is, using (16), so long as $f > -\rho f_0$. Thereafter, the appropriate condition is (13) which reduces to

$$(f^2 + 4q^2)(1 + \varrho)^2 + 4\varrho f f_0 = 0 \quad .. \quad .. \quad .. \quad .. \quad .. \quad (17)$$

or

$$\{f + 2\varrho f_0/(1 + \varrho)^2\}^2 + 4q^2 = 4\varrho^2 f_0^2/(1 + \varrho)^4 \quad .. \quad .. \quad .. \quad .. \quad (17a)$$

Formula (17a) applies until $f/(f^2 + 4q^2)^{1/2} < -(1 + \varrho)/2\varrho$; but the least possible value of the left-hand side is -1 (when $q = 0$) and $-1 > -(1 + \varrho)/2\varrho$ when $0 < \varrho < 1$. Therefore, the complete contour is defined by formulae (16) and (17). Taking $\varrho f_0/(\varrho + 2) = f_1$, so that f_1 is the apparent strength under uniaxial tension, the limiting condition for failure is plotted in Fig. 7 for values of ϱ from 0 to 1. On this diagram as in Figs. 1, 2 and 3, the horizontal and vertical scales are the same in terms of shear stress, that is $f = f_1$ represents a shear stress $\frac{1}{2}f_1$ due to tension. By this method of plotting, the condition (17) is represented by a semicircle with its centre at $(f/f_1) = -2(\varrho + 2)/(\varrho + 1)^2$ and $q = 0$, which passes through $f = 0$, $q = 0$. The dotted line across the curves of Fig. 7 indicates the boundary between conditions (16) and (17); this line corresponds to the upper dotted line in Fig. 5 or 6. When failure occurs at a limiting value of shear stress, or in any case if the applied stresses alternate, the sign of f becomes irrelevant and the whole behaviour is described by the upper quadrants of the curves in Fig. 7. In this case the ratio of the strength under pure shear (or torsion) to that under uniaxial direct stress (or bending) lies between $\frac{3}{4}$ and 1. The data for Silal cast iron given in Fig. 8, reproduced from Ref. 3, conform to formula (16) with $\varrho = 0{\cdot}2$ with a mean squared error of 2 per cent. On this evidence we might expect that the strength of Silal cast iron under uniaxial compression should be about six times its strength under uniaxial tension; the actual value of this ratio is just under 5.

I.5. *Comparison with Other Criteria of Failure.*—The upper parts of the curves of Fig. 7 all represent formula (16), and this formula may be expressed in the form,

$$\left(\frac{f_1}{q_1} - 1\right)\left(\frac{f}{f_1}\right)^2 + \left(2 - \frac{f_1}{q_1}\right)\left(\frac{f}{f_1}\right) + \left(\frac{q}{q_1}\right)^2 = 1 \quad .. \quad .. \quad .. \quad .. \quad (18)$$

where $f_1 = \varrho f_0/(\varrho + 2)$ and $q_1 = \varrho f_0/2(\varrho + 1)$. This form is identical with the 'general conic' defined in Ref. 3. Moreover, the original form (16) corresponds to the Guest law

$$(\tfrac{1}{4}f^2 + q^2)^{1/2} + \tfrac{1}{3}\lambda f = q_1 \quad .. \quad .. \quad .. \quad .. \quad (19)$$

if the undetermined parameter λ be identified with $3/2(1 + \varrho)$, or $3\left(2 - \frac{f_1}{q_1}\right)\Big/2\left(\frac{f_1}{q_1}\right)$, and q_1 with $\varrho f_0/2(1 + \varrho)$ as before. Finally, in the discussion on Ref. 3, Stanfield suggested the criterion $(s + \lambda p)_{\max} = \text{const.}$, where s and p are the shear and normal stress on any plane. This condition may be written in the form

$$[\tfrac{1}{2}f\lambda + (\tfrac{1}{2}f + \lambda q)\sin 2\theta + (q - \tfrac{1}{2}f\lambda)\cos 2\theta]_{\max} = \text{const.}$$

or

$$\tfrac{1}{2}f\lambda + (1 + \lambda^2)^{1/2}(\tfrac{1}{4}f^2 + q^2)^{1/2} = \text{const.} \quad .. \quad .. \quad .. \quad .. \quad (20)$$

which again is equivalent to (16) with $\lambda = 1/\{\varrho(\varrho + 2)\}^{1/2}$.

For any material tested under alternating stresses, the correspondence between the four criteria, elliptical holes of characteristic form, the Gough-Pollard general conic, the Guest law and the Stanfield criterion is formally complete; but, whereas the last three criteria permit any value of the ratio f_1/q_1 at least between 2 and 1, the criterion based on the presence of elliptical holes restricts this ratio to values between 1 and $\frac{4}{3}$. In practice values of f_1/q_1 exceeding $\frac{4}{3}$ are common for ductile materials and not uncommon for brittle ones; therefore, we must conclude that the failure of such materials cannot be due to the presence of elliptical cylindrical flaws. It is possible that ellipsoidal flaws may permit a wider variation of the ratio f_1/q_1; but at least we may conclude that experimental satisfaction under alternating stresses of the relation (16) or (18) neither proves nor disproves the existence of holes in the material. To put this question to the proof it is necessary to consider the behaviour of the material under static stresses.

Under static stresses the Gough-Pollard relation is irrelevant because it was proposed simply as an empirical formula to represent (as it does very well) the results of certain fatigue tests[3]. On the other hand the Guest and Stanfield criteria, which are virtually equivalent, imply that formula (16) or (18) should apply over the whole range of f including both positive and negative values. Whereas the ' holes ' criterion implies either the complete diagrams of Fig. 7, over the lower part of which condition (16) is replaced by condition (17), or only the upper part of the diagram, reflected (for negative values of f) in the axis of q (Fig. 1), according to whether the material fails by tension or by shear stress.

I.6. *Conclusion.*—The results of Sections I.2 and I.3 relate strictly to an infinite plane test piece pierced by a cylindrical hole with its axis perpendicular to the plane of stress. In applying the results to a circularly cylindrical test piece pierced by a radial hole and subjected to bending and torsion, allowance must be made for the differences between the two stressing cases. However, the comparison made in Fig. 2 suggests that, provided that the diameter of the radial hole is moderately small in relation to the diameter of the test piece (about 1/10th or less), the differences between the actual and idealized stressing cases may have no great effect. In respect of a circular hole drilled obliquely the application of the data summarized in Fig. 3 is more open to question; but at least it may be expected that these data should represent a first approximation.

The analysis of Section I.4 is related entirely to the fundamental question whether the low strength of all materials in relation to the estimates of their strengths based on thermodynamic data may be explicable by the hypothesis that all materials contain numerous sub-microscopic flaws. In respect of cylindrical flaws with their axes perpendicular to the plane of stress the present analysis shows clearly that this hypothesis accords with experimental results neither qualitatively nor quantitatively. Quantitatively there remains a possibility that ellipsoidal or other ' solid ' flaws might result in better agreement with experiment; but qualitatively it is clear that any system of flaws must always lead to a criterion for failure under combined bending and torsion which cuts the torsion axis obliquely (Fig. 1). Although some few materials yield experimental curves of this type, the majority conform to curves which cut the torsion axis orthogonally (Ref. 3). In such cases it is inconceivable that the materials actually fail at internal flaws. Other equally strong evidence against the flaw hypothesis, also based on stress concentration effects, is recorded in Part II.

PART II

Stress Concentration due to Holes and Grooves other than Elliptical in Form

Synopsis.—In order critically to compare the results of fatigue tests on pieces containing sharp V-notches and other abrupt changes of section with the theoretical values of stress concentration factors, a need was apparent for detailed theoretical investigation of the effect of the form of the discontinuity of section.

Following generally established methods of stress analysis the stress distributions round holes and grooves of a wide range of forms have been examined both under plane direct stress and under shear stress. These analyses have been applied to several particular cases and the results have been compared with approximate formulae based on the stress distribution round elliptical contours.

From the results it appears that the approximate formulae based on elliptical holes afford a reasonably accurate estimate of the maximum stress at any hole or groove under plane direct stress, but that the stress concentration under shear is influenced to a much greater extent by the general form of the hole or groove. Under both types of stress system, certain cases of anomaly arising from application of the approximate formulae are examined, and it is shown that all these anomalies are resolved by the more accurate formulae here derived. Incidentally, in this examination it is demonstrated that abrupt changes of curvature of the contour of a hole or groove cause no concentration of stress.

Comparisons are made with some measurements by the soap-film analogy method of the stresses at V-notches under shear, and moderately good agreement is found.

The stress distribution round very narrow ' hair ' cracks is investigated and the possible effect of such cracks in masking the stress concentration due to other larger notches and holes is examined. It is shown that, although the presence of hair cracks would suffice to explain why experimental values of stress concentration factor are usually markedly less than the theoretical values, the depth of the hair cracks necessary to have this effect is so great that they ought to be easily observable under the microscope; whereas, of course, no sign of such flaws has been observed.

II.1. *Introduction.*—It is well known that the actual reduction in strength of a piece containing a hole, groove or other discontinuity in comparison with the strength of a plain piece is usually very much less than the theoretical value of the ratio of the maximum stress round the discontinuity to the stress in the plain piece under the same load. So long as this discrepancy related only to the behaviour of pieces under static stresses, it appeared reasonable to attribute the lessened effect of the hole or notch in practice to the effect of yielding (with perhaps strain hardening of the material) in the regions of maximum stress round the hole. It is indeed doubtful whether this view was ever really justified, even in relation to static stresses, but, if the same argument be advanced as an explanation of the similar discrepancy between theory and experiment observed in fatigue tests, its insufficiency can be demonstrated fairly easily. It is not proposed here to attempt this demonstration in detail ; but briefly the rejection of this explanation is based on the following arguments.

(a) Yielding cannot change the shape of the hole so appreciably that the theoretical stress concentration factor is reduced to the experimental value.

(b) If yielding of the material in the regions of high stress occurs at each stress maximum in the load cycle, there is *a priori* no reason why similar yielding should not occur all over the regions of high stress in a plain piece; but, if this were the case, the strength of materials under alternating flexural stress should be *considerably* greater than the strength under alternating

direct stress uniform over the cross section. Moreover, continuous yielding, since it must involve dissipation of energy, should be reflected in increased damping of notched pieces in vibration; this increase has not been observed.

(c) If the material in the regions of high stress is strain hardened by repeated, but gradually diminishing, yield, the material must finally be brought into a state in which it can withstand the full theoretical range of stress. If this state can be reached at the bottom of a notch, why cannot it be reproduced throughout the piece?

The first argument (a) may be substantiated fairly easily by reference to any particular form of notch. It will be found that reduction of the curvature in one region of high stress is always accompanied by an increase in another.

The two latter arguments (b) and (c) present the essential dilemma. The material in the regions of high stress is either brought into an elastic condition or it remains plastic. If it is rendered elastic, it must also be rendered superstrong; if it remains plastic, it must be credited with a property hitherto unrecognized. In either case, it is clear that the mere statements that the material strain hardens or that it yields continuously cannot be regarded as sufficient, and that the meanings of these statements must be further examined.

In the discussion above, it has been tacitly assumed that the material may be regarded as a continuous medium. If it is not a continuous medium, the theory of elasticity based on the average properties of a large bulk of material is applicable only to stress distributions which are sensibly uniform over regions large in comparison with the fine structure of the material; if the stresses vary more rapidly the effect of the fine structure must be taken into account. On this basis, Griffith[4] sought to explain the differences between the theoretical estimates of the strength of materials based on their other physical properties and their actual practical strengths by postulating the presence in practical materials of numerous fine cracks or flaws of very small size; the same explanation has been advanced to account for the differences between theoretical and practical stress concentration factors due to discontinuities. This ' crack hypothesis ' is not now held in such favour as it was some years ago; but in relation to metals it has in some sense been superseded by the dislocation theory, and therefore, examination of the sufficiency of such hypotheses of discontinuities to the reconciliation of theoretical and experimental results is not out of place.

In attempting to review these and other possible explanations of the discrepancy between theoretical and practical values of stress concentration factors, it soon became apparent that the state of theoretical knowledge was insufficient. This was particularly remarked in considering the results of the fatigue tests carried out by Gough and Pollard[5] on pieces containing sharp V-grooves. From the results of these tests it appeared that the radius at the bottom of the notch had only a secondary effect on the fatigue strength, whereas according to the arguments advanced by Inglis[1] the stress concentration factor should vary in proportion to the root of this radius. On the other hand Inglis' conclusions were based entirely on results obtained for a hole of elliptical form and the application of these results to holes of other forms and to notches was supported only by general arguments, of which the validity was uncertain. Accordingly the possibility remained that the form of the hole or notch might have greater influence than Inglis considered, and that in certain cases this influence might predominate over that of the radius of curvature at the bottom of the hole or notch.

In this paper, therefore, an attempt is made to extend the analysis developed by Inglis to holes of forms more general than the ellipse and particularly to notches of quite arbitrary forms. At the same time, this more general analysis is applied to some cases of combinations of holes or notches and fine hair cracks, generally representative of the Griffith crack hypothesis in its original form.

II.2. *Synopsis of Analysis.*—The analysis is presented in eight sections. In Section II.3 the nature and some of the properties of the general epicyclic conformal transformation

$$x + iy = \sum_r \lambda_r e^{-r(\alpha+i\beta)}$$

are explained; in Section II.4 the device representing the hair crack is introduced; and in Section II.5 the use of the epicyclic series to represent a groove of arbitrary form is developed.

In Section II.6 the stress distribution round an infinitely long cylindrical hole in an infinite block due to shear parallel to the axis of the hole is worked out; and in Section II.7 the stress distribution round the same hole due to states of stress in planes perpendicular to the axis of the hole, and uniform at infinity, is found. In Section II.8 the results are applied to a class of holes differing appreciably from the elliptical form, and some general conclusions with regard to the relative importance of curvature and general form are drawn; in Section II.9 the effect of hair cracks in reducing the apparent stress concentration factors below the theoretical values is considered. General conclusions mainly relating to practical application of the results and to the use of the results in further examination of the criteria of fatigue failure are collected in Section II.10.

The general method of analysis used in Section II.7 follows that adopted by Inglis[1]; but the presentation has been considerably simplified and shortened. The analysis was first developed in terms exactly analogous to those used by Inglis, but it was quite obvious from the form of the results that they could be presented more simply. This simplification was eventually effected by adoption of complex variables throughout, and the work had been brought just to this stage when a paper by Stevenson[6] on the use of the complex variable in problems of elasticity was received. The first part of Section II.7 could now be omitted and the results quoted from Stevenson's paper or from other publications on the use of the complex variable in stress analysis[7,8]. On the other hand the complex variable method is not yet very well known, and therefore, for the sake of completeness the analysis of Section II.7 has been allowed to stand. For more complete and rigorous treatment Refs. 6, 7 and 8 should be consulted. It is, perhaps, worth adding that by Inglis' method, one arrives at $3s - 1$ simultaneous equations involving only $2s - 1$ unknowns, but s of the equations prove to be redundant. It was this fact, combined with the fact that Poisson's Ratio, which is involved throughout the early part of the analysis, later disappears from the results, which suggested that a more simple presentation must be possible.

II.3. *The General Epicyclic Transformation.*—(a) *Nature of the Transformation.* In an infinite block of material take Cartesian axes $Oxyz$ and transform to the curvilinear system of co-ordinates $\alpha\beta\gamma$ by the conformal transformation:

$$x + iy = \sum_n \lambda_n e^{-n(\alpha+i\beta)},$$
$$z = \gamma,$$

where n takes all values both positive and negative and the λ's are arbitrary. Then

$$x = \Sigma (\lambda_{-n} e^{n\alpha} + \lambda_n e^{-n\alpha}) \cos n\beta$$

and

$$y = \Sigma (\lambda_{-n} e^{n\alpha} - \lambda_n e^{-n\alpha}) \sin n\beta .$$

Any line of constant α is, therefore, an epicyclic cylinder about the axis Oz. By suitable choice of the values of λ_n and λ_{-n} any pair of such cylinders may be represented by the contours $\alpha = \pm \alpha_1$* and therefore, if the values of the stresses $\bar{\alpha}\bar{\alpha}$, $\bar{\alpha}\bar{\beta}$ and $\bar{\gamma}\bar{\alpha}$ may be made to assume assigned values at $\alpha = \pm \alpha_1$, the general expressions for these stresses and the corresponding expressions for the remaining stresses $\bar{\beta}\bar{\beta}$, $\bar{\gamma}\bar{\gamma}$ and $\bar{\beta}\bar{\gamma}$ represent the distribution of stress throughout the tube enclosed between the contours $\alpha = \pm \alpha_1$ under the action of the assigned surface tractions. In the present paper attention will be restricted to the effect of holes in infinite blocks and therefore we take $\lambda_{-1} = 1$ and $\lambda_{-n}(n > 1) = 0$. In this case when $\alpha \to \infty$, $x \to e^{\alpha} \cos \beta$ and $y \to e^{\alpha} \sin \beta$, so that the $\alpha\beta$-co-ordinate system tends to the circularly cylindrical. If of λ_n only λ_1 is different from zero, $x = (e^{\alpha} + \lambda_1 e^{-\alpha}) \cos \beta$ and $y = (e^{\alpha} - \lambda_1 e^{-\alpha}) \sin \beta$. Defining the contour of the hole as $\alpha = 0$, this system makes lines of constant α vary from the ellipse

$$x = (1 + \lambda_1) \cos \beta \text{ and } y = (1 - \lambda_1) \sin \beta$$

at the contour of the hole to the circle $x = e^{\alpha} \cos \beta$, $y = e^{\alpha} \sin \beta$ as $\alpha \to \infty$. This is the system of co-ordinates used by Inglis (*loc. cit.*)

* Or of course $\alpha = \alpha_1$ and $\alpha = \alpha_2$.

(b) *The Scale Factor h.*—

Writing

$$x + iy = \phi(\alpha + i\beta) \equiv \phi(\xi) \quad \text{(Definition)}$$

$$x - iy = \phi(\alpha - i\beta) \equiv \phi(\zeta) \quad \text{(Definition)}$$

Then

$$\delta x + i\,\delta y = \phi'(\xi)(\delta\alpha + i\,\delta\beta)$$

and

$$\delta x - i\,\delta y = \phi'(\zeta)(\delta\alpha - i\,\delta\beta)\,,$$

where a prime denotes differentiation with respect to the complete argument ξ or ζ, so that $(\delta s)^2 = (\delta x)^2 + (\delta y)^2 = \phi'(\xi)\phi'(\zeta)\{(\delta\alpha)^2 + (\delta\beta)^2\} = h^2\{(\delta\alpha)^2 + (\delta\beta)^2\}$.

The parameter $h = \{\phi'(\xi)\phi'(\zeta)\}^{1/2}$ is thus the scale factor describing the length represented by unit change in α or β. Further comments on the general characteristics of the $\alpha\beta$ system of co-ordinates are made in Section IV.2. When $\phi(\xi) = \sum_n \lambda_n e^{-n\xi}$,

$$\begin{aligned} h^2 &= \sum_n n\lambda_n e^{-n\xi} \sum_m m\lambda_m e^{-m\zeta} \\ &= \sum_n n^2\lambda_n^2 e^{-2n\alpha} + 2\sum_m \sum_n mn\lambda_m\lambda_n e^{-(m+n)\alpha}\cos(m-n)\beta,\ m > n\,. \\ r^2 &= \sum_n \lambda_n e^{-n\xi} \sum_m \lambda_m e^{-m\zeta} \\ &= \sum_n \lambda_n e^{-2n\alpha} + 2\sum_m \sum_n \lambda_m\lambda_n e^{-(m+n)\alpha}\cos(m-n)\beta,\ m > n\,. \end{aligned}$$

and the curvature $(1/\varrho)$ of a line of constant α is $\dfrac{1}{2h^3}\dfrac{\delta h^2}{\delta\alpha}$ (*see* Section IV.2) so that

$$|1/\varrho| = \{\sum_n n^3\lambda_n^2 e^{-2n\alpha} + \sum_m \sum_n mn(m+n)\,\lambda_m\lambda_n e^{-(m+n)\alpha}\cos(m-n)\beta\}/h^3,\ m > \mathrm{n}\,.$$

An important class of contour is that of regular n-sided polygons for which apart from the initial term λ_{-1}, only λ_{n-1}, λ_{2n-1}, λ_{3n-1}, etc., differ from zero.

II.4. *The Hair Crack.*—To the transformation $x + iy = \phi(\xi)$ representing any given hole at $\alpha = 0$, let the extra terms $(d/n)(e^{-\xi} + e^{-3\xi} + e^{-5\xi} + \ldots e^{-(2n+1)\xi})$ be added; x is then increased by $(d/n)\{\cos\beta + \cos 3\beta + \ldots + \cos(2n-1)\beta\} = d\sin 2n\beta/2n\sin\beta$; and y by $-(d/n)\{\sin\beta + \sin 3\beta + \ldots \sin(2n-1)\beta\} = -d(1-\cos 2n\beta)/2n\sin\beta$.

If n is large, the change in y is everywhere small, and the change in x is also small provided that β is not small. As $\beta \to 0$, however, the change in x tends to d. Using the results of Section II.3 (b), the radius of curvature at $\beta = 0$ may be found. The complete transformation, therefore, may be used to represent a hair crack of depth d and radius of curvature at its end

$$(1 - \Sigma m\lambda_m - nd)^2/\{1 + \Sigma m^2\lambda_m + (d/3)(4n^2 - 1)\}$$

(at $\beta = 0$ in the contour of the hole defined by $x + iy = e^{\xi} + \sum_m \lambda_m e^{-m\xi}$).

The extent to which the crack affects the contour of the hole in regions remote from $\beta = 0$ depends upon the value of n, the general form of the hole being the better maintained the higher the value of n. For the radius of curvature at the end of the crack to be positive nd must be less than $1 - \Sigma m\lambda_m$. In order than n should be large, d must therefore be small in comparison with $1 - \Sigma m\lambda_m$, this condition implies that the depth of the crack can be only a small fraction of the width $1 - \Sigma\lambda_m$ of the hole (at $\beta = \pi/2$).

To deeper cracks the general method of the following Section II.5 may be applicable.

II.5. *Representation of a Groove of any Form by an Epicyclic Series.*—(a) *General method of representing a groove.*—The contour of the hole is represented by the series:

$$x = (\lambda_{-1} + \lambda_1') \cos\beta + \lambda_2 \cos 3\beta + \ldots \ *$$

$$y = (\lambda_{-1} - \lambda_1') \sin\beta - \lambda_2 \sin 3\beta + \ldots$$

Or, writing, $\lambda_1 = \lambda_{-1} + \lambda_1'$,

$$x = \lambda_1 \cos\beta + \lambda_2 \cos 3\beta + \ldots$$

$$y = 2\lambda_{-1} \sin\beta - (\lambda_1 \sin\beta + \lambda_2 \sin 3\beta + \ldots) .$$

If λ_1, λ_2, etc., be so chosen that the function $\lambda_1 \cos\beta + \lambda_2 \cos 3\beta + \ldots$, etc., is finite over the ranges

$$-\frac{\pi}{2(2n-1)} < \beta < \frac{\pi}{2(2n-1)} \text{ and } \pi - \frac{\pi}{2(2n-1)} < \beta < \pi + \frac{\pi}{2(2n-1)}$$

and zero in between, where n is large, then within these ranges

$$x = \lambda_1 \cos\beta + \lambda_2 \cos 3\beta + \ldots$$

and approximately $y = \{2\lambda_{-1} - \sum_r (2r-1)\lambda_r\}\beta$.

And, if λ_1, λ_2, etc., be small in comparison with λ_{-1}, outside these ranges $x = 0$ and approximately $y = 2\lambda_{-1}\sin\beta$. Obviously the accuracy of the two approximate formulae for y is limited, but the error in the form for y when $x \equiv 0$ does not matter at all, whilst the error in the other form for y affects only values for which $\beta \to \pm\pi/2(2n-1)$. It will be seen later that, by the method of use of these approximate forms here developed, the effect of this error is slightly to round off the edges of the groove. The width w of the groove (neglecting the rounding of the outer edges) is $\{2\lambda_{-1} - \Sigma(2r-1)\lambda_r\}\{\pi/(2n-1)\}$, and its depth $a = \sum_r \lambda_r$; the radius of curvature at $\beta = 0$ (the bottom of the groove) $\varrho = \dfrac{(2n-1)^2 w^2}{\pi^2 a} \dfrac{\Sigma \lambda_r}{\Sigma (2r-1)^2 \lambda_r}$

(b) *Representation of given form of groove.*—Suppose the groove to be defined by Fourier Series

$$x = a\left(K_1 \cos\frac{\pi y}{w} + K_2 \cos\frac{3\pi y}{w} + \ldots\right), \text{ with } \sum_m K_m = 1$$

$$= a \sum_m K_m \cos(2m-1)(2n-1)\beta \text{ in the range } -\frac{\pi}{2(2n-1)} < \beta < \frac{\pi}{2(2n-1)}$$

and zero elsewhere in the range $-\pi/2 < \beta < \pi/2$.

Denoting by $\lambda_{r,m}$ the contribution of the K_m term to λ_r ,

$$\lambda_{r,m} = \frac{2a}{\pi}\int_{-\pi/2(2n-1)}^{\pi/2(2n-1)} K_m \cos(2m-1)(2n-1)\beta \cos(2r-1)\beta \, d\beta$$

$$= \frac{2aK_m}{\pi}\left[\frac{\sin[\{(2m-1)(2n-1)+(2r-1)\}\{\pi/2(2n-1)\}]}{(2m-1)(2n-1)+(2r-1)} + \frac{\sin[\{(2m-1)(2n-1)-(2r-1)\}\{\pi/2(2n-1)\}]}{(2m-1)(2n-1)-(2r-1)}\right]$$

$$= (-1)^{m-1}\frac{4aK_m}{\pi}\frac{(2m-1)(2n-1)}{(2m-1)^2(2n-1)^2-(2r-1)^2}\cos\left\{\frac{2r-1}{2n-1}\frac{\pi}{2}\right\} .$$

* In this section, λ_r is used in place of λ_{2r-1} for brevity.

Of course, by definition $\sum_r \lambda_{r,m} \cos(2r-1)\beta \equiv aK_m \cos(2m-1)(2n-1)\beta$ over the range of integration; so that, substituting $\beta = 0$, $\sum_r \lambda_{r,m} = aK_m$. This result follows also by forming the sum $\sum_r \lambda_{r,m}$. Moreover, $\Sigma \lambda_r = \sum_r \sum_m \lambda_{r,m} = \sum_m \sum_r \lambda_{r,m} = \sum_m aK_m = a$, because $\sum_m K_m = 1$.

Then

$$\sum_r (2r-1)\lambda_{r,m} = \sum_r (-1)^{m-1} \frac{4aK_m}{\pi} \frac{(2m-1)(2n-1)(2r-1)}{(2m-1)^2(2n-1)^2 - (2r-1)^2} \cos\left\{\frac{2r-1}{2n-1}\frac{\pi}{2}\right\}$$

$$= (-1)^{m-1}\frac{4aK_m}{\pi}(2m-1)(2n-1)$$

$$\sum_r \frac{(2m-1)(2n-1) - \{(2m-1)(2n-1) - (2r-1)\}}{(2m-1)^2(2n-1)^2 - (2r-1)^2} \cos\left\{\frac{2r-1}{2n-1}\frac{\pi}{2}\right\}$$

$$= (2m-1)(2n-1)\sum_r \lambda_{r,m} + (-1)^m (2m-1)(2n-1) \times$$

$$\frac{4aK_m}{\pi} \sum_r \frac{\cos[\{(2m-1)(2n-1) + (2r-1)\}\{\pi/2(2n-1)\} - (2m-1)(\pi/2)]}{(2m-1)(2n-1) + (2r-1)}$$

$$= (2m-1)(2n-1)aK_m$$

$$- (2m-1)(2n-1)\frac{4aK_m}{\pi} \sum_{r=1}^{r=\infty} \frac{\sin\{(2m-1)(2n-1) + (2r-1)\}\varepsilon}{(2m-1)(2n-1) + (2r-1)}$$

where $\varepsilon = \{\pi/2(2n-1)\}$

$$= (2m-1)(2n-1)(4aK_m/\pi)[(\pi/4) - \sum_1^{\infty}\{(\sin 2r\varepsilon)/2r\} + \sum_1^{2mn-m-n}\{(\sin 2r\varepsilon)/2r\}]$$

$$= (2m-1)(2n-1)(4aK_m/\pi)\sum_1^{2mn-m-n}\{(\sin 2r\varepsilon)/2r\}, \text{ because } \sum_1^{\infty}\{(\sin 2r\varepsilon)/2r\} = (\pi/4)$$

$$= (2m-1)(2n-1)(4aK_m/\pi)\sum_1^{2mn-m-n}\int_0^{\varepsilon}\cos 2r\theta\, d\theta, \text{ using } \theta \text{ as current variable}$$

$$= (2m-1)(2n-1)(4aK_m/\pi)\int_0^{\varepsilon}(\sum_1^{2mn-m-n}\cos 2r\theta)\, d\theta, \text{ assuming absolute convergence}$$

$$= (2m-1)(2n-1)(4aK_m/\pi)\int_0^{\varepsilon}[\{\sin(2m-1)(2n-1)\theta - \sin\theta\}/2\sin\theta]\, d\theta .$$

If ε is very small, that is if n is large,

$$\int_0^{\varepsilon}\{\sin(2m-1)(2n-1)\theta/\sin\theta\}\, d\theta \text{ is approximately equal to}$$

$$\int_0^{\varepsilon}\{\sin(2m-1)(2n-1)\theta/\theta\}\, d\theta = \mathrm{Si}\{(2m-1)(2n-1)\varepsilon\}$$

$$= \mathrm{Si}\{(2m-1)(\pi/2)\}$$

and ε is negligible in comparison.

Hence $\sum_r (2r-1)\lambda_{r,m} = (2m-1)(2n-1)(2aK_m/\pi)\,\mathrm{Si}\{(2m-1)(\pi/2)\}$.

Also

$$\sum_r (2r-1)^2 \lambda_{r,m} = \sum_r (-1)^{m-1} \frac{4aK_m}{\pi} \frac{(2m-1)(2n-1)(2r-1)^2}{(2m-1)^2(2n-1)^2-(2r-1)^2} \cos\left\{\frac{2r-1}{2n-1}\frac{\pi}{2}\right\}$$

$$= (-1)^{m-1}\frac{4aK_m}{\pi}(2m-1)^3(2n-1)^3 \sum_r \left\{\frac{1}{(2m-1)^2(2n-1)^2-(2r-1)^2} - \frac{1}{(2m-1)^2(2n-1)^2}\right\} \cos\left\{\frac{2r-1}{2n-1}\frac{\pi}{2}\right\}$$

$$= (2m-1)^2(2n-1)^2 \sum_r \lambda_{r,m} + (-1)^m \frac{4aK_m}{\pi}(2m-1)(2n-1) \sum_r \cos\left\{\frac{2r-1}{2n-1}\frac{\pi}{2}\right\}.$$

So that $\Sigma(2r-1)^2\lambda_{r,m}/(2n-1)^2 = (2m-1)^2 aK_m$, the second term being negligible in comparison with the first.

(c) *Summary of Results.*—Collecting these results, the width of the groove,

$w = \{2\lambda_{-1} - \sum_r (2r-1)\lambda_r\}\{\pi/(2n-1)\} = \{2\pi\lambda_{-1}/(2n-1)\} - 2a\sum_m (2m-1)\,\mathrm{Si}\{(2m-1)\pi/2\}K_m$

and the curvature $(1/\varrho)$ at the root is $\{\pi^2 a \sum_m (2m-1)^2 K_m\}/w^2$,

where $a = \sum_r \lambda_r$ is the depth of the groove, and its shape is defined by the Fourier Series

$$x = a\sum_m K_m \cos(2m-1)(\pi y/w).$$

Also

$$\lambda_r = \sum_m \lambda_{r,m} = \frac{4a}{\pi}\cos\left\{\frac{2r-1}{2n-1}\frac{\pi}{2}\right\} \sum_m (-1)^{m-1} K_m \frac{(2m-1)(2n-1)}{(2m-1)^2(2n-1)^2-(2r-1)^2}$$

and

$$\sum_r (2r-1)\lambda_r = \sum_m \sum_r (2r-1)\lambda_{r,m} = \{2a(2n-1)/\pi\} \sum_m (2m-1)\mathrm{Si}\{(2m-1)(\pi/2)\}K_m$$

but the m summations cannot be performed until the K's be specified.

II.6. *Stresses round a Hole Due to Uniform Shear Parallel to the Axis of the Hole.*—(a) *Solution of Stress Equation of Equilibrium.*—One of the three stress equations of equilibrium (Ref. 8, Section 58, page 89) is

$$h_1h_2h_3\left\{\frac{\partial}{\partial\alpha}\left(\frac{\bar\gamma\bar a}{h_2h_3}\right) + \frac{\partial}{\partial\beta}\left(\frac{\bar\beta\bar\gamma}{h_3h_1}\right) + \frac{\partial}{\partial\gamma}\left(\frac{\bar\gamma\bar\gamma}{h_1h_2}\right)\right\} + \bar\beta\bar\gamma h_2h_3\frac{\partial}{\partial\beta}\left(\frac{1}{h_3}\right)$$
$$+ \bar\gamma\bar a h_3h_1\frac{\partial}{\partial\alpha}\left(\frac{1}{h_3}\right) - \bar\beta\bar\beta h_2h_3\frac{\partial}{\partial\gamma}\left(\frac{1}{h_2}\right) - \bar a\bar a h_3h_1\frac{\partial}{\partial\gamma}\left(\frac{1}{h_1}\right) = 0.$$

In our case, the stress distribution must be independent of γ, h_3 is constant, and $h_1 = h_2 = 1/h$ in our notation; the equation, therefore, reduces to

$$\frac{\partial}{\partial\alpha}(h\bar\gamma\bar a) + \frac{\partial}{\partial\beta}(h\bar\beta\bar\gamma) = 0.$$

But $\bar\beta\bar\gamma = Ge_{\beta\gamma}$ and $\bar\gamma\bar a = Ge_{\gamma\alpha}$, whilst $e_{\beta\gamma} = \dfrac{\partial u_\gamma}{h\,\partial\beta}$ and $e_{\gamma\alpha} = \dfrac{\partial u_\gamma}{h\,\partial\alpha}$.

(Ref. 8, Section 20; h, u_α and u_β are all independent of γ.)

Therefore

$$\left(\frac{\partial^2}{\partial\alpha^2} + \frac{\partial^2}{\partial\beta^2}\right)u_\gamma = 0.$$

Using the solutions $u_\gamma = \sum_m A_m \cosh m\alpha \sin m\beta$ and similar terms

$\bar\beta\bar\gamma = (G/h)\sum_m mA_m \cosh m\alpha \cos m\beta$ and $\bar\gamma\bar a = (G/h)\sum_m mA_m \sinh m\alpha \sin m\beta$.

(b) *Case of Uniform Shear.*—As $\alpha \to \infty$, $h \to e^{\alpha}$ (taking $\lambda_{-1} = 1$), so that to make the stress at infinity finite, we may take $m = 1$ only. If the stress system at infinity is $\bar{y}\bar{z} = q$ and $\bar{z}\bar{x} = q'$, the appropriate solutions are

$$\bar{\beta}\bar{\gamma} = 2(q/h) \cosh \alpha \cos \beta + 2(q'/h) \cosh \alpha \sin \beta$$

$$\bar{\gamma}\bar{\alpha} = 2(q/h) \sinh \alpha \sin \beta + 2(q'/h) \sinh \alpha \cos \beta ,$$

conforming to the additional condition $\bar{\gamma}\bar{\alpha} = 0$ at $\alpha = 0$ (the contour of the hole). If $q' = 0$, at $\beta = (\pi/2)$, $\bar{\beta}\bar{\gamma} = 0$, so that the block may be cut through the plane $\beta = (\pi/2)$ to leave a semi-infinite block scored by a groove down one face and sheared by forces tending to distort this face.

The position of the maximum stress depends both on the ratio of q to q' and on the values of the λ's. However, if $q' = 0$ and the curvature of $\beta = 0$ is a maximum, the stress will normally be a maximum at this point in the contour of the hole ($\alpha = 0$ and $\beta = 0$). In this case the stress concentration factor

$$\mu_q = (\bar{\beta}\bar{\gamma}/q)_{\alpha=0,\,\beta=0} = 2/\{1 - \sum_r r\lambda_r\} = 2/(1 - \lambda_1 - 2\lambda_2 - 3\lambda_3 - \ldots) .$$

But ϱ at $\beta = 0$ (Section 3) $= (1 - \lambda_1 - 2\lambda_2 - \ldots)^2/(1 + \lambda_1 + 4\lambda_2 + \ldots)$ and a, the radius of the hole at $\beta = 0$, $= 1 + \lambda_1 + \lambda_2 + \ldots$, so that if λ_2, λ_3, etc., are zero, $\mu_q = 2/(1 - \lambda_1) = 1 + (1 + \lambda_1)/(1 - \lambda_1) = 1 + \sqrt{(a/\varrho)}$, the usual formula for the ellipse. Further examples of stress concentration in shear are given in Section II.8 and subsequent sections.

(c) *Stress Concentration Factor for General Groove.*—In the case of the general groove discussed in Section II.5, the stress concentration factor in shear $\mu_q = 2\lambda_{-1}/\{\lambda_{-1} - \Sigma\,(2r - 1)\lambda_r\}$, but the value of λ_1 to be used in this formula is the substantive value λ_1' (Section II.5 (a)). Substituting for $\lambda_1' = \lambda_1 - \lambda_{-1}$, $\mu_q = 2\lambda_{-1}/\{2\lambda_{-1} - \Sigma\,(2r - 1)\lambda_r\}$, where the values of λ_r are now those used in the remainder of Section II.5. It then follows that

$$\begin{aligned}\mu_q &= 2\lambda_{-1}/\{2\lambda_{-1} - \sum_r (2r - 1)\lambda_r\} \\ &= 1 + \{\pi/(2n - 1)w\} \sum_r (2r - 1)\lambda_r \\ &= 1 + (2a/w) \sum_m (2m - 1) \operatorname{Si}\{(2m - 1)(\pi/2)\}K_m\end{aligned}$$

or using the relation $a/\varrho = (\pi a/w)^2 \sum_m (2m - 1)^2 K_m$

$$\mu_q = 1 + \frac{2}{\pi}\left(\frac{a}{\varrho}\right)^{1/2} \frac{\sum_m (2m - 1) \operatorname{Si}\{(2m - 1)(\pi/2)\}K_m}{\{\sum_m (2m - 1)^2 K_m\}^{1/2}} .$$

As an example, if the groove approximates to a triangular notch of width w, and depth a its apex being rounded to a radius ϱ, K_m may be taken as $\{8/\pi^2(2m - 1)^2\}$ for values of m up to M and zero for all higher values of M. The appropriate value of M is defined by the relation

$$a/\varrho = (\pi a/w)^2 \sum_m (2m - 1)^2 K_m = 8(a/w)^2 M.$$

Then $\mu_q = 1 + J_M(a/\varrho)^{1/2}$, where

$$J_M = \frac{4}{\pi^2}\left(\frac{2}{M}\right)^{1/2} \sum_{m=1}^{m=M} \frac{\operatorname{Si}\{(2m - 1)(\pi/2)\}}{2m - 1} .$$

* If $K_M = 1$ where M is large and all the other K's are zero, $\operatorname{Si}\{(2M - 1)(\pi/2)\} \to (\pi/2)$ and $\mu_q \to 1 + (a/p)^{1/2}$. A continuous sinusoidal serration thus gives the same stress concentration as a single (half) elliptical groove having the same depth and same radius of curvature at its root, *cf.* Part III.

Values of J_M for values of M from 1 to 13 are given in Table 1 below.

TABLE 1

Values of J_M

M	1	2	3	4	5	6	7	8	9	10	11	12	13
J_M	0·785	0·773	0·732	0·699	0·669	0·644	0·622	0·604	0·587	0·572	0·559	0·546	0·535

For a semi-elliptical groove, the nominal value of M is $\frac{1}{2}$ and of course $J_M = 1$: this accords with the values for higher values of M listed in Table 1. For a given value of a/ϱ, M increases with w/a. Thus as w/a increases, a/ϱ being maintained constant J_M is reduced; this shows the effect of widening the groove. For a 90 deg notch $w/a = 2$ and $M = a/2\varrho$; values of $\mu_q = 1 + J_M(a/\varrho)^{1/2}$ for this case and for 60 deg and 120 deg notches are shown in Fig. 9 in comparison with the approximate formula $\mu_q = 1 + (a/\varrho)^{1/2}$. On the same diagram are shown results obtained by A. A. Griffith by the use of the soap-film method[10]. With reference to the grooves used by Gough and Pollard[3] taking $a = 0{\cdot}02$ in., $\varrho = 0{\cdot}0002$ in., $w/2a = \tan 55$ deg/2, $M =$ about $13{\cdot}5$ and $\mu_q = 6{\cdot}3$ in comparison with the approximate value $11{\cdot}0$.

II.7. *Stresses round a Hole Due to Systems of Uniform Plane Strain in the Plane Perpendicular to the Axis of the Hole.*—(a) *General Formulae for Stresses and Strains.*—By the general stress-strain equations $(1 - \sigma)\Delta + (1 - 2\sigma)\omega$ may be any function of $\alpha + i\beta$. If u_α and u_β are the displacements along the $\alpha\beta$ co-ordinate lines respectively and if $u = u_\alpha/h$ and $v = u_\beta/h$,

$$\Delta = \frac{\partial u}{\partial \alpha} + \frac{\partial v}{\partial \beta} - 2h\left(u\frac{\partial}{\partial \alpha} + v\frac{\partial}{\partial \beta}\right)\left(\frac{1}{h}\right) = \frac{1}{h^2}\left\{\frac{\partial(h^2 u)}{\partial \alpha} + \frac{\partial(h^2 v)}{\partial \beta}\right\}$$

and

$$\omega = \frac{1}{2h^2}\left\{\frac{\partial(h^2 v)}{\partial \alpha} - \frac{\partial(h^2 u)}{\partial \beta}\right\}.$$

Substituting $U = u + iv$, $V = u - iv$, $\xi = \alpha + i\beta$ and $\zeta = \alpha - i\beta$,

$$\partial/\partial\alpha = \partial/\partial\xi + \partial/\partial\zeta \quad \text{and} \quad \partial/\partial\beta = i(\partial/\partial\xi - \partial/\partial\zeta)$$

and therefore,

$$\Delta = \frac{1}{h^2}\left\{\frac{\partial(h^2 U)}{\partial \xi} + \frac{\partial(h^2 V)}{\partial \zeta}\right\} \quad \text{and} \quad \omega = \frac{1}{2ih^2}\left\{\frac{\partial(h^2 U)}{\partial \xi} - \frac{\partial(h^2 V)}{\partial \zeta}\right\}.$$

Thus $(1 - \sigma)\Delta + i(1 - 2\sigma)\omega = \frac{1}{2h^2}\left\{p\frac{\partial(h^2 U)}{\partial \xi} + \frac{\partial(h^2 V)}{\partial \zeta}\right\} = f(\xi)$

and $(1 - \sigma)\Delta - i(1 - 2\sigma)\omega = \frac{1}{2h^2}\left\{\frac{\partial(h^2 U)}{\partial \xi} + p\frac{\partial(h^2 V)}{\partial \zeta}\right\} = f(\zeta).$

where f is any function and $p = 3 - 4\sigma$ (a constant)

Therefore,

$$(p^2 - 1)\frac{\partial(h^2 U)}{\partial \xi} = 2h^2\{pf(\xi) - f(\zeta)\} \quad .. \quad .. \quad .. \quad .. \quad .. \quad (21)$$

$$(p^2 - 1)\frac{\partial(h^2 V)}{\partial \zeta} = 2h^2\{pf(\zeta) - f(\xi)\} \quad .. \quad .. \quad .. \quad .. \quad .. \quad (22)$$

and

$$\Delta = \{2/(1 + p)\}\{f(\xi) + f(\zeta)\}. \quad .. \quad .. \quad .. \quad .. \quad (23)$$

Moreover

$$e_{\alpha\alpha} - e_{\beta\beta} = \frac{\partial u}{\partial \alpha} - \frac{\partial v}{\partial \beta} = \frac{\partial V}{\partial \xi} + \frac{\partial U}{\partial \zeta} \quad .. \quad .. \quad .. \quad .. \quad .. \quad (24)$$

and

$$e_{\alpha\beta} = \frac{\partial v}{\partial \alpha} + \frac{\partial u}{\partial \beta} = i\left(\frac{\partial V}{\partial \xi} - \frac{\partial U}{\partial \zeta}\right) \quad .. \quad .. \quad .. \quad .. \quad .. \quad (25)$$

so that

$$e_{\alpha\alpha} - e_{\beta\beta} \pm ie_{\alpha\beta} = 2\frac{\partial U}{\partial \zeta} \text{ or } 2\frac{\partial V}{\partial \xi}. \quad .. \quad .. \quad .. \quad .. \quad .. \quad .. \quad (26)$$

For the stress values, we have

$$\bar{\alpha}\bar{\alpha} + \bar{\beta}\bar{\beta} = E\Delta/(1+\sigma)(1-2\sigma) = \{E/2(1-\sigma^2)(1-2\sigma)\}\{f(\xi) + f(\zeta)\} \quad (27)$$

$$\text{and } \bar{\alpha}\bar{\alpha} - \bar{\beta}\bar{\beta} - 2i\bar{\alpha}\bar{\beta} = \{E/(1+\sigma)\}(e_{\alpha\alpha} - e_{\beta\beta} \pm ie_{\alpha\beta})$$

$$= \frac{2E}{1+\sigma}\frac{\partial U}{\partial \zeta} \text{ and } \frac{2E}{1+\sigma}\frac{\partial V}{\partial \xi} \text{ respectively.} \quad .. \quad .. \quad .. \quad (28)$$

If the co-ordinate system be defined by $x + iy = \phi(\xi)$, so that $h^2 = \phi'(\xi)\phi'(\zeta)$ (Section II.3), write $f(\xi) = F'(\xi)/\phi'(\xi)$. Then from equation (21)

$$\frac{\partial(h^2U)}{\partial \xi} = \frac{2}{p^2-1}\{p\phi'(\zeta)F'(\xi) - \phi'(\xi)F'(\zeta)\},$$

and

$$h^2U = \frac{2}{p^2-1}\{p\phi'(\zeta)F(\xi) - \phi(\xi)F'(\zeta) + \psi(\zeta)\} \text{ where } \psi \text{ is any function,}$$

and

$$U = \frac{2}{p^2-1}\left\{p\frac{F(\xi)}{\phi'(\xi)} - \frac{\phi(\xi)F'(\zeta)}{\phi'(\xi)\phi'(\zeta)} + \frac{\psi(\zeta)}{\phi'(\xi)\phi'(\zeta)}\right\}^* \quad .. \quad .. \quad (29)$$

Hence finally,

$$\bar{\alpha}\bar{\alpha} + \bar{\beta}\bar{\beta} = \frac{E}{2(1-\sigma^2)(1-2\sigma)}\left\{\frac{F'(\xi)}{\phi'(\xi)} + \frac{F'(\zeta)}{\phi'(\zeta)}\right\}, \quad .. \quad .. \quad .. \quad (30)$$

and using equation (28),

$$\bar{\alpha}\bar{\alpha} - \bar{\beta}\bar{\beta} + 2i\bar{\alpha}\bar{\beta} = \frac{E}{2(1-\sigma^2)(1-2\sigma)}\left[-\frac{\phi(\xi)}{\phi'(\xi)}\frac{\partial}{\partial \zeta}\left\{\frac{F'(\zeta)}{\phi'(\zeta)}\right\} + \frac{1}{\phi'(\xi)}\frac{\partial}{\partial \zeta}\left\{\frac{\psi(\zeta)}{\phi'(\zeta)}\right\}\right].$$

$$.. \quad .. \quad .. \quad (31)$$

Since F and ψ are entirely arbitrary, these expressions may be expressed in the simpler forms:

$$\bar{\alpha}\bar{\alpha} + \bar{\beta}\bar{\beta} = G(\xi) + G(\zeta) \quad .. \quad .. \quad .. \quad .. \quad .. \quad .. \quad (30a)$$

and

$$\bar{\alpha}\bar{\alpha} - \bar{\beta}\bar{\beta} + 2i\bar{\alpha}\bar{\beta} = \{-\phi(\xi)G'(\zeta) + H(\zeta)\}/\phi'(\xi), \quad .. \quad .. \quad .. \quad .. \quad (31a)$$

but the forms given by (30) and (31) are better adapted to our present purpose.

We note that $\bar{\alpha}\bar{\alpha} + i\bar{\alpha}\bar{\beta}$ is proportional to

$$F'(\xi) + \frac{F'(\zeta)\phi'(\xi)}{\phi'(\zeta)} - \phi(\xi)\frac{\partial}{\partial \zeta}\left\{\frac{F'(\zeta)}{\phi'(\zeta)}\right\} + \frac{\partial}{\partial \zeta}\left\{\frac{\psi(\zeta)}{\phi'(\zeta)}\right\}. \quad .. \quad .. \quad (32)$$

* Expressions for u_α and u_β may easily be written down, but they are needed only in problems involving specified displacements.

(b) *Solutions Appropriate to Epicyclic Contours.*—We have $\phi(\xi) = \sum_r \lambda_r e^{-r\xi}$, where r takes the values defined in Section II.3, that is $\lambda_{-1} = 1$ and $\lambda_{-r}\,(r > 1) = 0$, and we take

$$\left.\begin{aligned} \frac{E}{2(1-\sigma^2)(1-2\sigma)}\,F'(\xi) &= \sum_n (A_n + iC_n)e^{-n\xi} \\ \frac{E}{2(1-\sigma^2)(1-2\sigma)}\,F'(\zeta) &= \sum_n (A_n - iC_n)e^{-n\zeta}\,* \\ \frac{E}{2(1-\sigma^2)(1-2\sigma)}\,\psi(\zeta) &= \sum_n (B_n + iD_n)e^{-(n-1)\zeta} \end{aligned}\right\}$$ where n may take all integral values both positive and negative,

λ, A, B, C and D being all real numerical constants.

(c) *Stresses at Infinity.*—As $\alpha \to \infty$, $\bar{\alpha}\bar{\alpha} + \bar{\beta}\bar{\beta} \to 2A_{-1} + e^{\alpha}$ (terms in A_{-2}, A_{-3}, etc.). Since the stresses are to remain finite at infinity we take A_{-2}, etc., zero. For the same reason we take B_{-2}, D_{-2}, etc., zero, when as $\alpha \to \infty$,

$$\bar{\alpha}\bar{\alpha} - \bar{\beta}\bar{\beta} + 2\bar{\alpha}\bar{\beta} \to (B_{-1} + iD_{-1})e^{(\zeta-\xi)} = (B_{-1} + iD_{-1})e^{-2i\beta}\,.$$

But, as $\alpha \to \infty$,

$$\left.\begin{aligned} \bar{\alpha}\bar{\alpha} &\to f' \cos^2\beta + f \sin^2\beta + 2q \sin\beta\cos\beta \\ \bar{\beta}\bar{\beta} &\to f' \sin^2\beta + f \cos^2\beta - 2q \sin\beta\cos\beta \\ \bar{\alpha}\bar{\beta} &\to (f'-f)\sin\beta\cos\beta + q(\cos^2\beta - \sin^2\beta) \end{aligned}\right\}$$ where f', f and q are the values of $\bar{x}\bar{x}$, $\bar{y}\bar{y}$ and $\bar{x}\bar{y}$ respectively, at infinity.

or $\bar{\alpha}\bar{\alpha} + \bar{\beta}\bar{\beta} \to f + f'$

and $\bar{\alpha}\bar{\alpha} - \bar{\beta}\bar{\beta} + 2i\bar{\alpha}\bar{\beta} \to \{(f' - f) + 2iq\}(\cos 2\beta - i \sin 2\beta)$.

Hence $A_{-1} = \frac{1}{2}(f + f')$, $B_{-1} = f' - f$ and $D_{-1} = 2q$.

(d) *Stresses at the Edge of the Hole* ($\alpha = 0$).—It is required to render both $\bar{\alpha}\bar{\alpha}$ and $\bar{\alpha}\bar{\beta}$ identically zero over the contour $\alpha = 0$; this is done most conveniently by rendering $\bar{\alpha}\bar{\alpha} + i\bar{\alpha}\bar{\beta}$ identically zero. At $\alpha = 0$, $\xi = -\zeta = i\beta$, and it is convenient to write $i\beta = \theta$.

Then, omitting signs of summation with respect to n, $\bar{\alpha}\bar{\alpha} + i\bar{\alpha}\bar{\beta}$ at $\alpha = 0$ is proportional to

$$(A_n + iC_n)e^{-n\theta} + (A_n - iC_n)\,e^{n\theta}\frac{\Sigma r\lambda_r e^{-r\theta}}{\Sigma r\lambda_r e^{r\theta}} - \Sigma\lambda_r e^{-r\theta}\frac{d}{d\theta}\left\{\frac{(A_n - iC_n)e^{n\theta}}{\Sigma r\lambda_r e^{r\theta}}\right\}$$
$$+ \frac{d}{d\theta}\left\{\frac{(B_n + iD_n)e^{(n-1)\theta}}{\Sigma r\lambda_r e_r^{\theta}}\right\},$$

or

$$-\frac{1}{n}(A_n + iC_n)\frac{de^{-n\theta}}{d\theta} - (A_n - iC_n)\frac{d}{d\theta}\left\{\frac{e^{n\theta}\,\Sigma\lambda_r e^{-r\theta}}{\Sigma r\lambda_r e^{r\theta}}\right\} + (B_n + iD_n)\frac{d}{d\theta}\left\{\frac{e^{(n-1)\theta}}{\Sigma r\lambda_r e^{r\theta}}\right\}.$$

Therefore, we have to make

$$\sum_n \left[\frac{1}{n}(A_n + iC_n)e^{-n\theta}\,\Sigma r\lambda_r e^{r\theta} + (A_n - iC_n)e^{n\theta}\,\Sigma\lambda_r e^{-r\theta} - (B_n + iD_n)e^{(n-1)\theta}\right]$$

identically zero.†

* When ξ is changed to ζ the sign of C_n must be changed, so that $F'(\xi) + F'(\zeta)$ shall be entirely real.

† Or strictly a multiple of $\Sigma r\lambda_r e_{r\theta}$.

Obviously the AB and CD solutions are entirely separate. Equating to zero the coefficients of $e^{s\theta}$, we have:

$$B_{s+1} = \sum_r \left(\frac{r}{r-s} \lambda_r A_{r-s} + \lambda_r A_{r+s} \right)$$

$$D_{s+1} = \sum_r \left(\frac{r}{r-s} \lambda_r C_{r-s} - \lambda_r C_{r+s} \right)$$

but the structure of these relations is better shown in tabular form below. In this table (Table 2*) the individual equations are represented in vertical columns; the B coefficients, each of which enters into one equation only are shown in the second row, whilst the coefficients of each individual A in the separate equations are shown in the succeeding rows, λ_{-1} has been taken equal to unity as before.

TABLE 2

Relations between A and B coefficients

$e^{-10\theta}$	$e^{-8\theta}$	$e^{-6\theta}$	$e^{-4\theta}$	$e^{-2\theta}$	1	$e^{2\theta}$	$e^{4\theta}$	$e^{6\theta}$	$e^{8\theta}$	$e^{10\theta}$	
				$-B_{-1}$	$-B_1$	$-B_3$	$-B_5$	$-B_7$	$-B_9$	$-B_{11}$	
λ_9	λ_7	λ_5	λ_3	λ_1	1						A_{-1}
					1	$-\lambda_1$	$-3\lambda_3$	$-5\lambda_5$	$-7\lambda_7$	$-9\lambda_9$	
λ_{11}	λ_9	λ_7	λ_5	λ_3	λ_1	1					A_1
				-1	λ_1	$3\lambda_3$	$5\lambda_5$	$7\lambda_7$	$9\lambda_9$	$11\lambda_{11}$	
λ_{13}	λ_{11}	λ_9	λ_7	λ_5	λ_3	λ_1	1				A_3
			$-1/3$	$1/3\,\lambda_1$	λ_3	$5/3\,\lambda_5$	$7/3\,\lambda_7$	$9/3\,\lambda_9$	$11/3\,\lambda_{11}$	$13/3\,\lambda_{13}$	
λ_{15}	λ_{13}	λ_{11}	λ_9	λ_7	λ_5	λ_3	λ_1	1			A_5
		$-1/5$	$1/5\,\lambda_1$	$3/5\,\lambda_3$	λ_5	$7/5\,\lambda_7$	$9/5\,\lambda_9$	$11/5\,\lambda_{11}$	$13/5\,\lambda_{13}$	$15/5\,\lambda_{15}$	
λ_{17}	λ_{15}	λ_{13}	λ_{11}	λ_9	λ_7	λ_5	λ_3	λ_1	1		A_7
	$-1/7$	$1/7\,\lambda_1$	$3/7\,\lambda_3$	$5/7\,\lambda_5$	λ_7	$9/7\,\lambda_9$	$11/7\,\lambda_{11}$	$13/7\,\lambda_{13}$	$15/7\,\lambda_{15}$	$17/7\,\lambda_{17}$	
λ_{19}	λ_{17}	λ_{15}	λ_{13}	λ_{11}	λ_9	λ_7	λ_5	λ_3	λ_1	1	A_9
$-1/9$	$1/9\,\lambda_1$	$3/9\,\lambda_3$	$5/9\,\lambda_5$	$7/9\,\lambda_7$	λ_9	$11/9\,\lambda_{11}$	$13/9\,\lambda_{13}$	$15/9\,\lambda_{15}$	$17/9\,\lambda_{17}$	$19/9\,\lambda_{19}$	

The table for the CD solution is similar, except that the first row of coefficients for each A becomes negative. As a result the coefficients of all the C's in the centre column became zero, and D_1 is therefore always zero.

If λ_{2s-1} is the highest order λ to be included, the negative powers of e^{θ} give s relations between the s unknowns A_1 to A_{2s-1} and the two known coefficients A_{-1} and B_{-1}; the remaining $s+1$ equations give the values of the $s+1$ unknowns B_1 to B_{2s+1}, and it will be noticed that $B_{2s+1} = 0$ in all cases. Table 2*a* indicates the limits of the table when $s = 5$.

* This table and the greater part of the subsequent discussion is restricted to λ's of odd orders; it will be seen that the inclusion of λ's of even order necessitates the insertion in Table 2 of rows and columns in between those shown, but from the structure of the table it is clear that if the λ's of even order be omitted, the AB coefficients of even order also disappear. On the other hand, if λ's of even order *only* are included, the AB coefficients of odd order, do *not* disappear. This is due to the coefficient -1 for A_1 in the column headed $e^{-2\theta}$, since this column includes the coefficient $B_{-1}(=f'-f)$, A_1 can never be identically zero.

TABLE 2a

Relations between A and B coefficients

$e^{-10\theta}$	$e^{-8\theta}$	$e^{-6\theta}$	$e^{-4\theta}$	$e^{-2\theta}$	1	$e^{2\theta}$	$e^{4\theta}$	$e^{6\theta}$	$e^{8\theta}$	$e^{10\theta}$	
				$-B_{-1}$	$-B_1$	$-B_3$	$-B_5$	$-B_7$	$-B_9$	$-B_{11}$	
λ_9	λ_7	λ_5	λ_3	λ_1	1 1	 $-\lambda_1$	 $-3\lambda_3$	 $-5\lambda_5$	 $-7\lambda_7$	 $-9\lambda_9$	A_{-1}
	λ_9	λ_7	λ_5	λ_3 -1	λ_1 λ_1	1 $3\lambda_3$	 $5\lambda_5$	 $7\lambda_7$	 $9\lambda_9$		A_1
		λ_9	λ_7 $-1/3$	λ_5 $1/3\,\lambda_1$	λ_3 λ_3	λ_1 $5/3\,\lambda_5$	1 $7/3\,\lambda_7$	 $9/3\,\lambda_9$			A_3
		 $-1/5$	λ_9 $1/5\,\lambda_1$	λ_7 $3/5\,\lambda_3$	λ_5 λ_5	λ_3 $7/5\,\lambda_5$	λ_1 $9/5\,\lambda_5$	1			A_5
	 $-1/7$	 $1/7\,\lambda_1$	 $3/7\,\lambda_3$	λ_9 $5/7\,\lambda_5$	λ_7 λ_7	λ_5 $9/7\,\lambda_9$	λ_3	λ_1	1		A_7
 $-1/9$	 $1/9\,\lambda_1$	 $3/9\,\lambda_3$	 $5/9\,\lambda_5$	 $7/9\,\lambda_7$	λ_9 λ_9	λ_7	λ_5	λ_3	λ_1	1	A_9

The determination of the values of the A's and B's (or C's and D's) for any given set of numerical values of the λ's is straightforward, and in Tables 3 and 4 below the values are given in terms of A_{-1} and A_1 for λ's up to λ_5; but if higher order λ's are included, this general solution becomes very cumbersome. However, if all the λ's of order higher than λ_1 and up to a certain higher order (λ_{2n-1}, say) are equal to ε, where ε is small, an approximate solution is possible. On the other hand, if only one of the higher order λ's is different from zero, the exact solution is easy. These special solutions are described below.

TABLE 3

*Relations between the A and B coefficients for λ's up to λ_5**

	A_{-1}	A_1
A_5	$5\lambda_5$	
A_3	$3(\lambda_3+\lambda_1\lambda_5)$	$3\lambda_5$
B_{-1}	$\lambda_1+\lambda_1\lambda_3+3\lambda_1\lambda_5^2+6\lambda_3\lambda_5+\lambda_1^2\lambda_5$	$-1+\lambda_3+\lambda_1\lambda_5+3\lambda_5^2$
B_1	$2+6\lambda_3^2+10\lambda_5^2+6\lambda_1\lambda_3\lambda_5$	$2\lambda_1+6\lambda_3\lambda_5$
B_3	$-\lambda_1+3\lambda_1\lambda_3+5\lambda_1\lambda_5^2+10\lambda_3\lambda_5+3\lambda_1^2\lambda_5$	$1+3\lambda_3+3\lambda_1\lambda_5+5\lambda_5^2$
B_5	$8\lambda_1\lambda_5$	$8\lambda_5$

* Note : When only λ_1 differs from zero, the AB coefficients correspond with those in Inglis' solution with the following substitutions :—

Present Solution :	λ_1	A_{-1}	A_1	B_{-1}	B_1	B_3
Inglis' Solution :	$e^{-2\alpha_0}$	A_{-1}	$A_1 e^{-2\alpha_0}$	$-B_{-3}$	$-B_{-1}e^{-2\alpha_0}$	$-B_1 e^{-4\alpha_0}$.

TABLE 4

Relations between the C and D coefficients for λ's up to λ_5

	C_{-1}	C_1
C_5	$-5\lambda_5$	
C_3	$-3(\lambda_3+\lambda_1\lambda_5)$	$-3\lambda_5$
D_{-1}	$-\lambda_1-\lambda_1\lambda_3+3\lambda_1\lambda_5^2-\lambda_1^2\lambda_5$	$-1-\lambda_3-\lambda_1\lambda_5+3\lambda_5^2$
D_3	$-\lambda_1+3\lambda_1\lambda_3-5\lambda_1\lambda_5^2+3\lambda_1^2\lambda_5$	$-1+3\lambda_3+3\lambda_1\lambda_5-5\lambda_5^2$
D_5	$8\lambda_1\lambda_5$	$8\lambda_5$

(e) *Stress Concentration Factors.*—For the value of the stress $\bar{\beta}\bar{\beta}$ at the edge of the hole, we have

$$\bar{\beta}\bar{\beta} = \bar{\alpha}\bar{\alpha} + \bar{\beta}\bar{\beta} \text{ (since } \bar{\alpha}\bar{\alpha} = 0) = \frac{\sum_n A_n e^{-ni\beta}}{-\sum_r r\lambda_r e^{-ri\beta}} + \frac{\sum_n A_n e^{ni\beta}}{-\sum_r r\lambda_r e^{ri\beta}}.$$

The value of $\bar{\beta}\bar{\beta}$ at $\beta = 0$ is then $-2\sum_n A_n / \sum_r r\lambda_r$.

Example. If only λ_1 is different from zero

$$A_1 = \lambda_1 A_{-1} - B_{-1} \text{ (from Table 3),}$$

and

$$\sum_n A_n = A_{-1} + A_1 = (1 + \lambda_1)A_{-1} - B_{-1} = \tfrac{1}{2}(1 + \lambda_1)(f + f') - (f' - f)$$
$$= \tfrac{1}{2}(3 + \lambda_1)f + \tfrac{1}{2}(\lambda_1 - 1)f'$$

and

$$\sum_r r\lambda_r = -1 + \lambda_1.$$

Therefore

$$\bar{\beta}\bar{\beta}_{\beta=0} = \{(3 + \lambda_1)/(1 + \lambda_1)\}f - f' = \{1 + 2(a/b)\}f - f' \text{ or } \{1 + 2(a/\varrho)^{1/2}\}f - f'$$ where $2a$ and $2b$ are the lengths of the major and minor axes of the ellipse, so that

$$a/b = (1 + \lambda_1)/(1 - \lambda_1) = (a/\varrho)^{1/2} \text{ (}see\text{ Section II.3).}$$

For any given set of λ's the values of $\bar{\beta}\bar{\beta}$ at $\alpha = 0$ and $\beta = 0$ may easily be found, and the value at other values of β can be calculated without much difficulty; to calculate the values of the stresses at values of α different from zero (away from the contour of the hole) is considerably more difficult.

II.8. *Stresses round Special Types of Hole.*—(a) *Simple Polygonal Holes.*—(i) *Geometry of Hole.*—The transformation $x + iy = e^{\xi} + \lambda_r e^{-r\xi}$ represents a series of polygonal holes with $r + 1$ sides (including the ellipse as a special case, when $r = 1$). The maximum and minimum radii are $1 \pm \lambda_r$ and the corresponding radii of curvature are respectively $(1 - r\lambda_r)^2/(1 + r^2\lambda_r)$ and $(1 + r\lambda_r)^2/(1 - r^2\lambda_r)$ (Section II.3).

(ii) *Stress Concentration under Shear Parallel to Axis of Hole.*—The stress concentration factor at $\beta = 0$ under shear along the axis of the hole parallel to the plane $\beta = 0$ is (Section II.6),

$$\mu_q = \frac{2}{1 - r\lambda_r}.$$

Using the relation $(1 + \lambda_r)(1 + r^2\lambda_r)/(1 - r\lambda_r)^2 = a/\varrho$ to eliminate λ_r, we find

$$\mu_q = 1 + \{1/(r + 1)\}\{4r(a/\varrho) + (r - 1)^2\}^{1/2}$$
$$= 1 + [1 + 4r\{(a/\varrho) - 1\}/(r + 1)^2]^{1/2}.$$

If $r = 1$, $\mu_q = 1 + (a/\varrho)^{1/2}$ as previously for the ellipse.

In general, as $r \to \infty$, $\mu_q \to 2$ independently of a/ϱ so long as a/ϱ remains finite. In the special case where $\lambda_r = 1/r^2$, $a/\varrho = 2(1 + r^2)/(r - 1)^2$ and the other principal radius of curvature is infinite, so that the hole consists of a polygon with nearly flat sides and rounded corners; in this case $\mu_q = 2r/(r - 1)$ or $1 + \{(a/\varrho) - 1\}^{1/2}$. As $r \to \infty$, $\mu_q \to 2$, whereas $a/\varrho \to 2$ so that $1 + (a/\varrho)^{1/2} \to 1 + \sqrt{2}$. In this case, therefore, the approximate formula for μ_q overestimates its value by 20 per cent. Comparison of μ_q and $1 + (a/\varrho)^{1/2}$ for other shapes of flat-sided holes is afforded in Table 5 below. The error of the approximate formula in other more general cases is illustrated in Fig. 10. In this figure the dotted line connects the series of flat-sided holes (for which $\lambda_r = 1/r^2$); to the left of this dotted line the contours of the holes are rounded, to the right they are re-entrant.

(iii) *Stress Concentration under Direct Stress across Hole.*—The stress concentration factor at $\beta = 0$ under direct stress (f) across the plane $\beta = 0$ is $2 \sum_n A_n/(1 - r\lambda_r)$, where $A_{-1} = f/2$, $B_{-1} = -f$ and the remaining A's have to be found from Table 2. From this table, it is clear that, if r be odd, $A_r = r\lambda_r A_{-1}$, $A_{r-2} = (r - 2)\lambda_1 A_1$, $\lambda_r A_{r-2} - A_1 = B_{-1}$ and all the other A's are zero. The stress concentration factor is then

$$\mu_f = \left\{ 1 + r\lambda_r + 2\,\frac{1 + (r - 2)\lambda_r}{1 - (r - 2)\lambda_r^2} \right\} \Big/ (1 - r\lambda_r) .$$

In this case elimination of λ_r does not lead to a simple expression for μ_f; but when $\lambda_r = 1/r^2$,

$$\mu_f = \left\{ r + 1 + \frac{2r^3(r^2 + r - 2)}{r^4 - r + 2} \right\} \Big/ (r - 1) \text{ and, as } r \to \infty,\ \mu_f \to 3,$$

whereas $1 + 2(a/\varrho)^{1/2} \to 1 + 2\sqrt{2}$. Values of μ_f for the range of flat-sided polygonal holes are given in Table 5, together with the corresponding values of $1 + 2(a/\varrho)^{1/2}$.

The values of μ_f for the whole class of simple polygonal holes are shown in Fig. 11; this figure is to be compared with Fig. 10. The dotted line in the lower part of the diagram again marks the division between rounded and re-entrant contours; the sketch in Fig. 11 illustrates a typical example of the latter type, of which an enlarged view is given in Fig. 12.

Comparison of Figs. 10 and 11 affords a good indication of the relative importance of the form of the hole in relation to the approximate formulae $1 + (a/\varrho)^{1/2}$ for shear and $1 + 2(a/\varrho)^{1/2}$ for direct stress. When r is large a good approximation to μ_f is afforded by the formula

$$3\{r + (a/\varrho)\}/\{r - (a/\varrho)\} .$$

TABLE 5

Values of μ_f and μ_q for flat-sided polygonal holes

Description of Hole	Square	Hexagon	Octagon	Decagon	Dodecagon	—
Value of r	3	5	7	9	11	∞
Value of μ_f	5·375	4·314	3·910	3·697	3·564	3
$1 + 2\sqrt{\frac{a}{\varrho}}$	5·472	4·608	4·333	4·201	4·124	3·828
Value of μ_q	3·000	2·500	2·333	2·250	2·200	2
$1 + \sqrt{\frac{a}{\varrho}}$	3·236	2·804	2·667	2·600	2·562	2·414

(b) *Deep Grooves.*—A class of hole which illustrates still more clearly the relative importance of curvature and general form is that defined by the three coefficients λ_1, λ_3 and λ_5 under the conditions:

$$1 - \lambda_1 + 9\lambda_3 - 25\lambda_5 = 0$$
$$1 + \lambda_1 + \lambda_3 + \lambda_5 \quad = K(1 - \lambda_1 + \lambda_3 - \lambda_5) ,$$

where K is a constant.

The former condition provides that the curvature at $\beta = \pi/2$ shall be zero, the latter that the ratio of the depth of the hole a to its width b shall be K. If K is fairly large, the (half) hole takes the form of a deep narrow groove, with a radius of curvature at its end, ϱ, defined by:

$$\frac{a}{\varrho} = (1 + \lambda_1 + \lambda_3 + \lambda_5)(1 + \lambda_1 + 9\lambda_3 + 25\lambda_5)/(1 - \lambda_1 - 3\lambda_3 - 5\lambda_5)^2 .$$

By assigning suitable values to λ_1 and by using the two conditions to determine λ_3 and λ_5, a series of grooves with almost parallel sides is defined, for which the ratio a/b $(= K)$ is constant, but in which the ratio a/ϱ can be varied at will. A series of such grooves, corresponding to $K = 10$ is shown in Fig. 13, and the stress concentration factors μ_q and μ_f for these grooves are plotted in Fig. 14, where the values are compared with the values $1 + (a/\varrho)^{1/2}$ and $1 + 2(a/\varrho)^{1/2}$ appropriate to true elliptical holes.

It will be seen that under direct stress the approximate formula $\mu_f = 1 + 2(a/\varrho)^{1/2}$ affords a very close estimate of the true maximum stress, but that in shear the approximate formula $1 + (a/\varrho)^{1/2}$ is far from accurate. In fact, up to a value of $(a/\varrho)^{1/2}$ of about 10, the true value of μ_q is approximately midway between the values $1 + (a/\varrho)^{1/2}$ and $1 + (a/b)$ $(= 11$ in this case).

(c) *Square Holes.*—Any square hole with rounded corners may be represented to any desired accuracy by the following means. Using the transformation of Section II.3 (b), we have

$$x = \lambda_{-1} \cos\beta + \lambda_3 \cos 3\beta + \lambda_7 \cos 7\beta + \lambda_{11} \cos 11\beta + \ldots$$
$$y = \lambda_{-1} \sin\beta - \lambda_3 \sin 3\beta - \lambda_7 \sin 7\beta - \lambda_{11} \sin 11\beta - \ldots$$

and the perpendicular distance of a point on this curve from the line $x + y = 1$ is

$$\lambda_{-1}(\cos\beta + \sin\beta) + \lambda_3(\cos 3\beta - \sin 3\beta) + \ldots - 1 .$$

Squaring this perpendicular distance, integrating from 0 to $\pi/2$ and then differentiating with respect to λ_{-1}, λ_3, etc., in succession and equating to zero, the conditions are found that the curve $x + iy = \Sigma \lambda_r e^{ri\beta}$ should conform as closely as possible to the line $x + y = 1$. These conditions are sufficient to define the values of all the λ's up to the highest order λ included, so that the radius of curvature at $x = 0$* is also determined. In order to make the radius of curvature at $x = 0$ take some assigned value, two ' best fitting ' sets of λ's are taken, the first set including λ's up to λ_{4r-1}, the second including one more λ, namely λ_{4r+3}. From these two sets a new set is formed by taking the sum of an arbitrary proportion X of the first and a proportion $(1 - X)$ of the second. The expression for the radius of curvature ϱ then takes the form $\varrho = (A + BX)^2/(C + DX)$, where A, B, C and D are known constants. Given the value of ϱ (or more conveniently of a/ϱ) the appropriate value of X and the composite set of λ's corresponding to this value of X may thus be found; this composite set of λ's represents the best possible approach using λ's up to λ_{4r+3} to a square hole with corners rounded to a specified radius. A similar procedure is obviously applicable to any regular polygonal hole; but for irregular polygons the appropriate limits of integration for β have to be found by trial and error.

The numerical work has been carried out for a set of λ's up to λ_{19}. The contours of one quadrant of the holes thus defined are shown in Fig. 15. The approach to a straight line boundary is in general so good that in the complete diagram, Fig. 15a, only the worse case, corresponding to

* Or $y = 0$, the two radii in this case are, of course, identical.

a value of $a/\varrho = 0$ at $\beta = 0$, is shown. In the diagram Fig. 15b, the detail of the contours near the corner of the square is shown for values of a/ϱ from 0 to 144 to a scale 10 times larger than that of Fig. 15a. For values of $(a/\varrho)^{1/2}$ greater than 5, the approximation afforded to the prescribed form of the hole appears quite sufficiently close. For low values of a/ϱ, the method is really inappropriate, because it seeks to make the contour follow the line $x + y = 1$ well into the corner of the hole; as a result at low values of a/ϱ, the maximum curvature of the contour occurs away from the actual corner (*see* Fig. 15b). For values of $(a/\varrho)^{1/2}$ less than 5, a better representation is afforded by the simple polygonal hole discussed in Section (a) above; this representation is most accurate at $(a/\varrho)^{1/2} = 2{\cdot}236$, for then the contour is flat at $\beta = \pi/4$.

Calculated values of μ_f and μ_q for this range of square holes with rounded corners are shown plotted against values of $(a/\varrho)^{1/2}$ in Fig. 16. Although continuous curves over the whole range of $(a/\varrho)^{1/2}$ down to zero are shown, it must be remembered that these values represent the stresses at $\beta = 0$ in the contours shown in Fig. 15b. In Fig. 16, the values of μ_f and μ_q for simple polygonal holes are also shown, and for values of $(a/\varrho)^{1/2}$ less than 5, these curves represent a better approximation to the practical case of a square hole with rounded corners; the two asterisks in Fig. 16 mark the values of μ_f and μ_q for a simple square hole with flat sides ($\varrho = \infty$ at $\beta = \pi/4$). For comparison the curve of μ_q against $(a/\varrho)^{1/2}$ derived by the method of Section II.6(c) is also reproduced in Fig. 16 (from Fig. 9). The discrepancy between these values of μ_q and those now found appears surprisingly large; but the range (around $(a/\varrho)^{1/2} = 2$ to 3) over which comparison may fairly be made is too short to permit close analysis.

Although the contours of Fig. 15b for values of $(a/\varrho)^{1/2}$ less than 5 are not of much practical interest, they do provide a good illustration of a class of hole for which the approximate formulae $1 + (a/\varrho)^{1/2}$ and $1 + 2(a/\varrho)^{1/2}$ are very inaccurate. The true stress concentrations are at least as great as those shown in Fig. 16, for still greater stresses may be set up near the points of maximum curvature; this is, of course, a result of the general shape of the contour, which differs so radically from an ellipse.

II.9. *Hair Cracks.*—(a) *Stress Concentration in Shear.*—For a given form of hole or groove, $a = 1 + \Sigma\lambda_r$, $\varrho = (1 - \Sigma r\lambda_r)^2/(1 + \Sigma r^2\lambda_r)$ and $\mu_q = 2/(1 - \Sigma r\lambda_r)$. The radius of curvature ϱ' at the end of a hair crack, defined by n and d, at the root of this groove is (Section II.4) $(1 - \Sigma r\lambda_r - dn)^2/\{1 + \Sigma r^2\lambda_r + (d/3)(4n^2 - 1)\}$ and the new stress concentration factor $\mu_q = 2/(1 - \Sigma r\lambda_r - dn)$. The 'order' n' of a hair crack having the same depth d and the same radius of curvature ϱ' at its root in a plain test piece* is defined by the equation $\varrho' = 3(2 - dn')^2/d(4n'^2 - 1)$; the stress concentration factor for this case is $\mu_0 = 2/(2 - dn')$. Since n and n' are assumed to be large, unity may be neglected in comparison with either $4n^2$ or $4n'^2$. With this approximation it may be shown that the apparent stress concentration factor

$$\mu_{qa}\left(=\frac{\mu_q'}{\mu_0}\right) = \frac{(\mu_0 - 2)\mu_q}{[\{(\mu_0 - 1)^2 + (3d/4\varrho)\mu_0(\mu_0 - 2)\}^{1/2} - 1]}$$

or approximately, if μ_0 be large, $\mu_{qa} = \mu_q/\{1 + (3d/4\varrho)\}^{1/2}$, and if $(d/\varrho) \to 0$, $\mu_{qa} \to \mu_q$.

For a semi-elliptical groove, $\mu_{qa} = \{1 + (a/\varrho)^{1/2}\}/\{1 + (3d/4\varrho)\}^{1/2}$. The maximum value of this approximate expression for μ_{qa} for variation of ϱ when the values of d and a are specified occurs when $\varrho = 9d^2/16a$ and is $(\mu_{qa})_{\max} = \{1 + (4a/3d)\}^{1/2}$. Values of μ_{qa} for values of $(a/\varrho)^{1/2}$ down to 5 and for values of d/a from $0{\cdot}05$ to $0{\cdot}40$ are shown in Fig. 17.

(b) *Stress Concentration under Direct Stress.*—The determination of the stress concentration due to a complex hole or groove is very much more complicated in the case of direct stress than in the case of shear. Accordingly in the case of direct stress consideration is restricted to grooves of elliptical form; previous examples (Section II.8(b) and (c)) suggest that under direct stress, the stress concentrations due to holes far from elliptical in form do not differ much from the

* The surface of a plane test piece is represented by putting $\lambda_1 = -1$, giving an infinitely long narrow ellipse with its major axis lying along $\beta = \pi/2$.

concentrations due to the equivalent ellipses. In what follows λ_{-1} is taken as unity (as previously), λ is written for λ_1 and all the other λ's of odd orders up to λ_{2n-1} are put equal to $\varepsilon = d/n$ (Section II.4).

By inspection of Table 2, it will be seen that A_{2n-1} is equal to $(2n-1)\varepsilon A_{-1}$. Since $\varepsilon = d/n$ is of the order $1/n^2$ (nd being comparable with unity), A_{2n-1} is of the order $(1/n)A_{-1}$. The contribution of each of the A terms, when they are multiplied by ε, is thus of the order $(1/n^3)A_{-1}$, and the sum of n such terms is of the order $(1/n^2)A_{-1}$, which is negligible in comparison with A_{-1}. Accordingly Table 2 may be rewritten.

TABLE 6

					B_{-1}	
. . .	ε	ε	ε	ε	λ	A_{-1}
. . . .		ε	ε	ε	-1	A_1
				-1	λ	$\frac{1}{3}A_3$
			-1	λ		$\frac{1}{5}A_5$
		-1	λ			$\frac{1}{7}A_7$
	-1	λ				$\frac{1}{9}A_9$
. . . . .						

By adding λ times the first (left-hand) column to the second column, then adding λ times the new second column to the third, etc.

TABLE 7

					B_{-1}	
ε	$(1+\lambda)\varepsilon$	$(1+\lambda+\lambda^2)\varepsilon$	$\frac{1-\lambda^{n-2}}{1-\lambda}\varepsilon$	$\frac{1-\lambda^{n-1}}{1-\lambda}\varepsilon$	λ	A_{-1}
	ε	$(1+\lambda)\varepsilon$	$\frac{1-\lambda^{n-3}}{1-\lambda}\varepsilon$	$\frac{1-\lambda^{n-2}}{1-\lambda}\varepsilon$	-1	A_1
				-1	λ	$\frac{1}{3}A_3$
			-1			$\frac{1}{5}A_5$
. . . . .						
		-1				$\frac{1}{2n-5}A_{2n-5}$
	-1					$\frac{1}{2n-3}A_{2n-3}$
-1						$\frac{1}{2n-1}A_{2n-1}$

So that

$$A_{2n-2r+1} = (2n-2r+1)\varepsilon\{(1-\lambda^r)A_{-1} + (1-\lambda^{r-1})A_1\}/(1-\lambda)\,,$$

and

$$A_3 + A_5 + \ldots A_{2n-1} = \frac{\varepsilon}{1-\lambda}\left[\left\{n^2 - 1 + \frac{\lambda^n - 3\lambda^{n+1}}{(1-\lambda)^2}\right\}A_{-1} + \left\{(n-1)^2 + \frac{\lambda^{n-1} - 3\lambda^n}{(1-\lambda)^2}\right\}A_1 + \frac{(2\lambda-1)(1+\lambda)}{(1-\lambda)^2}(A_{-1}+A_1)\right].$$

Since λ is less than 1, we may neglect λ^n and neglecting also unity in comparison with n, $A_3 + A_5 + \ldots A_{2n-1}$ is approximately equal to

$$\varepsilon\{n^2 + (2\lambda - 1)(1 + \lambda)/(1 - \lambda)^2\}(A_{-1} + A_1)/(1 - \lambda) ,$$

so that approximately

$$A_{-1} + A_1 + A_3 + \ldots A_{2n-1} = \left[1 + \frac{nd}{1 - \lambda}\left\{1 + \frac{(2\lambda - 1)(1 + \lambda)}{n^2(1 - \lambda)^2}\right\}\right](A_{-1} + A_1) .$$

Moreover, $B_{-1} = \lambda A_{-1} - A_1 + 1/3\,\lambda A_3$, and $A_3 = 3\varepsilon(A_{-1} + A_1)/(1 - \lambda)$ approximately.

Thus, approximately

$$B_{-1} = \lambda\{1 + \varepsilon/(1 - \lambda)\}A_{-1} - \{1 - \lambda\varepsilon/(1 - \lambda)\}A_1 .$$

Provided λ does not approach unity, $1 - \lambda$ may be regarded as comparable with nd. The terms in ε are then of order $1/n^2$ and may be neglected. Hence $A_1 = \lambda A_{-1} - B_{-1}$ and

$$2(A_{-1} + A_1) = (\lambda - 1)f + (3 + \lambda)f' ,$$

as for the groove without the hair crack.

The term $(2\lambda - 1)(1 + \lambda)/n^2\,(1 - \lambda)^2$ in the expression for ΣA may be written $(2\lambda - 1)/n^2\varrho$, where $\varrho = (1 - \lambda)^2/(1 + \lambda)$ is the radius of curvature at the root of the elliptical groove (ignoring the hair crack). We are interested in cases for which ϱ is of the same order as d, so that this term may be regarded as of order $(2\lambda - 1)/n^2d$ or $(2\lambda - 1)/n(1 - \lambda)$. This term is of order higher than $1/n$ but unless λ be very nearly equal to unity, it may probably safely be neglected.

The stress concentration factor μ_f' (for the stress f) is then

$$\mu_f' = (3 + \lambda)\{1 + nd/(1 - \lambda)\}/(1 - \lambda - nd) .$$

If nd is zero, the value $\mu_f = (3 + \lambda)/(1 - \lambda)$ is that for the semi-elliptical groove alone, whilst if $\lambda < -1$, the factor

$$\mu_0 = (2 + n'd)/(2 - n'd)$$

is that for a hair crack of order n' and depth d in the surface of a plain test piece.

If the radius of curvature at the root of the hair crack is the same in the two cases,

$$\frac{(2 - n'd)^2}{(4/3)n'^2d^2} = \frac{(1 - \lambda - nd)^2}{\{1 + \lambda^2 + (4/3)n^2d\}d} = \frac{(1 - \lambda - nd)^2}{(1 - \lambda)^2\,(d/\varrho) + (4/3)n^2d^2} .$$

Eliminating λ and $n'd$ by use of the relations $1 - \lambda = 4/(\mu_f + 1)$ and $n'd = 2(\mu_0 - 1)/(\mu_0 + 1)$ and writing $nd/(1 - \lambda) = m$,

$$(1 - m)^2/\{(3d/4\varrho) + m^2\} = 4/(\mu_0 - 1)^2 \quad \text{and} \quad \mu_f'/\mu_f = (1 + m)/(1 - m) .$$

Then, by elimination of m ,

$$\frac{\mu_f'}{\mu_f} = \frac{\mu_0(\mu_0 - 2) - (3d/4\varrho)}{\{(\mu_0 - 1)^2 + (3d/4\varrho)(\mu_0 - 3)(\mu_0 + 1)\}^{1/2} - 1 + (3d/4\varrho)}$$

and

$$\mu_{fa} = \frac{\mu_f'}{\mu_0} = \frac{\mu_f\{\mu_0 - 2 - (3d/4\varrho\,\mu_0)\}}{\{(\mu_0 - 1)^2 + (3d/4\varrho)(\mu_0 - 3)(\mu_0 + 1)\}^{1/2} - 1 + (3d/4\varrho)}$$

(if $(d/\varrho) \to 0$, $\mu_{fa} \to \mu_f$) .

If $\mu_0 \to \infty$, $\mu_{fa} \to \mu_f/\{1 + (3d/4\varrho)\}^{1/2}$, a form similar to that found for the case of shear. Putting $\mu_f = 1 + 2(a/\varrho)^{1/2}$, the maximum value of μ_{fa} for variation of ϱ, when the values of a and d are specified, occurs when $\varrho = 9d^2/64a$ and is $(\mu_{fa})_{\max} = \{1 + (16a/3d)\}^{1/2}$. Values of μ_{fa} for values of $(a/\varrho)^{1/2}$ down to 5 and for values of d/a from 0·05 to 0·40 are shown in Fig. 18.

The many approximations that have had to be made in deriving an expression for μ_{fa} render it extremely difficult to judge the accuracy of the result or to delimit its range of application. Strictly, these approximations would appear to invalidate the results over practically the whole field covered by Fig. 18; but by analogy with the shear case, for which the results are exempt from similar doubt, it appears that the final results may be reasonably close to the truth. At least it is thought that the curves of Fig. 18 express a qualitative truth, that the effect of hair cracks will be to reduce the apparent stress concentration and to render its value less sensitive to changes in the ratio a/ϱ.

II.10. *Conclusions.*—(*a*) *Effect of General Form of Hole.*—The types of hole for which stress concentration factors have been worked out are all included in the general class of polygonal holes; but the results suffice to indicate the nature and order of the differences between the true concentration factors and the approximate values $1 + (a/\varrho)^{1/2}$ and $1 + 2(a/\varrho)^{1/2}$. Generally it appears that the latter value is a far better approximation to the true value under direct stress than the former is to the true concentration factor in shear. Nevertheless, the error of the form $\mu_f = 1 + 2\,(a/\varrho)^{1/2}$ may be considerable, particularly for holes in which the radius of curvature varies rapidly round the contour near the point of maximum stress. This point is illustrated by Fig. 16 at low values of a/ϱ; but it is brought out most clearly in the case of a simple polygonal hole with an infinite number of sides. In this case the hole is indistinguishable from a true circle and the stress factor μ_f takes the value 3, as would be expected; but in fact the radius of curvature of the contour oscillates indefinitely rapidly between $a/2$ and infinity, so that the value of $1 + 2\,(a/\varrho)^{1/2}$ oscillates between 1 and $1 + 2\sqrt{2}$.

The reason why the approximation $\mu_q = 1 + (a/\varrho)^{1/2}$ should usually be so much more in error than the approximation $\mu_f = 1 + 2\,(a/\varrho)^{1/2}$ is not apparent; but it appears to be generally so (*cf.* Part III).

(*b*) *Application to Specific Forms of Hole.*—Two practicable methods for successively approximating to a given form of hole by the transformation $x + iy = \sum_r \lambda_r e^{-r\xi}$ have been described. Unfortunately neither of these methods is automatically applicable to any given case; but certain artifices are available to meet special difficulties. Another general method is outlined in Part IV.

(*c*) *Effect of Hair Cracks.*—The analysis of the effect of hair cracks on the apparent value of μ_q appears to be reliable within ascertainable limits; but the estimate of the apparent value of μ_f is much less certainly established. It does, however, appear safe to conclude that the presence of hair cracks will reduce the apparent values of μ_q and μ_f and render these values less sensitive to changes in the ratio a/ϱ (in comparison with the approximate formulae $\mu_q = 1 + (a/\varrho)^{1/2}$ and $\mu_f = 1 + 2\,(a/\varrho)^{1/2}$). On the other hand, in order to explain on this basis the whole discrepancy between theoretical and experimental results it would be necessary to admit the existence of hair cracks of quite considerable depth; these necessary depths of hair cracks appear to be much greater than would by other evidence appear admissible.

PART III

The Effect of Surface Irregularities on Fatigue Strength

Synopsis.—It is perhaps not generally recognized that the approximate formulae $1 + \sqrt{(a/\varrho)}$ and $1 + 2\sqrt{(a/\varrho)}$ for the stress concentrations under shear and under direct stress due to a groove of depth a and root radius ϱ are applicable not only when the ratio a/ϱ is large but equally when it is small; indeed the accuracy of these approximate formulae improves as a/ϱ decreases. This is demonstrated by computation by exact theory of the stress concentration due to a continuous nearly sinusoidal undulation of the surface of a test piece, and it is shown incidentally that when a and ϱ are both negative, so that the groove is inverted into a protrusion, the ' de-concentration ' of stress is represented very closely by the approximate formulae $1 - \sqrt{(a/\varrho)}$ and $1 - 2\sqrt{(a/\varrho)}$. It is shown further that these factors applied as corrections to computed stress factors under torsion for an approximation to a square shaft with rounded corners suffice to reconcile these results to the established solution for a square shaft under torsion.

The presence of the radical in the approximate formulae implies that long shallow grooves cause appreciable stress concentration; for instance a groove of which the depth is only one hundredth of the radius at its root increases the local value of applied direct stress in the ratio 1·2 : 1. Such shallow grooves are present on the surface of every practical test piece and therefore this purely geometrical effect of surface condition on the fatigue strength may be important. Certain actual surface finishes are analysed in this aspect and their relative merits are reviewed. It is concluded that substantial improvement of the geometrical factor by ordinary methods of machining may be difficult to achieve, but that it is likely to result from other treatments, which are generally thought to improve the fatigue resistance by entirely different means.

III.1. *Introduction.*—The stress at the end of the principal axis $2a$ of an elliptical cylindrical hole in an infinite block under direct stress perpendicular to this axial plane is $1 + 2(a/b)$, where $2b$ is the other principal axis of the ellipse; the shear stress at the same point due to shear parallel to the principal axial plane in the direction of the axis of the hole is $1 + (a/b)$. These formulae apply equally whether $a > b$ or $b > a$. Since the radius of curvature ϱ at the end of the principal axis $2a$ is b^2/a, the formulae may be written $1 + 2\sqrt{(a/\varrho)}$ and $1 + \sqrt{(a/\varrho)}$.

These formulae, which relate strictly only to elliptical holes, are in fact applicable much more widely. Several comparisons are made in Part II between stress concentration factors accurately computed for divers types of holes and grooves and the values indicated by the approximate formulae. Apart from one or two rather extreme cases the differences are seldom large. On the other hand, for complex forms of hole or groove, although the meaning of ϱ is always specific, the interpretation to be placed on a, ' the depth of the groove, or half-depth of the hole ', is sometimes not obvious. In order, therefore, to demonstrate the validity of the approximate formulae for long shallow grooves, when the ratio a/ϱ is small, it appears desirable to derive the formulae afresh on the basis of an appropriate example accurately computed.

III.2. *Stress Concentration due to a Continuous Undulation of the Surface of a Test Piece.*—It is shown in Sections II.8 (ii) and (iii), that the stress concentrations at $\beta = 0$ caused by a cylindrical hole

$$\left.\begin{aligned} x &= R\cos\beta + a\cos n\beta \\ y &= R\sin\beta - a\sin n\beta \end{aligned}\right\} \quad \text{for which } r^2 = x^2 + y^2 = R^2 + a^2 + 2Ra\cos(n+1)\beta \qquad \ldots\ \ldots\ \ldots\ \ldots \quad (33)$$

are $\mu_q = 2/\{1 - (na/R)\}$ under shear on the plane $x = 0$ in the direction parallel to the axis of the cylinder $\ldots\ \ldots$ (34)

and $\mu_f = [1 + (na/R) + 2\{1 + (n-2)(a/R)\}/\{1 - (n-2)(a/R)^2\}]/\{1 - (na/R)\}$ under direct stress perpendicular to the plane $x = 0$ $\ldots\ \ldots$ (35)

The maximum and minimum radii of the hole are

$R + a$ at $\beta = 0,\ 2\pi/(n+1),\ 4\pi/(n+1)$, etc.

and $R - a$ at $\beta = \pi/(n+1),\ 3\pi/(n+1)$, etc.

At these points $x = R\cos\{\pi/(n+1)\} + a\cos\{n\pi/(n+1)\} = (R-a)\cos\{\pi/(n+1)\}$

$y = R\sin\{\pi/(n+1)\} - a\sin\{n\pi/(n+1)\} = (R-a)\sin\{\pi/(n+1)\}$

so that $\theta = \tan^{-1}(y/x) = \pi/(n+1)$, etc.

and the half wavelength $= R\theta = \pi R/(n+1)$.

The radius of curvature ϱ at $\beta = 0$ is $R\{1-(na/R)\}^2/\{1+(n^2a/R)\}$ and that at $\beta = \pi/(n+1)$ is $R\{1+(na/R)\}^2/\{1-(n^2a/R)\}$, the latter value corresponding to that at $\beta = 0$ is a if made negative.

If we make R and n both tend to infinity, whilst the ratio R/n remains finite, we have

$$(a/\varrho) = (na/R)^2/\{1-(na/R)\}^2 \text{ at } \beta = 0$$

and $(-a/\varrho) = (na/R)^2/\{1+(na/R)\}^2$ at $\beta = \pi/(n+1)$

Then
$$\left.\begin{aligned}\mu_q &= 2/\{1-(na/R)\} = 2\{1+\sqrt{(a/\varrho)}\} \text{ at } \beta = 0\\ &\text{or } 2/\{1+(na/R)\} = 2\{1-\sqrt{(-a/\varrho)}\} \text{ at } \beta = \pi/(n+1)\end{aligned}\right\} \quad .. \quad (36)$$

and
$$\left.\begin{aligned}\mu_f &= 3\{1+(na/R)\}/\{1-(na/R)\} = 3\{1+2\sqrt{(a/\varrho)}\} \text{ at } \beta = 0.\\ &\text{or } 3\{1-(na/R)\}/\{1+(na/R)\} = 3\{1-2\sqrt{(-a/\varrho)}\} \text{ at } \beta = \pi/(n+1)\end{aligned}\right\} \quad .. \quad (37)$$

Now, since R is indefinitely large and since $m\theta (= m\pi/(n+1)$, where m is finite) is indefinitely small, the part of the contour including any finite number of undulations is in effect based on a flat surface, and the whole of the material in the region round $\beta = 0$ is subjected to twice the nominal shear stress and three times the nominal direct stress due to the concentrations caused by the (infinitely large) circular hole. Thus the separate local stress concentrations due to the undulations are represented by the formulae $1 + \sqrt{(a/\varrho)}$, etc.

The form of the undulation is not quite sinusoidal. Writing $\alpha = n\beta$ so that α is finite, the formulae (33) reduce to

$$\left.\begin{aligned}x - R &= a\cos\alpha\\ \text{and } y &= a\{(R/na)\alpha - \sin\alpha\} = a\{(\lambda/a)(\alpha/\pi) - \sin\alpha\}\end{aligned}\right\} \quad .. \quad .. \quad .. \quad (38)$$

where $\lambda = \pi R/n$ is the half wavelength of the undulation. If λ/a is very large, approximately $\alpha = \pi y/\lambda$ and $x - R = a\cos(\pi y/\lambda)$; but if λ/a is comparable with π, the trough of the undulation is narrower than the crest. This is illustrated in Fig. 19, which shows the forms of the undulation for $\lambda/a = 4$, 8, 16 and 32. For values of $\lambda/a > 30$ the undulation does not differ appreciably from a true sine curve.

Although strictly formulae (36) and (37) are applicable only to the special form of undulation represented by formula (38) and Fig. 19, it seems probable that the forms $1 + \sqrt{(a/\varrho)}$ should be moderately accurate in application to more general forms. For such application it appears that the depth a should be measured from the median line of the undulating surface and that, disregarding the signs of a and ϱ, the local stress concentration factors are approximately $\mu_f = 1 \pm 2\sqrt{(a/\varrho)}$ and $\mu_q = 1 \pm \sqrt{(a/\varrho)}$, the positive sign being used for a trough and the negative sign for a crest.

III.3. *Application of Local Stress Concentration Factors to the Torsion of a Square Section Shaft.*—In order to test this hypothesis, reference is made to a solution of the torsion problem for a nearly square shaft with rounded corners. This solution, described in Part IV, is exact, but the

sides of the shaft as represented by the analytical form are not truly plane; the undulating form of the section boundary is shown in Fig. 20. The values of the shear stress along the section boundary computed for this actual undulating contour are given as values of q in Table 8; the values of a and ϱ computed from the analytical form of this contour are also listed, together with the values of a/ϱ and $\sqrt{(a/\varrho)}$, the latter being taken as negative when both a and ϱ are negative. The corrected values q' of the stress found by dividing q by the appropriate value of local stress concentration factor $1 \pm \sqrt{(a/\varrho)}$ define a reasonably smooth curve of which the value near $\beta = 0$ agrees quite closely with the value $q' = 1{\cdot}351$ found for a square shaft by another method[10].

TABLE 8

Shear stress distribution in a square section shaft under torsion

β	0	5	10	15	20	25	30	35	40	45
$100a$ ..	+0·500	−0·352	−0·428	+0·631	−0·335	−0·823	+1·016	−0·378	−2·263	+8·341
ϱ ..	+0·118	−0·411	−0·327	+0·114	−0·570	−0·287	+0·136	−1·945	−0·356	−0·381
a/ϱ ..	$0{\cdot}042_5$	$0{\cdot}008_5$	0·013	0·055	0·006	0·029	0·075	0·002	0·064	—
$\sqrt{(a/\varrho)}$ ..	0·206	−0·092	−0·114	0·236	−0·077	−0·170	0·273	−0·045	−0·252	—
q ..	1·624	1·235	1·192	1·617	1·200	1·041	1·482	0·919	0·693	0·637
q' ..	1·348	1·360	1·344	1·308	1·301	1·252	1·163	0·961	0·927	0·637

By this test the formulae (36) and (37) appear likely to be widely applicable; their implications in respect of ordinary surface finishes of engineering components are examined below.

III.4. *Stress Concentration due to the Geometry of Surface Finishes.*—The methods available for the measurement of roughness of machined surfaces do not afford a complete and accurate record of the surface profile; for instance, where an exploring probe is used, the point of the probe cannot penetrate into a groove which may be narrower than the probe itself. On the other hand the measurements available do afford conservative estimates of the depths of the larger irregularities and of their ' wavelengths '. A depression of depth a and length λ corresponds to a value of $\sqrt{(a/\varrho)} = K(a/\lambda)$, the value of the coefficient K depending upon the form of the groove; it is least for a circular profile, for which $\varrho = (\lambda^2/8a)$, so that $K = 2\sqrt{2}$; for a sinusoidal profile of half amplitude a and half wavelength λ, $K = \pi$; and for practical grooves of less regular form considerably greater values of K are to be expected. In order, therefore, to form a conservative estimate of the stress concentrating effect of some typical surface finishes, we may take values of a and λ from the records available[11] and then assume $\sqrt{(a/\varrho)} = 4(a/\lambda)$. The values of the stress concentration factors thus found (Table 9) are probably all very much less than the true values,

TABLE 9

Minimum stress concentration factors due to typical surface finishes

Description of Surface Finish	Reference (Fig. Nos. of Ref. 12)	a		λ		μ_f	μ_q
		(10^{-6} in.)	Microns	(10^{-6} in.)	Microns		
Rough ground	6	60	1·52	400	10·1	2·2	1·6
Fine ground	19	10	0·25	130	3·4	1·6	1·3
Fine ground	6	10	0·25	200	5·1	1·4	1·2
Honed	20	3	0·08	120	3·0	1·2	1·1

(53510)

but at least these values serve to show that the stress concentrations due to the geometry of the surface are by no means negligible. The stress concentrating effect of a surface finish depends as much on the length λ of the irregularities as on their depth a. For that reason a treatment which reduces the value of a is ineffective if at the same time it reduces λ in the same proportion. Thus the difference between rough and fine grinding may not be marked if the shape of the abrading particles on coarse and fine wheels is much the same. It is notable that the honed finish with an average roughness of only $1\frac{1}{2}$ micro-inches still causes a stress concentration under direct stress of at least $1 \cdot 2$. This is due to a few rather deeper grooves, which are widely spaced but rather narrow. Such grooves may well differ markedly from the circular or sinusoidal form and the estimated values of the stress concentration factors are probably far too low.

A rolled surface may be appreciably better than a machined one, not principally because the irregularities may be shallower but rather because they are likely to be wider. Unfortunately no records of rolled surfaces are available for analysis.

Although there is also a lack of records of shot-peened surfaces, in this case we know the approximate value of ρ and we may guess the value of a. The radius ρ is presumably greater than the radius of the shot used and a may be slightly less than the penetration of the individual shot into the surface. Shot $0 \cdot 1$ inch in diameter indenting to a depth of $0 \cdot 001$ inch may thus leave a surface roughness of 500 micro-inches and yet cause a stress concentration of no more than $1 \cdot 2$ under direct stress; this value is comparable with that resulting by polishing or honing.

For optimum shot-peening in this aspect the shot should be as large as possible and their speed of impact should be such that they indent to a depth greater but not much greater than the depth of the irregularities in the original surface. Very light peening with large shot of a surface previously honed or polished might be expected to afford the highest possible fatigue resistance. For instance a surface roughness not exceeding 20 micro-inches produced by peening with shot $0 \cdot 1$ inch in diameter should cause a stress concentration under direct stress of about $1 \cdot 04$.

Detailed analysis of records of surface roughness and perhaps more accurate analysis of the stress concentrations due to particular wave forms would be required in order to render the survey strictly quantitative. On the other hand, the few cases quoted all represent minimum estimates, and they afford sufficient evidence in support of the claims that the stress concentration due to the geometry of the surface is vitally important and that allowance for this effect must be made before the other effects of special surface treatments may be properly assessed.

It should be added that, although the surface irregularities left by machining are small they are nevertheless large enough in relation to the atomic structure for the application of the ordinary theory of elasticity to be valid. On the other hand there is evidence to indicate that materials are relatively insusceptible to such highly localized concentrations of stress.

PART IV

Stress Concentration in Twisted Shafts

Synopsis.—A straightforward method for computing the stress distribution in a twisted shaft of specified cross-section is developed, and the method is illustrated by application to a round shaft with a single flat on one side and to a six-splined shaft. In these applications use is made of the process of correction for local irregularities described in Part III, and some general comments are made on the means to represent complex boundaries by analytical forms, which supplement the techniques described in Part II. An approximate formula for the concentration of shear stress in the fillet at the root of the spline of a splined shaft under torsion is proposed and the accuracy of this formula is tested by three examples. One example of a hollow shaft with a lobed external contour and a wide variation of wall thickness is worked out, and it is shown that over the smooth inner boundary the shear stress is very nearly inversely proportional to the wall thickness, whereas at the lobed outer boundary marked concentration of stress occurs at the grooves between the lobes.

IV.1. *Introduction.*—The problem of torsion of a cylindrical shaft is usually stated by reference to rectilinear axes *Oxyz*, *Oz* being parallel to the axis of the cylinder: that is, a solution is sought to the differential equation $\frac{\partial^2\psi}{\partial x^2} + \frac{\partial^2\psi}{\partial y^2} = 0$ subject to the condition that $\psi = \frac{1}{2}\tau(x^2 + y^2)$ over the boundary of the shaft, where τ is the angle of twist in unit length. Subsequently the stresses are evaluated from the formulae $\bar{z}\bar{x} = -G\left(\frac{\partial\psi}{\partial y} + \tau y\right)$ and $\bar{y}\bar{z} = G\left(\frac{\partial\psi}{\partial x} + \tau x.\right)$ (Refs. 9, 11, 13, 14).

This method of approach is that originally devised by St. Venant, and it has been applied by St. Venant himself and by many others to the solution of the torsion problem for a wide range of particular shapes of boundary. Yet the method has two disadvantages; one is that it appears rather indirect and that the physical meaning of the torsion function ψ is not emphasised; the other is that the solution of the problem in elasticity is not clearly separated from the process of transformation into the special co-ordinate system appropriate to each particular boundary. The latter fault of the St. Venant method becomes most apparent when the problem concerns some specified boundary. There appear to be no straightforward means to define the appropriate form for ψ, and there seems to be no alternative to a process of trial and error.

By the method of approach described below the problem is stated from the outset by reference to curvilinear axes, chosen to conform to the specified boundary. The solution in terms of shear stress is derived directly from the conditions of equilibrium and from the boundary conditions, so that the appropriate form for ψ can be written down by inspection. Moreover, the physical meaning of ψ is made clear and its relation to the warping of cross sections is emphasised. By this approach it is made apparent that the solution of the torsion problem for any boundary consists merely in defining a suitable system of curvilinear co-ordinates; once the co-ordinate system has been defined, the remainder of the solution is straightforward computation.

IV.2. *General Cylindrical Co-ordinates.* (*See* also Section II.3).—Any system of curvilinear cylindrical co-ordinates may be defined intrinsically without reference to any other co-ordinate system; but the intrinsic formulation merely relates the curvature of each co-ordinate line to distance measured along that line, so that this method of representation does not afford a ready picture of the shape of the system. For that reason and also for ease of satisfaction of the condition that the co-ordinate lines shall intersect at right-angles, it is convenient to relate the orthogonal curvilinear system (α, β) to a rectilinear system (x, y) by specifying $x + iy = \phi(\alpha + i\beta)$, where ϕ is any continuous function. Then also $x - iy = \phi(\alpha - i\beta)$, and $r^2 = x^2 + y^2 = \phi(\alpha+i\beta).\phi(\alpha - i\beta)$.

Moreover, $\delta x + i\delta y = \phi'(\alpha + i\beta).(\delta\alpha + i\delta\beta)$, where the prime denotes differentiation with respect to the complete argument $\alpha + i\beta$, and $\delta x - i\delta y = \phi'(\alpha - i\beta)(\delta\alpha - i\delta\beta)$. Hence, $\delta s^2 = \delta x^2 + \delta y^2 = \phi'(\alpha + i\beta).\phi'(\alpha - i\beta)(\delta\alpha^2 + \delta\beta^2) = h^2(\delta\alpha^2 + \delta\beta^2)$. Thus unit change in α or β represents a length h, and the value of the space factor h, which is equal to $\{\phi'(\alpha + i\beta).\ \phi'(\alpha - i\beta)\}^{1/2}$, varies over the field in a manner determined simply by the form of the function ϕ.

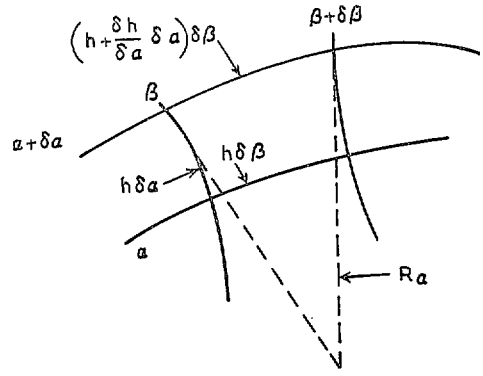

The length of the α-line between β and $\beta + \delta\beta$ is then $h\,\delta\beta$ and the length of the $\alpha + \delta\alpha$-line between the same limits is $\left(h + \frac{\partial h}{\partial\alpha}\delta\alpha\right)\delta\beta$; but the lines α and $\alpha + \delta\alpha$ are $h\,\delta\alpha$ apart, so that the tangents to the lines β and $\beta + \delta\beta$ meet at a distance R_α, such that $\frac{h\,\delta\beta}{R_\alpha} = \frac{\partial h}{\partial\alpha}\delta\alpha\,\delta\beta/h\,\delta\alpha$, or $\frac{1}{R_\alpha} = \frac{1}{h^2}\frac{\partial h}{\partial\alpha}$. Since the α and β lines intersect at right-angles*, R_α is the radius of curvature of the α-line. Similarly $\frac{1}{R_\beta} = \frac{1}{h^2}\frac{\partial h}{\partial\beta}$, where R_β is the radius of curvature of the β-line. These are, in fact, the intrinsic formulae to which reference was made above and they alone could be used as definitions of the co-ordinate system. In the slightly simpler forms $\frac{1}{R_\alpha} = -\frac{\partial}{\partial\alpha}\left(\frac{1}{h}\right)$ and $\frac{1}{R_\beta} = -\frac{\partial}{\partial\beta}\left(\frac{1}{h}\right)$† it is apparent that $\frac{\partial}{\partial\beta}\left(\frac{1}{R_\alpha}\right) = \frac{\partial}{\partial\alpha}\left(\frac{1}{R_\beta}\right)$; this restriction results from the condition that the α and β lines shall be orthogonal. It is perhaps worth noticing that in general $\frac{1}{h}$ is *not* a plane harmonic function.

IV.3. *The Torsion of a Cylinder.*—We assume that the section distant z from one end of the shaft rotates without distortion through an angle $f(z)$ about an axis parallel to the generators of the cylinder; for the present there is no restriction on the form of the function $f(z)$. Then the displacement of any point in the plane of the section is $rf(z)$ normal to the radius vector r from the centre of rotation, and the displacements along the α and β co-ordinate lines are $u_\alpha = -\frac{r}{h}\frac{\partial r}{\partial\beta}f(z)$ and $u_\beta = \frac{r}{h}\frac{\partial r}{\partial\alpha}f(z)$. (It can readily be checked that the strain $e_{\alpha\alpha} = \frac{1}{h}\frac{\partial u_\beta}{\partial\alpha} + \frac{u_\beta}{h^2}\frac{\partial h}{\partial\beta}$ is zero, as also are the strains $e_{\beta\beta}$ and $e_{\alpha\beta}$; but of course this is clear from the nature of the displacement specified).

* The tangent to the β-line at α, β has the slope $(S - 1)/i(S + 1)$, where $S = \phi'(\alpha + i\beta)/\phi'(\alpha - i\beta)$ and the slope of the tangent to the α-line is similar with $-S$ for S. Thus the product of the two slopes is -1 and the lines cut at right-angles.

† Some authors (*cf.*, for example, Ref. 8) define h by the reciprocal of the definition here adopted. Neither definition appears markedly more convenient than the other; but it is a pity that both are used, because care needs to be exercised to avoid confusion.

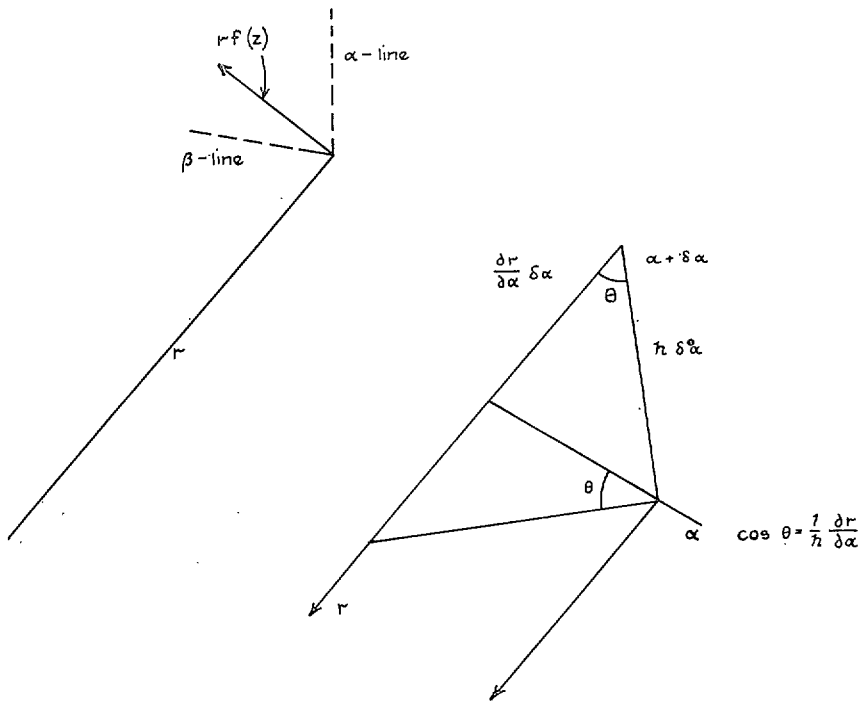

If the displacement out of the plane of the section parallel to the axis Oz is w, the shear stresses and strains

$$\bar{a}\bar{z} = Ge_{az} = G\left(\frac{\partial u_\alpha}{\partial z} + \frac{\partial w}{h\,\partial \alpha}\right)$$

and $$\bar{\beta}\bar{z} = Ge_{\beta z} = G\left(\frac{\partial u_\beta}{\partial z} + \frac{\partial w}{h\,\partial \beta}\right)$$

or, by substitution for u_α and u_β

$$\bar{a}\bar{z} = G\left\{-\frac{r}{h}\frac{\partial r}{\partial \beta}f'(z) + \frac{\partial w}{h\,\partial \alpha}\right\} \text{ and } \bar{\beta}\bar{z} = G\left\{\frac{r}{h}\frac{\partial r}{\partial \alpha}f'(z) + \frac{\partial w}{h\,\partial \beta}\right\} . \quad .. \quad .. \quad .. \quad (39)$$

If we assume now that $\partial w/\partial z = \text{const.}$, the stresses $\bar{a}\bar{a}$, $\bar{a}\bar{\beta}$, $\bar{\beta}\bar{\beta}$ and $\bar{z}\bar{z}$ are all independent of α and β. Then for equilibrium $\partial \bar{a}\bar{z}/\partial z = 0$ and $\partial \bar{\beta}\bar{z}/\partial z = 0$, which merely demands $f''(z) = 0$; thus $f'(z) = \tau$ and must be constant. Finally for equilibrium $\partial(h\,.\,\bar{a}\bar{z})/\partial\alpha + \partial(h\,.\,\bar{\beta}\bar{z})/\partial\beta = 0$ which requires $\dfrac{\partial^2 w}{\partial \alpha^2} + \dfrac{\partial^2 w}{\partial \beta^2} = 0$*, so that w is a plane harmonic function.

With w we may therefore associate its harmonic conjugate ψ such that $\partial w/\partial\alpha = \partial\psi/\partial\beta$ and $\partial w/\partial\beta = -\partial\psi/\partial\alpha$, and of course $\Delta^2\psi = 0$. Then formulae (39) may be re-written

$$\bar{a}\bar{z} = G\frac{1}{h}\frac{\partial}{\partial\beta}(\psi - \tfrac{1}{2}\tau r^2) \text{ and } \bar{\beta}\bar{z} = -G\frac{1}{h}\frac{\partial}{\partial\alpha}(\psi - \tfrac{1}{2}\tau r^2) . \quad .. \quad .. \quad .. \quad .. \quad (40)$$

---

* The space function h takes care of all curvature effects, so that Δ^2 has the same form in the $\alpha\beta$ system as in Cartesians. It may readily be shown that $\dfrac{\partial}{\partial\alpha} + i\dfrac{\partial}{\partial\beta} = 2\phi'(\alpha - i\beta)\left(\dfrac{\partial}{\partial x} + i\dfrac{\partial}{\partial y}\right)$ and that $\dfrac{\partial}{\partial\alpha} - i\dfrac{\partial}{\partial\beta} = 2\phi'(\alpha + i\beta)\left(\dfrac{\partial}{\partial x} - i\dfrac{\partial}{\partial y}\right)$. Hence $\dfrac{\partial^2}{\partial\alpha^2} + \dfrac{\partial^2}{\partial\beta^2} = 4h^2\left(\dfrac{\partial^2}{\partial x^2} + \dfrac{\partial^2}{\partial y^2}\right)$. Note, however, that $\left(\dfrac{\partial^2}{\partial x^2} + \dfrac{\partial^2}{\partial y^2}\right)^2 = \dfrac{1}{4h^2}\left(\dfrac{\partial^2}{\partial\alpha^2} + \dfrac{\partial^2}{\partial\beta^2}\right)\left\{\dfrac{1}{4h^2}\left(\dfrac{\partial^2}{\partial\alpha^2} + \dfrac{\partial^2}{\partial\beta^2}\right)\right\}$, so that $(\Delta^2)^2$ is *not* invariant (*see* Section II.7).

If $\bar{\alpha}\bar{z}$ is zero round the contour of the cylindrical surface defined by $\alpha =$ constant, $\psi - \frac{1}{2}\tau r^2$ is constant (independent of β) round that contour. But r^2 is defined as a function of β for the given value of α by the relation $r^2 = \phi(\alpha + i\beta) \,.\, \phi(\alpha - i\beta)$, so that the plane harmonic (torsion) function ψ may at once be written down by inspection; the values of $\bar{\beta}\bar{z}$ and w (the warping) follow.

The value of the torque transmitted is

$$T = \int_\alpha \int_\beta (\bar{\beta}\bar{z} \cos\theta + \bar{\alpha}\bar{z} \sin\theta) \,.\, r \,.\, h\, d\alpha \,.\, h\, d\beta$$

where $\cos\theta = \dfrac{1}{h}\dfrac{\partial r}{\partial \alpha}$ and $\sin\theta = -\dfrac{1}{h}\dfrac{\partial r}{\partial \beta}$ (*see* diagram, page 37).

Substituting for $\bar{\beta}\bar{z}$ and $\bar{\alpha}\bar{z}$ from formulae (40), the formula may be written in the form

$$T = -\tfrac{1}{2}G \int_\alpha \int_\beta \left\{ \frac{\partial}{\partial \alpha}(\psi - \tfrac{1}{2}\tau r^2) \frac{\partial r^2}{\partial \alpha} + \frac{\partial}{\partial \beta}(\psi - \tfrac{1}{2}\tau r^2) \frac{\partial r^2}{\partial \beta} \right\} d\alpha\, d\beta \quad .. \quad .. \quad (41)$$

IV. 4. *Periodic Co-ordinate Systems.*—The boundary of the section of any cylindrical shaft is of course a closed curve; therefore, if this be represented by $\alpha = \alpha_0$, the co-ordinate system must be periodic in β. A wide range of co-ordinate systems satisfying these conditions may be represented in the form $x + iy = \phi(\alpha + i\beta) = \sum_n \lambda_n e^{n(\alpha+i\beta)}$, where the coefficients λ_n are arbitrary constants. It is indeed probable that *any* closed curve may be represented in this form, subject only to limitations as to continuity similar to those governing expansions in Fourier series. The general similarity to Fourier series is of course apparent, but the differences are such as to render proof of the general proposition far from easy. However, in practice the form $\sum_n \lambda_n e^{n(\alpha+i\beta)}$ may be adjusted fairly readily to approximate to prescribed forms of boundary by particular methods based on Fourier forms, and in respect of stress analysis rules for complete expansion in infinite series would not be of much practical use for a reason which will appear later (Section IV.9).

If the shaft be solid, the co-ordinate system must include the point $x = 0$, $y = 0$ which is taken within the shaft contour; for solid shafts, therefore, we are limited* to negative values of either n or α. It is convenient to take α and β always positive and to represent a solid shaft by the form $x + iy = \sum_n \lambda_{-n} e^{-n(\alpha+i\beta)}$, so that the point $x = 0, y = 0$ corresponds to $\alpha \to \infty$. Then $r^2 = \sum_m \sum_n \lambda_{-m}\lambda_{-n} e^{-(m+n)\alpha} \cos(m-n)\beta$, both m and n being taken over complete ranges, or $r^2 = \sum_n \lambda_{-n}^2 e^{-2n\alpha} + 2\sum_m \sum_n \lambda_{-m}\lambda_{-n} e^{-(m+n)\alpha} \cos(m-n)\beta$, where $m > n$. At the boundary it is convenient to take $\alpha = 0$ and then $r^2 = \text{const.} + 2\sum_m \sum_n \lambda_{-m}\lambda_{-n} \cos(m-n)\beta$, $m > n$, so that the torsion function $\psi = \tau \sum_m \sum_n \lambda_{-m}\lambda_{-n} e^{-(m-n)\alpha} \cos(m-n)\beta$, $m > n$, and the warping $w = \tau \sum_m \sum_n \lambda_{-m}\lambda_{-n} e^{-(m-n)\alpha} \sin(m-n)\beta$, $m > n$. The terms with $e^{(m-n)\alpha}$ are excluded by the condition that ψ and w must remain finite at $x = 0$, $y = 0$ (when $\alpha \to \infty$).

If the shaft be hollow, the pole $x = 0, y = 0$ may be taken within the inner boundary and need not be included by the $\alpha\beta$ co-ordinate system. Then the complete transformation $x + iy = \sum_n \lambda_n e^{n(\alpha+i\beta)}$ may be used with both positive and negative values of n, and the part of the formula for r^2, which depends on β, becomes

$$2\sum_m \sum_n \{\lambda_{-m}\lambda_{-n} e^{-(m+n)\alpha} + \lambda_m \lambda_n e^{(m+n)\alpha}\} \cos(m-n)\beta,\ m > n.$$

* The ellipse is an exception to this rule.

The torsion function is then

$$\psi = \tau \sum_m \sum_n \{X e^{(m-n)\alpha} + Y e^{-(m-n)\alpha}\} \cos (m-n)\beta.$$

where the values of X and Y are defined by the equations

$$X e^{(m-n)\alpha_1} + Y e^{-(m-n)\alpha_1} = \lambda_m \lambda_n e^{(m+n)\alpha_1} + \lambda_{-m} \lambda_{-n} e^{-(m+n)\alpha_1}$$

and $$X e^{(m+n)\alpha_2} + Y e^{-(m-n)\alpha_2} = \lambda_m \lambda_n e^{(m-n)\alpha_2} + \lambda_{-m} \lambda_{-n} e^{-(m+n)\alpha_2}$$

and $\alpha = \alpha_1$, and $\alpha = \alpha_2$ define the inner and outer boundaries of the hollow shaft.

There are still degrees of freedom and of restriction in respect of choice of the values of α_1 and α_2, but this concerns only the representation of the two boundaries in the form $x + iy = \sum_n \lambda_n e^{n\alpha_1}$ $(\cos n\beta + i \sin n\beta)$ and does not affect the torsion problem itself. The range of double boundaries which may thus be represented is limited, but for any that can be represented the torsion problem is solved by the formulae above. The same conclusion is valid also for any multiply-connected section; once a co-ordinate system has been found by which all the boundaries are represented by curves belonging all to one of the two co-ordinate families, the solution of the torsion problem follows automatically. Representation of multiply-connected regions by a single system of co-ordinates is seldom straightforward and the subject will be pursued no further here; one example of a hollow shaft is worked in Section IV.11.

IV.5. *The Stress System in a Twisted Polygonal Solid Shaft.*—For convenience the general transformation will be rewritten as $x + iy = \sum_{n=1}^{n=\infty} \lambda_n e^{-n(\alpha+i\beta)}$ and the external contour will be taken at $\alpha = 0$.

Then $$r^2 = \sum_n \lambda_n^2 e^{-2n\alpha} + 2 \sum_m \sum_n \lambda_m \lambda_n e^{-(m+n)\alpha} \cos (m-n)\beta, \; m > n$$

$$\psi = \tau \sum_m \sum_n \lambda_m \lambda_n e^{-(m-n)\alpha} \cos (m-n)\beta, \; m > n.$$

$$\bar{\beta}\bar{z} = \frac{G}{h} \frac{\partial}{\partial \alpha} (\tfrac{1}{2}\tau r^2 - \psi)$$

$$= -\frac{G\tau}{h} [\sum_n n\lambda_n^2 e^{-2n\alpha}$$

$$+ \sum_m \sum_n \lambda_m \lambda_n \{(m+n)e^{-(m+n)\alpha} - (m-n)e^{-(m-n)\alpha}\} \cos (m-n)\beta \,] \quad m > n \quad .. \quad (42)$$

and $$h^2 = \sum_n n^2 \lambda_n^2 e^{-2n\alpha} + 2 \sum_m \sum_n mn\lambda_m \lambda_n e^{-(m+n)\alpha} \cos (m-n)\beta, \quad m > n. \quad .. \quad .. \quad .. \quad (43)$$

At the boundary, $\alpha = 0$

$$|\bar{\beta}\bar{z}| = G\tau\{\sum_n n\lambda_n^2 + 2 \sum_m \sum_n n\lambda_m \lambda_n \cos (m-n)\beta\} / \{\sum_n n^2 \lambda_n^2$$

$$+ 2 \sum_m \sum_n mn\lambda_m \lambda_n \cos (m-n)\beta\}^{1/2}, \quad m > n. \quad .. \quad .. \quad .. \quad .. \quad .. \quad (44)$$

The area of section is $\pi \sum_n n\lambda_n^2$. By applying formula (41), the modulus of section may be found from the torque T transmitted in the form

$$J = \frac{T}{G\tau} = \frac{\pi}{2} \left\{ \sum_n n\lambda_n^4 + 4 \sum_m \sum_n n\lambda_m^2 \lambda_n^2 + 4 \sum_n \sum_s n\lambda_{2n+s} \lambda_{n+s}^2 \lambda_n + 8 \sum_m \sum_n \sum_s n\lambda_{m+s} \lambda_{n+s} \lambda_m \lambda_n \right\} \quad (45)$$

where $m > n$ and in the last term $(n + s) > m$. (A slightly more concise form may be written, but that given emphasises the four types of product which contribute to the torque).

IV.6. *Two-Term Contours.*—In order to illustrate the application of formula (44), it is convenient to consider the class of contours for which only λ_1 and λ_n differ from zero. The contour $\alpha = 0$ is then $\lambda_1^2 + \lambda_n^2 + 2\lambda_1\lambda_n \cos(n-1)\beta$; the maximum and minimum radii are $\lambda_1 \pm \lambda_n$, and they are spaced at angular intervals $\pi/(n-1)$. The shafts are thus regular polygons with $(n-1)$ sides: when $n = 2$ the shaft is more or less circular with a slightly flattened region at one side. Along the boundary $\alpha = 0$, $h^2 = \lambda_1^2 + n^2\lambda_n^2 + 2n\lambda_1\lambda_n \cos(n-1)\beta$ and the maximum and minimum of $h = \lambda_1 \pm n\lambda_n$ correspond with the maximum and minimum of the radius r. The value of the shear stress is

$$\bar{\beta z} = G\tau\{\lambda_1^2 + n\lambda_n^2 + 2\lambda_1\lambda_n \cos(n-1)\beta\}/\{\lambda_1^2 + n^2\lambda_n^2 + 2n\lambda_1\lambda_n \cos(n-1)\beta\}^{1/2}$$

the torque $T = \frac{1}{2}\pi G\tau(\lambda_1^4 + 4\lambda_1^2\lambda_n^2 + n\lambda_n^4)$, the area of section is $\pi(\lambda_1^2 + n\lambda_n^2)$ and the radius of curvature of the contour is

$$\varrho = \{\lambda_1^2 + n^2\lambda_n^2 + 2n\lambda_1\lambda_n \cos(n-1)\beta\}^{3/2}/\{\lambda_1^2 + n^3\lambda_n^2 + n(n+1)\lambda_1\lambda_n \cos(n-1\beta\}.$$

The principal values of $\bar{\beta z}$ and ϱ are

at	Radius (r/λ_1)	Shear stress $(\bar{\beta z}/G\tau\lambda_1)$	Radius of curvature (ϱ/λ_1)
$\beta = 0$	$1 + d$	$(1 + 2d + nd^2)/(1 + nd)$	$(1 + nd)^2/(1 + n^2d)$
$\beta = \pi/(n-1)$	$1 - d$	$(1 - 2d + nd^2)/(1 - nd)$ where $d = \lambda_n/\lambda_1$	$(1 - nd)^2/(1 - n^2d)$

When $d < 1/n^2$ the contour of the shaft is everywhere convex outwards: when $d = 1/n^2$ the contour has a flat in the middle of each side: when $d > 1/n^2$ the shaft is grooved: and when $d \to 1/n$, the groove sharpens into a cusp. The values of the stresses for the series of flat-sided shafts when $d = 1/n^2$ are

Number of sides:		1	2	3	4	5	6	7	8	9	10	∞
$\frac{\bar{\beta z}}{G\tau\lambda_1}$	Max.	1·250	1·222	1·187	1·160	1·139	1·122	1·109	1·099	1·090	1·083	1
	Min.	1·083	0·944	0·912	0·907	0·909	0·913	0·918	0·923	0·928	0·933	1

the higher stress occurring at the middle of the flat side, and the lower at the corner. It should be noticed that a shaft with a very large number of flats having between these flats a radius of curvature equal to half its own radius has no concentration of stress under torsion (*cf.* Section II.8).

If $nd = 1 - \varepsilon$, where ε is small, the value of the stress at the bottom of the narrow groove is approximately $1 + (1 - 1/n)/\varepsilon$. The value of the radius of curvature (ϱ) here is about $(\varepsilon^2/(n-1) = d(\varepsilon^2/(1 - 1/n)$, since nd is approximately unity. Therefore, the stress concentration factor $1 + (1 - 1/n)/\varepsilon = 1 + \{(1 - 1/n)(d/\varrho)\}^{1/2}$ which approximates to $1 + (d/\varrho)^{1/2}$, when n is large (*cf.* Section III.2.)

IV.7. *The Square Shaft.*—The square shaft in Section IV.6 above has corners very well rounded, the diagonal width being only $\frac{1}{12}$th greater than the width across the flats. A better approach to the square shaft may be achieved by using the series λ_1, λ_5, λ_9, λ_{13}, etc., and by making $\lambda_1 \cos\beta + \lambda_5 \cos 5\beta + \lambda_9 \cos 9\beta + \ldots$, etc., fit as closely as possible to unity over the range $0 < \beta < \pi/4$. The best fit afforded by the first six terms of this series has $\lambda_1 = 1{\cdot}080$, $\lambda_5 = -0{\cdot}109$, $\lambda_9 = 0{\cdot}046$, $\lambda_{13} = -0{\cdot}027$, $\lambda_{17} = 0{\cdot}019$ and $\lambda_{21} = -0{\cdot}014$. Using these values in formula (44), the distribution of shear stress is at β (deg).

	0	5	10	15	20	25	30	35	40	45
$\frac{\bar{\beta z}}{G\tau}$	1·624	1·235	1·192	1·617	1·200	1·041	1·482	0·919	0·693	0·637

and the torque is $1{\cdot}4384(\pi/2)G\tau$.

The apparently erratic variation of $\bar{\beta}\bar{z}$ along the flat side of the shaft is actually quite regular and the variation is due to local stress concentrations. The form defined by the values of the λ's listed above differs from a true square with corners rounded to a radius of about $\frac{1}{7}$th of the side of the square by less than 2 per cent over the whole contour. On the other hand the curvature varies much more, and these local variations of curvature are responsible for marked local concentrations of stress. The process of correction for the effect of these local irregularities has been described in Section III.3 and is illustrated by Fig. 20.

IV.8. *The Round Shaft with a Single Flat.*—As a further illustration of the process of correction of stress factors in respect of local undulations we take the case of a round shaft with a single flat. If we take $\lambda_2 = -0{\cdot}3\lambda_1$

$$(\bar{\beta}\bar{z}/G\tau\lambda_1) = (1{\cdot}18 - 0{\cdot}6\cos\beta)/(1{\cdot}36 - 1{\cdot}2\cos\beta)^{1/2}$$

$$(\varrho/\lambda_1) = (1{\cdot}36 - 1{\cdot}2\cos\beta)^{3/2}/(1{\cdot}72 - 1{\cdot}8\cos\beta)$$

and $(a/\lambda_1) = \cos\beta - 0{\cdot}3\cos 2\beta - 0{\cdot}7080.$

the term 0·7080 being the mean distance of the flat from the origin. Then as before

β	0	5	10	15	20	25	30	35	40	45
$100(a/\lambda_1)$	−0·80	−0·72	−0·51	−0·19	0·19	0·55	0·80	0·86	0·59	−0·10
(ϱ/λ_1)	−0·800	−0·912	−1·430	−4·841	3·931	1·603	1·127	0·943	0·858	0·818
$100(a/\varrho)$	1·000	0·803	0·356	0·039	0·048	0·343	0·710	0·911	0·688	—
$(a/\varrho)^{1/2}$	0·100	0·090	0·060	0·020	−0·022	−0·059	−0·084	−0·095	−0·083	—
$(\overline{\beta z}/G\tau\lambda_1)$	1·450	1·435	1·396	1·340	1·278	1·219	1·166	1·121	1·085	1·057
$\frac{(\overline{\beta z}/G\tau\lambda_1)}{1+(a/\varrho)^{1/2}}$	1·318	1·317	1·316	1·314	1·307	1·295	1·273	1·238	1·183	(1·057)

The torque transmitted is $1{\cdot}376(\pi/2\ G\tau\lambda_1{}^4)$. The stress in a round shaft of radius λ_1 under this torque would be $1{\cdot}376G\tau\lambda_1$; the stress in a round shaft of radius $1{\cdot}15\ \lambda_1$, that is the shaft shown in Fig. 21 without the flat, would be $0{\cdot}905G\tau\lambda_1$. The stress in a round shaft of the same area under the same torque would be $1{\cdot}074G\tau\lambda_1$, and by this comparison the flat may be said to cause a stress concentration of $1{\cdot}318/1{\cdot}074 = 1{\cdot}227$.

Although in this example no other solution is available for comparison, it will be seen that the corrected stress values form a smooth series and that the stress in the middle of the flat region varies only very slowly. The shape of the section and the distribution of shear stress round its boundary are shown in Fig. 21.

Correction by means of the formulae $1 \pm (a/\varrho)^{1/2}$ is feasible only so long as the amplitude a of the undulation is small, say 1 to 2 per cent of the mean radius of the shaft. For larger amplitudes the choice of the mean height of the undulating surface becomes rather vague, and the estimate of shear stress is likely to be inaccurate.

A further example of the distribution of shear stress in a round shaft with a flat on one side is described in Fig. 22; again the values of the stresses after correction for the effect of local curvature form a smooth series.

IV.9. *Representation of Splined Shafts.*—Shafts of technical importance in engineering practice are usually circular over the greater part of their contours, and their greatest and least radii seldom differ very greatly. A typical class is that of splined shafts, with heights of splines 5 to 10 per cent of the mean shaft diameter.

The radius r of the contour $\alpha = 0$ of the system $x + iy = \sum_n \lambda_n e^{-n(\alpha+i\beta)}$ is given by

$$r^2 = \sum_n \lambda_n{}^2 + 2\sum_m \sum_n \lambda_m \lambda_n \cos(m-n)\beta, \quad m > n\ .$$

If λ_1 is considerably greater than λ_2 λ_3 etc. (say about ten times) this formula differs only slightly from

$$r^2 = \text{const.} + 2\lambda_1 \sum_n \lambda_n \cos(n-1)\beta$$

because the terms $\lambda_m\lambda_n$, where neither m nor n is unity, are ten times smaller than the terms $\lambda_1\lambda_n$. Moreover, to the same order of accuracy $r = \lambda_1 + \sum_n \lambda_n \cos(n-1)\beta$, so that the variation of r is represented by the Fourier series $\Sigma_n \lambda_n \cos(n-1)\beta$.

If, then, we take the sequence λ_1, λ_{n+1}, λ_{2n+1}, etc., we define a regular n-sided shaft of which the shape between $\beta = 0$ and $\beta = 2\pi/n$ is represented approximately in terms of β by the Fourier series $\sum_s \lambda_{sn+1} \cos sn\beta$, provided that λ_{sn+1}/λ_1 is moderately small (about one-tenth, say). By writing λ_s for λ_{sn+1} and γ for $n\beta$, we may apply the same Fourier series $\sum_s \lambda_s \cos s\gamma$ to any polygonal shaft merely by assigning the appropriate value to n. The distortion of the form due to the difference between γ and $\theta(= \tan^{-1}(y/x))$ will be discussed later; but it may be mentioned here that this distortion tends to narrow the groove, to reduce the radius of curvature at its sides, to widen the spline and to round its edges. In some measure it is practicable to anticipate these effects by so choosing the basic Fourier series $\sum_s \lambda_s \sin s\gamma$ that the subsequent distortion results in the actual contour required; but sharp outstanding edges cannot readily be represented.

If the Fourier series $\sum_s \lambda_s \cos s\gamma$ represents a function having a finite number of discontinuities in the range 0 to π, the coefficients λ_s eventually converge as the sequence $1/s$. By each integration the eventual order of convergence improves, so that a function, which may be differentiated m times before discontinuities appear, eventually converges as $1/s^{m+1}$. In order, therefore, to achieve a satisfactory degree of eventual convergence, so that no great number of Fourier terms shall be required to approximate closely to a specified function, it is desirable first to represent the function by abrupt changes not in itself but in some moderately high order differential.

On the other hand it can be shown that if a function has discontinuities in its mth differential, the coefficient of the sth term in the Fourier series representing the function is of the order $\sin^m s\alpha/s^{m+1}$, where α is *least* distance between discontinuities (the whole period of the function being 2π). Thus when α is small, as it must be if the changes of height of the function itself are to be abrupt, the first terms in the Fourier series are small and the eventual order of convergence as $1/s^{m+1}$ is scarcely established until s reaches values comparable with π/α.

The latter effect more than offsets the former, so that a greater number of terms in the Fourier series is needed when the transitions of the function are smoothed than when they are made abrupt. At the same time the actual convergence to the smoothed function is decidedly better than that to the unsmoothed. It is essential to smooth at least to the extent of relegating actual discontinuities to the second differential, because otherwise the *curvature* of the contour varies erratically, and curvature has immediate effect upon stress. Discontinuities of curvature do not in themselves affect the stress distribution (*see* Sections IV.6 and II.8), so that this degree of smoothing suffices; but a considerable improvement in general smoothness may be achieved by relegating discontinuities to the fourth differential. In practice, except for special purposes, the choice extends no further; because the number of Fourier terms required increases by about 50 per cent for each double differentiation. Whereas, using the lesser degree of smoothing six or seven terms may often suffice, with the greater smoothing nine or ten may be required, and the volume of computation increases roughly in proportion to the square of the number of Fourier terms.

Two examples of splined forms represented by these means are illustrated in Figs. 23 and 25. The first is based on a function discontinuous in its second differential and is represented by five terms of the Fourier series; although these five are in effect nine because by symmetry four intermediate terms are identically zero, the actual basis may be regarded as seven, because the last one of the five is almost negligible. The second example is based on a function discontinuous in its fourth differential and is represented by ten terms of the Fourier series. The basic function for the first example has its second differential zero from $\beta = 0$ to 10 deg and from 20 to 30 deg, unity from 10 to 15 deg and negative unity from 15 to 20 deg. When this symmetrical form is

' wrapped ' round the circular shaft the width of the spline is increased at the expense of the width of the groove and the outstanding corner is rounded to a large radius, whilst the inner corner is sharpened. These effects are accentuated the greater the height of the spline in relation to the diameter of the shaft, and a limit is reached when the inner corner becomes a cusp. The basic function for the second example has its fourth differential zero from $\beta = 0$ to 5 deg and from 15 to 30 deg, 24 from $\beta = 5$ to 6 deg, -40 from 6 to 7 deg, 5 from 7 to 11 deg and -1 from 11 to 15 deg. This asymmetrical function limits both the rounding of the outstanding corner and the sharpening of the inner corner and results in near equality between the widths of spline and groove. The particular height of spline chosen is that which renders the inner end of the side of the spline radial.

These two examples illustrate the scope and indicate some of the limitations of the means proposed for the representation of specified forms. A much more elaborate exposition would be needed in order fully to demonstrate the possibilities of the method. The relative widths of spline and groove may be fixed fairly easily by fixing the final limit of all the discontinuities ($\beta = 20$ deg in the first example and $\beta = 15$ deg in the second); but the relative radii of curvature of the two corners are much less easy to fix, because they are influenced much more by the height of the spline. Although certain principles may be established, their statement would be wearisome save to those who might actually seek to apply them, and these few may be left to find their own enjoyment in discovering these (and probably other) principles for themselves.

The two examples suffice as they stand to point certain general conclusions in respect of stress distribution.

IV.10. *Stresses in Splined Shafts.*—Once the form of the shaft in terms of the λ's has been decided, evaluation of the stress distribution proceeds by direct application of formula (44). The complete stress distribution over the boundary of the section illustrated in Fig. 23 is shown in Fig. 24, but in Fig. 25 only the peak of stress round $\beta = 12$ deg is illustrated, together with the values of the stress at $\beta = 0$ deg and $\beta = 30$ deg. The latter values have been corrected for the effect of the slight undulations of the nearly circular contour in this region in the manner described in Section IV.7; but here of course the effective ' radius of local curvature ' is the reciprocal of the difference between the curvatures of the actual contour and the true circle. In the region $\beta = 0$ deg to 2 deg of Fig. 25, the radius of the contour varies by about $\pm 0{\cdot}2$ per cent, and the resulting variation of stress is about ± 7 per cent; in the region $\beta = 28$ to 30 deg, the radius varies by about $\pm 0{\cdot}025$ per cent and the resulting variation of stress is $\pm 1{\cdot}2$ per cent. The corrected stress values vary by less than $0{\cdot}05$ per cent in the range $\beta = 28$ to 30 deg and the total variation of $2{\cdot}1$ per cent over the range $\beta = 0$ to 2 deg represents in part a real variation (*cf.* Fig. 24), so that the actual accuracy is probably about $0{\cdot}04$ per cent.

In Fig. 24, the inset diagram shows the actual stress values adjacent to the inner corner of the spline compared with the formula $1 + \frac{1}{2}(a/\varrho)^{1/2}$ where a is the height of the spline and ϱ is the radius of local curvature. For this comparison unit stress is taken to be that at the surface of a circular shaft of the same median radius subjected to the same twist ; the basis for this comparison is discussed further below. For the second example the maximum stress is $4{\cdot}45$, whereas on the same basis the expression $1 + \frac{1}{2}(a/\varrho)^{1/2} = 4{\cdot}90$. In a third example (not illustrated) the maximum stress was $2{\cdot}79$ and the value of $1 + \frac{1}{2}(a/\varrho)^{1/2}$ was $3{\cdot}27$. These values of $1 + \frac{1}{2}(a/\varrho)^{1/2}$ are, however, based on the local values of $1/\varrho$ actually at the point of maximum stress. If instead we substitute the average value of $1/\varrho$ over the whole corner, that is from $\beta = 12$ deg to $\beta = 13$ deg in Fig. 25, the corresponding values of $1 + \frac{1}{2}(a/\varrho)^{1/2}$ become $4{\cdot}37$ for the case shown in Fig. 25 and $2{\cdot}87$ for the third case not illustrated. For the case illustrated in Figs. 23 and 24 the similar comparison gives $1 + \frac{1}{2}(a/\varrho)^{1/2} = 2{\cdot}36$ (actual maximum value $2{\cdot}43$); the correction to average curvature makes less difference in this case because the curvature round the corner is fairly uniform.

These comparisons indicate that the expression $1 + \frac{1}{2}(a/\varrho)^{1/2}$ affords a very fair approximation to the value of the maximum stress; but the comparison would be both more soundly based and more useful in practice, if unit stress could readily be defined otherwise, for instance as the stress

at the surface of a circular shaft of the same area of section under the same torque. In order to evaluate this stress, however, it would be necessary to compute the value of the torque from formula (45), and in the second example (Fig. 25) this expression comprises over 100 quartic terms. Although a great many of these terms are negligibly small, the computation of the torque is still very tedious, and, since the value of the unit stress as thus defined is unlikely to differ appreciably from that previously adopted, the extra computation has not been thought worth while. On the evidence here presented, it suffices to claim that the inner corner of a spline, representing as it does a sort of half groove, causes a stress concentration of about $1 + \frac{1}{2}(a/\varrho)^{1/2}$, where a is the height of the spline and ϱ is the average radius of curvature at its root, leaving unit stress to be defined in any convenient manner. More precise statement would really be pointless, because if greater precision were needed it would be unwise to rely on any approximate formula.

IV.11. *Hollow Shafts.*—The method of dealing with hollow shafts has already been explained in Section IV.4 and it was remarked there that the only real difficulty is to specify a suitable co-ordinate system. Following the procedure outlined in Section IV.9 the outer contour might be represented as closely as desired in the form $x + iy = \sum_n \lambda_n e^{-n(\alpha+i\beta)}$; if then the inner boundary were circular and not too close to the outer one, it might suffice to use this form unaltered, because the transform $x + iy = \sum_n \lambda_n e^{-n(\alpha+i\beta)}$ rapidly approaches a true circle as α increases. For instance in the case of the shaft illustrated in Fig. 25, the contour $\alpha = \log_e 2$ differs from a true circle by about $\pm$ 1 per cent, so that a hollow shaft with this external boundary and a circular bore not more than half the median diameter of the outside could reasonably be treated in this way.

The torsion function ψ must still include exponentials with positive indices, because without these terms the condition $\bar{a}\bar{z} = 0$ cannot be satisfied at both boundaries. Yet this amendment to the analysis makes comparatively little difference to the stress distribution, because as the contour $\alpha =$ constant approaches a circle, so also does $\bar{a}\bar{z}$ approximate more and more closely to zero. In effect, therefore, for hollow shafts in which the bore is circular and fairly small, say less than half the median diameter of the external contour, it is permissible to apply the results for a solid shaft of the same external form; but of course the torque-twist relationship is affected and must be recomputed.

For hollow thin walled shafts the relationship between the transforms for the inner and outer boundaries is too close for the simple mode of treatment outlined and it becomes essential to re-specify the transform in the complete form $x + iy = \sum_n \lambda_n e^{n(\alpha+i\beta)} + \lambda_{-n} e^{-n(\alpha+i\beta)}$. For instance, in the case where the inner boundary is circular the elementary form

$$x + iy = e^{-(\alpha+i\beta)} + \lambda_{-n} e^{-n(\alpha+i\beta)} + \lambda_{n-2} e^{(n-2)(\alpha+i\beta)}$$

leads to

$$\begin{aligned} r^2 = x^2 + y^2 &= e^{-2\alpha} + \lambda_{-n}{}^2 e^{-2n\alpha} + \lambda_{n-2}{}^2 e^{2(n-2)} \\ &+ (2\lambda_{-n} e^{-(n+1)\alpha} + 2\lambda_{n-2} e^{(n-3)\alpha}) \cos (n-1)\beta \\ &+ 2\lambda_{-n}\lambda_{n-2} e^{-2\alpha} \cos 2(n-1)\beta. \end{aligned}$$

Then we may choose the values of λ_{-n} and λ_{n-2} so that the coefficient of $\cos (n-1)\beta$ in the formula for r^2 disappears over the inner boundary (at $\alpha = \alpha_1$), and, since λ_{-n} and λ_{n-2} are necessarily of order $1/n$ or less, the variation of r over this boundary is thus reduced to order $1/n^2$ or less. Application of this procedure is illustrated in Fig. 26, which relates to the shaft defined by $x + iy = e^{-(\alpha+i\beta)} + 0{\cdot}1e^{-7(\alpha+i\beta)} - 0{\cdot}025e^{5(\alpha+i\beta)}$ with outer boundary at $\alpha = 0$ and inner boundary at $\alpha = (1/6)\log_e 2$. The two boundaries are then

$$r_0^2 = 1{\cdot}010625 + 0{\cdot}15 \cos 6\beta - 0{\cdot}005 \cos 12\beta$$

and $r_1^2 = 0{\cdot}7937(1{\cdot}005 - 0{\cdot}005 \cos 12\beta)$

and r_1 varies by $\pm$ 1 per cent only.

The form of this shaft section is shown in Fig. 26 together with the distribution of shear stress. It is interesting to note that the product of the stress at the inner boundary with the local wall thickness varies only about $\pm$ 20 per cent over the whole range of β; but the effect of true stress concentration as opposed to load concentration is of course much greater over the outer boundary.

IV.12. *Conclusions.*—The principal purpose of this paper has been to demonstrate that the solution of the torsion problem for any arbitrary section depends solely upon the specification of an appropriate system of co-ordinates. Once the co-ordinate system has been devised the remainder of the work is straightforward computation. Methods of constructing peculiar co-ordinate systems have been described; but no attempt has been made to devise a comprehensive system (on the lines of the Schwarz-Christoffel transformation), because in stress analysis a comprehensive system would be virtually useless on account of its singularities. In place of a comprehensive method for exact representation of specified contours, a procedure for correction of stress distributions in fairly rough approximate forms has been devised. This process of correction can be carried through very quickly and the corrected results are likely to be highly accurate.

From the one or two examples worked out in illustration of the general method, it appears that a fillet of radius ϱ at the foot of a change of section of depth a will cause a stress concentration under shear of about $1 + \frac{1}{2}(a/\varrho)^{1/2}$. Several more examples need, of course, to be worked in order to test the accuracy of this formula more thoroughly; but from the three cases computed its accuracy seems likely to be better than $\pm$ 5 per cent.

REFERENCES

No.	*Author*	*Title, etc.*
1	C. E. Inglis	Stresses in a Plate due to Presence of Cracks and Sharp Corners. *Trans. Instn. Nav. Archit.*, Vol. 55, Part I, p. 219. 1913.
2	R. C. A. Thurston and J. E. Field	The Fatigue Strength under Combined Stresses of Test Pieces with Diametral Holes. Eng. Div. 218/46. (As yet unpublished.)
3	H. J. Gough and H. V. Pollard	The Strength of Metals under Combined Alternating Stresses. *Proc. Instn. Mech. Engrs.*, Vol. 131, p. 3. 1935. A.R.C. 4270.
4	A. A. Griffith	The Phenomena of Rupture and Flow in Solids. *Phil. Trans.*, A, Vol. 221, p. 163. 1921.
5	A. C. Stevenson	Complex Potentials in Two-Dimensional Elasticity. *Proc. Roy. Soc.*, A, Vol. 184, pp. 129 and 218. 1945.
6	N. I. Mushelisveli	*Math. Ann.*, Vol. 107, pp. 282–312. 1932.
7	I. S. Sokolnikoff and R. D. Specht	*Mathematical Theory of Elasticity.* McGraw Hill Book Co. Inc., New York.
8	A. E. H. Love	*Mathematical Theory of Elasticity.* 3rd Edition. 1920. Cambridge University Press.
9	A. A. Griffith and G. I. Taylor	The Use of Soap Films in Solving Torsion Problems. *Proc. Instn. Mech. Engrs.*, Vol. 2, p. 755. 1917.
	A. A. Griffith	A.R.C. Report No. T 1275, December, 1918. (Unpublished.)
10	S. Timoskhenko	*Theory of Elasticity.* 1st Edition. 1934. McGraw Hill Book Co. Inc.
11	Inst. Mech. Engrs.	Conference on Surface Finish. *Proc.*, Vol. 153, p. 331.
12	J. Prescott	*Applied Elasticity.* 1st Edition. 1924. Longmans, Green & Co.
13	R. V. Southwell	*Theory of Elasticity.* 1st Edition. 1936. Oxford, Clarendon Press.
14	H. Neuber	*Kerbspannungslehre.* 1937. Springer, Berlin.
15	Battelle Memorial Institute	*Prevention of the Failure of Metals under Repeated Stress.* (Handbook prepared for the Bureau of Aeronautics, Navy Department, U.S.A. 1941).
16	Melbourne University Press	*The Failure of Metals by Fatigue.* Proceedings of a Symposium held in the University of Melbourne. 1947.
17	R. Cazaud	*La Fatigue des Métaux.* 1948. Dunod, Paris.

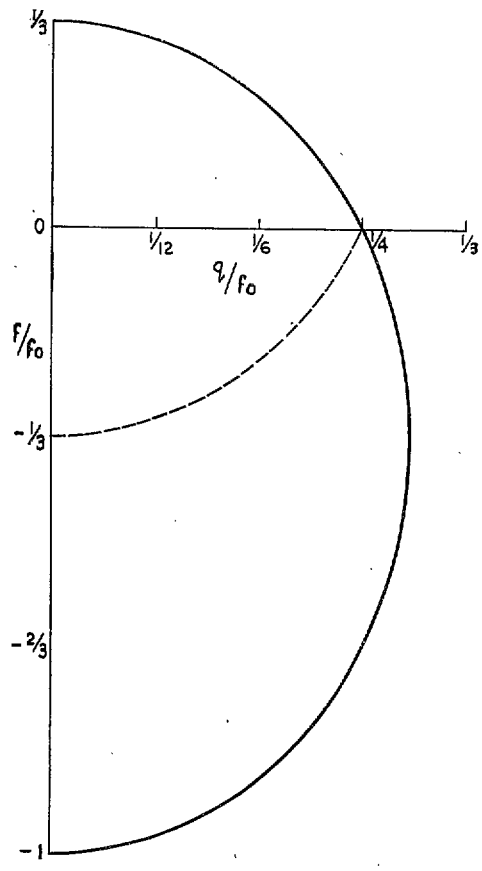

FIG. 1. Limiting condition for failure of a test piece containing a circular hole.

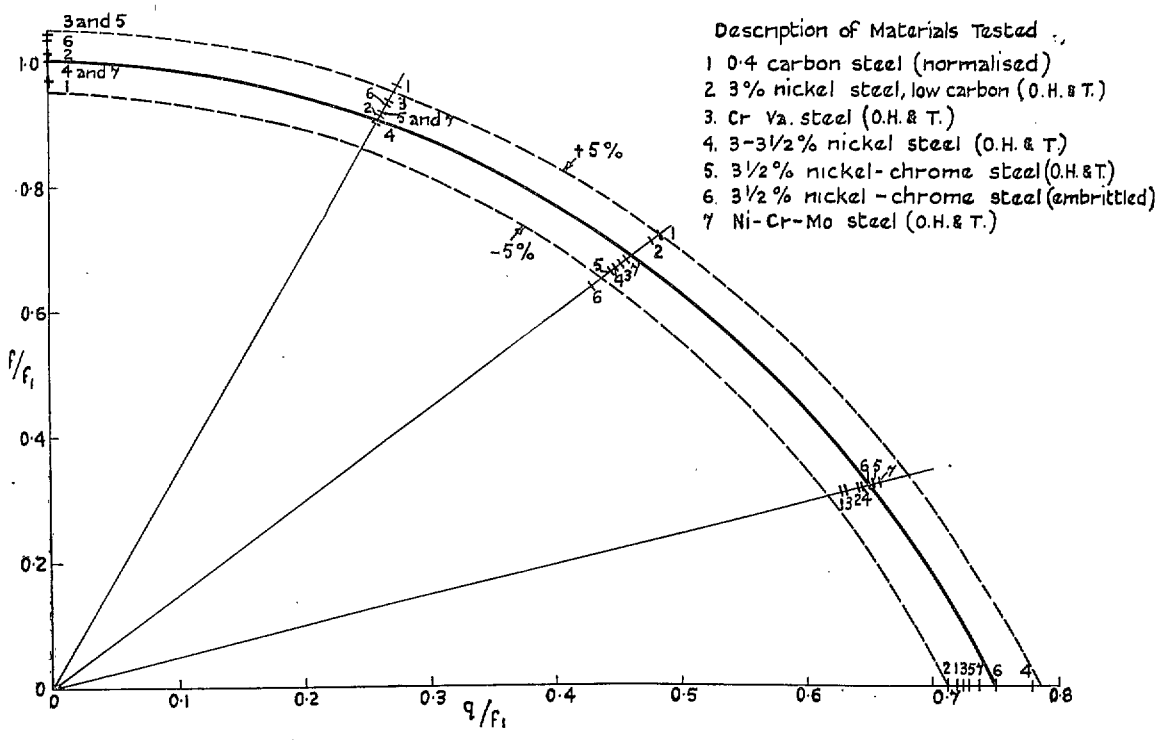

FIG. 2. Comparison of fatigue test data on test pieces containing circular holes with theoretical curve.

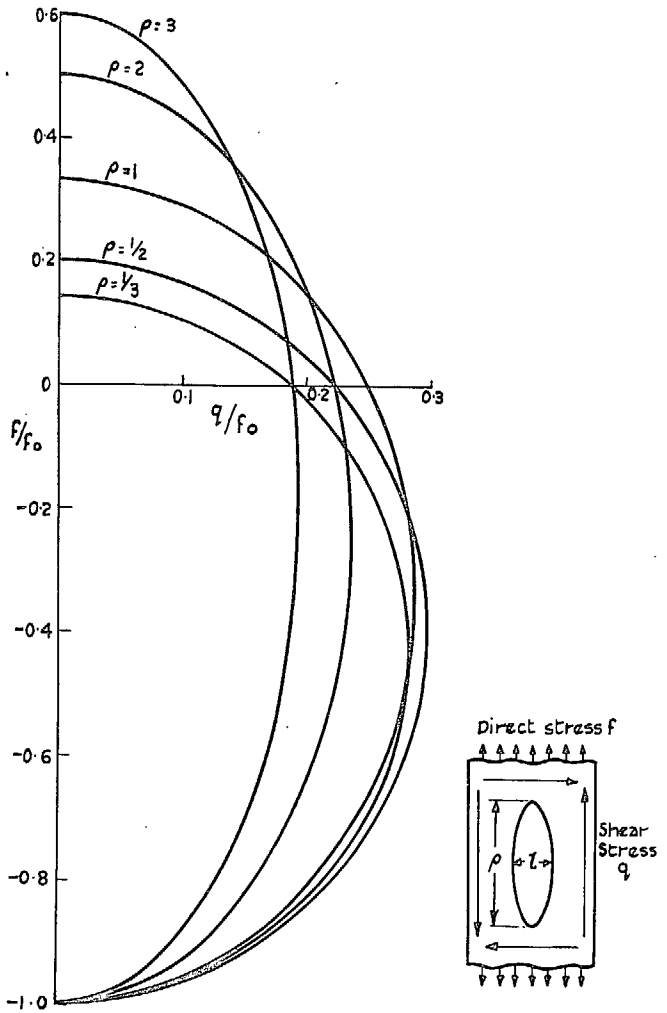

FIG. 3. Limiting conditions for failure of test pieces containing elliptical holes, stressed parallel to axes of hole.

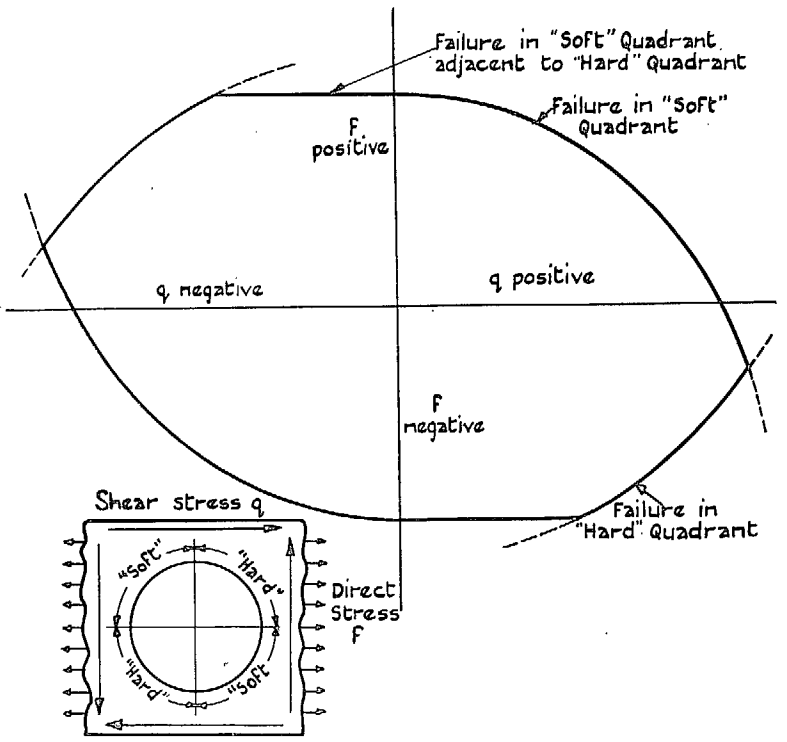

FIG. 4. Effect of differential hardening round a circular hole.

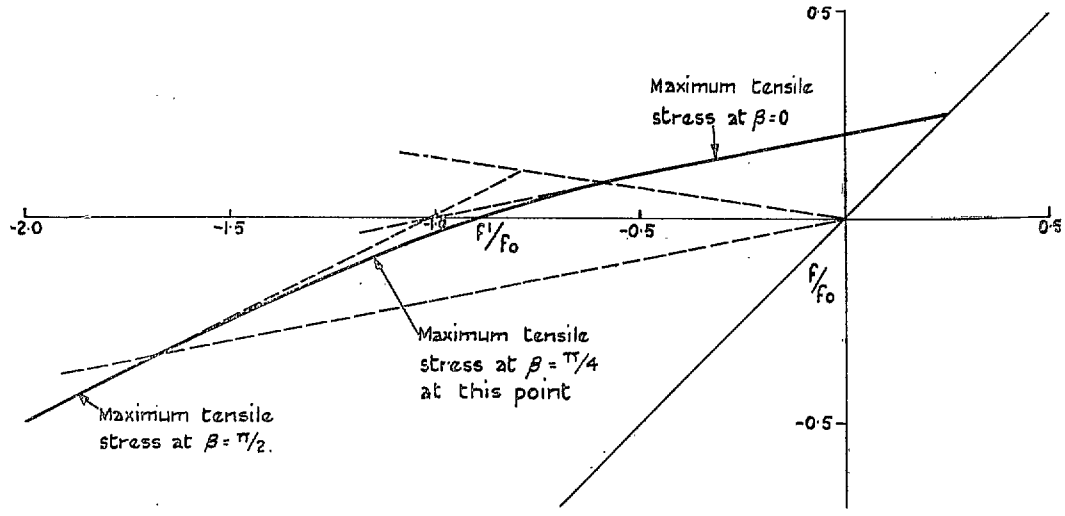

FIG. 5. Limiting condition for failure of test pieces containing elliptical holes oriented at random (ratio of axes of elliptical hole 2 : 1).

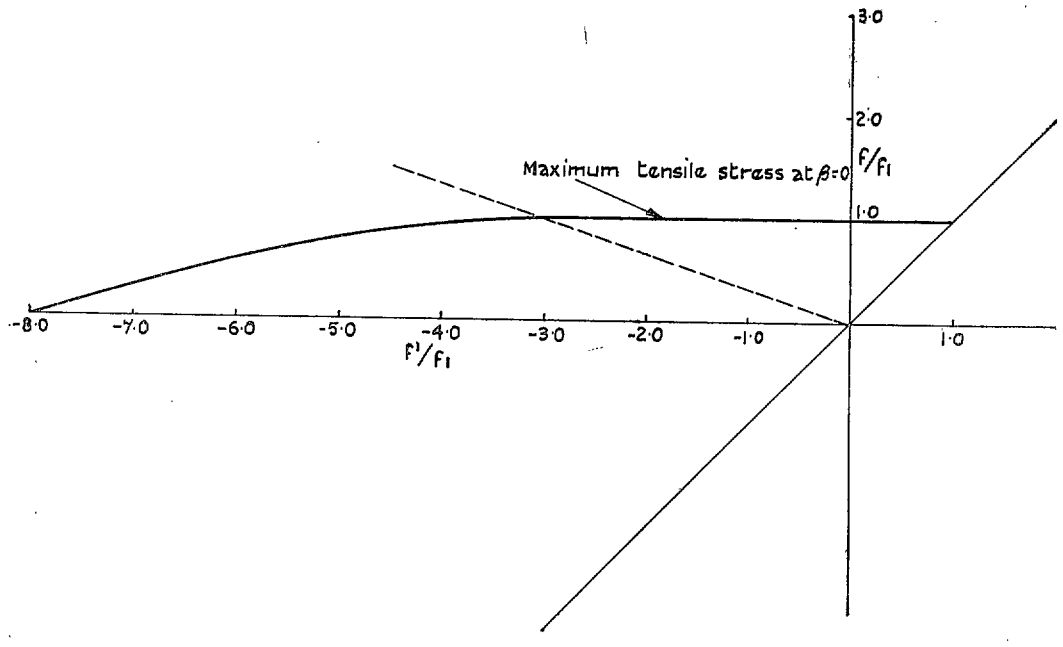

FIG. 6. Limiting condition for failure of test pieces containing elliptical holes oriented at random (infinitely narrow elliptical hole).

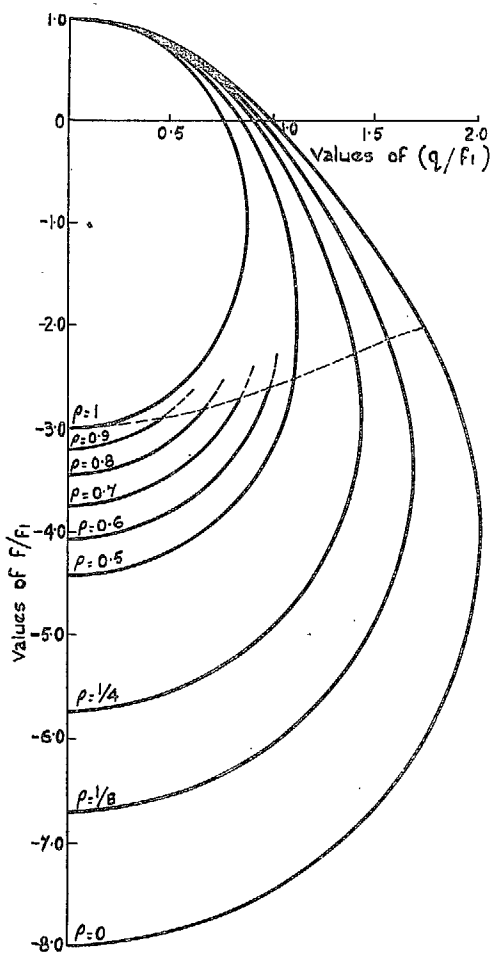

FIG. 7. Limiting conditions for failure under combined direct stress and shear of test pieces containing elliptical holes oriented at random.

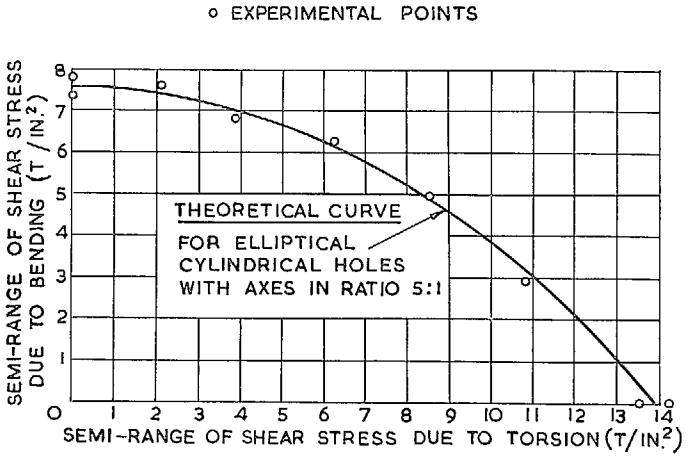

FIG. 8. Results of fatigue tests under combined alternating bending and torsion on ' silal ' cast iron.

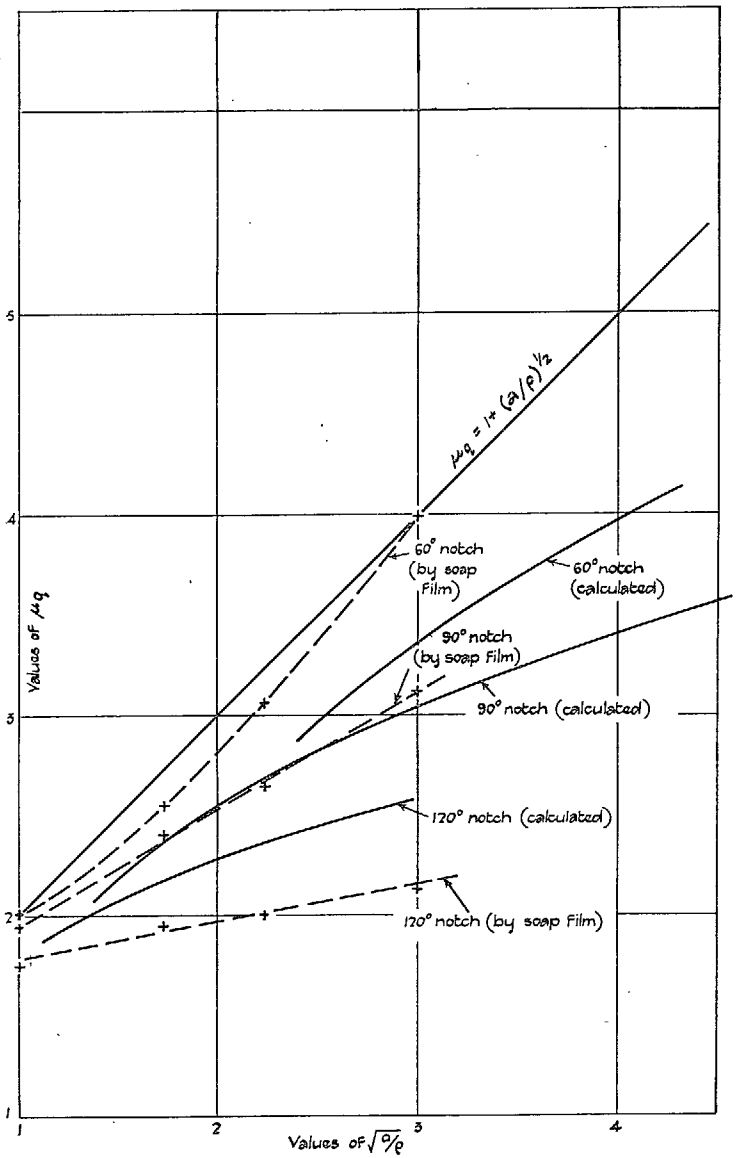

FIG. 9. Shear stress concentration factors for V-notches. The crosses joined by dotted lines represent results obtained by A. A. Griffith using the soap-film method[10].

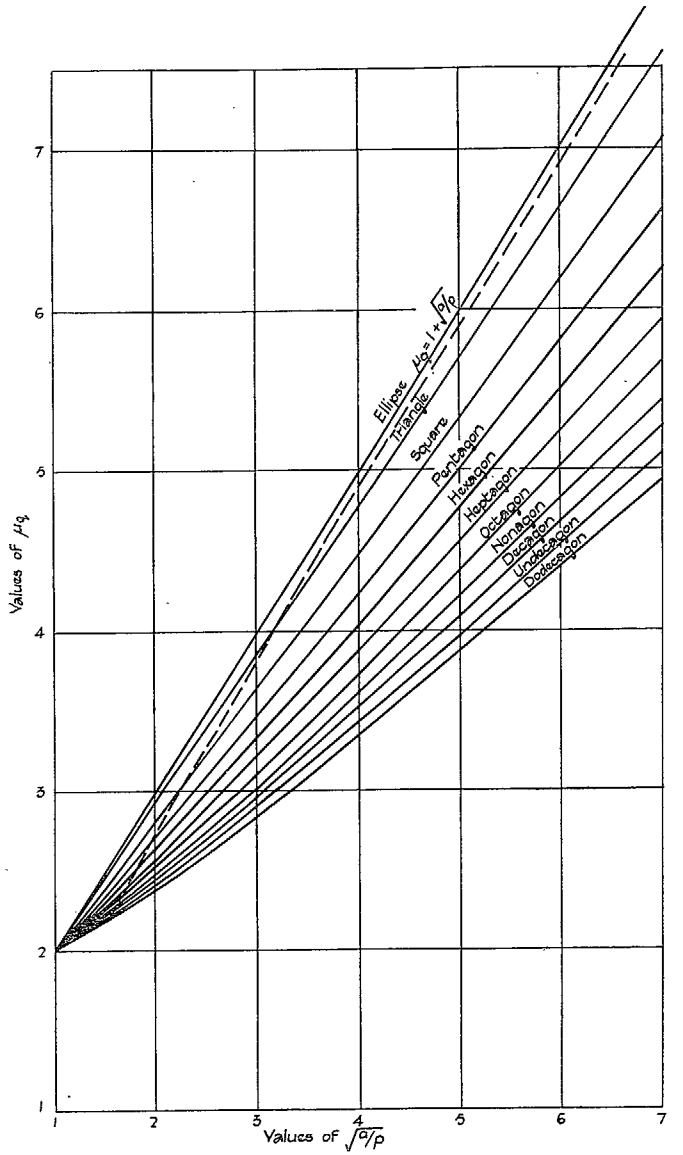

FIG. 10. Shear stress concentration factors for simple polygonal holes.

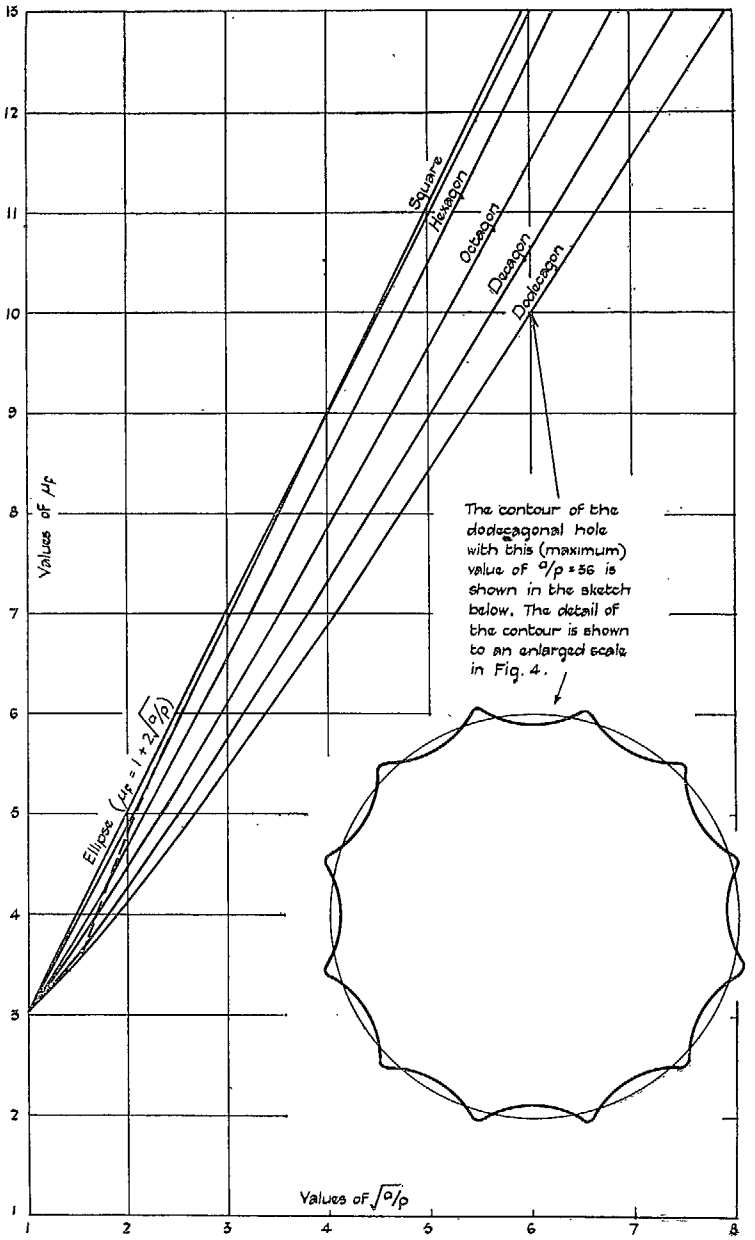

FIG. 11. Direct stress concentration factors for simple polygonal holes.

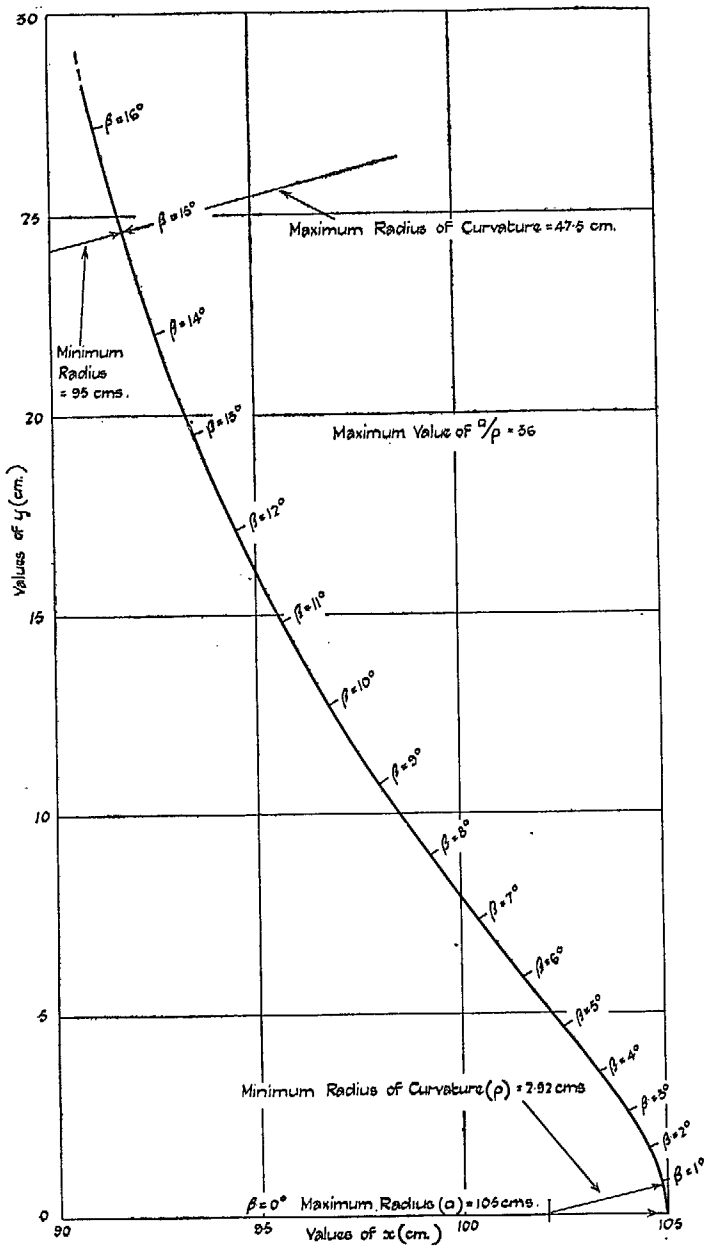

FIG. 12. Contour of typical simple dodecagonal hole.

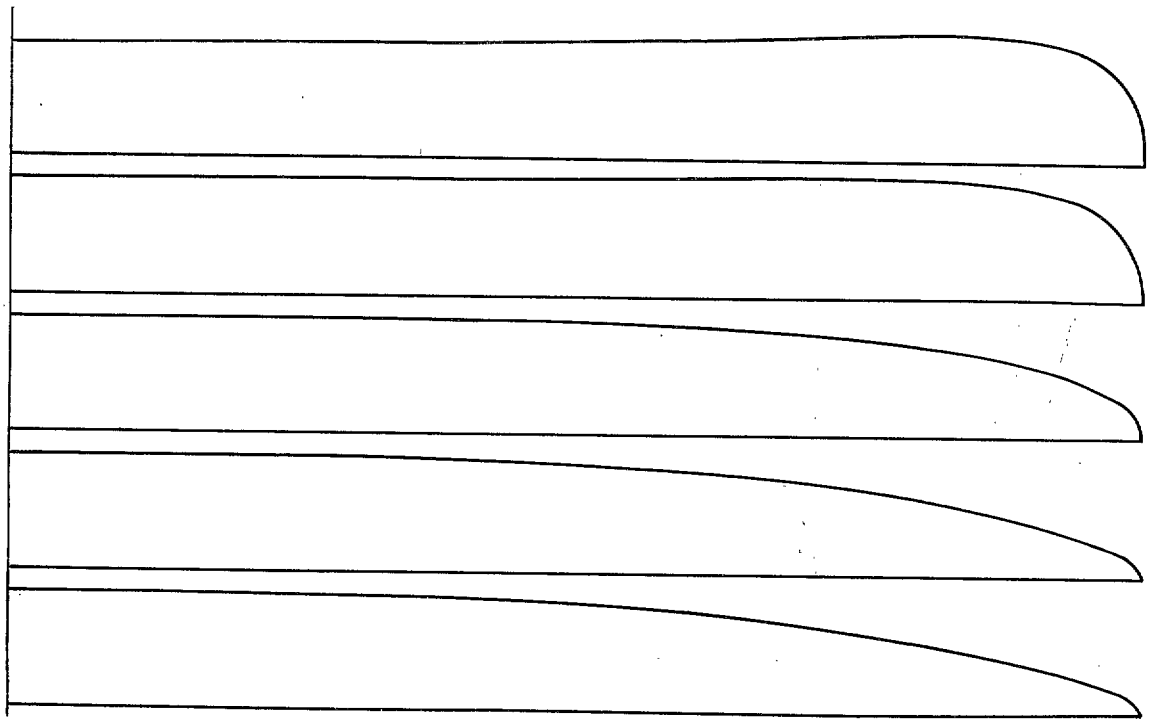

FIG. 13. Forms of deep narrow groove.

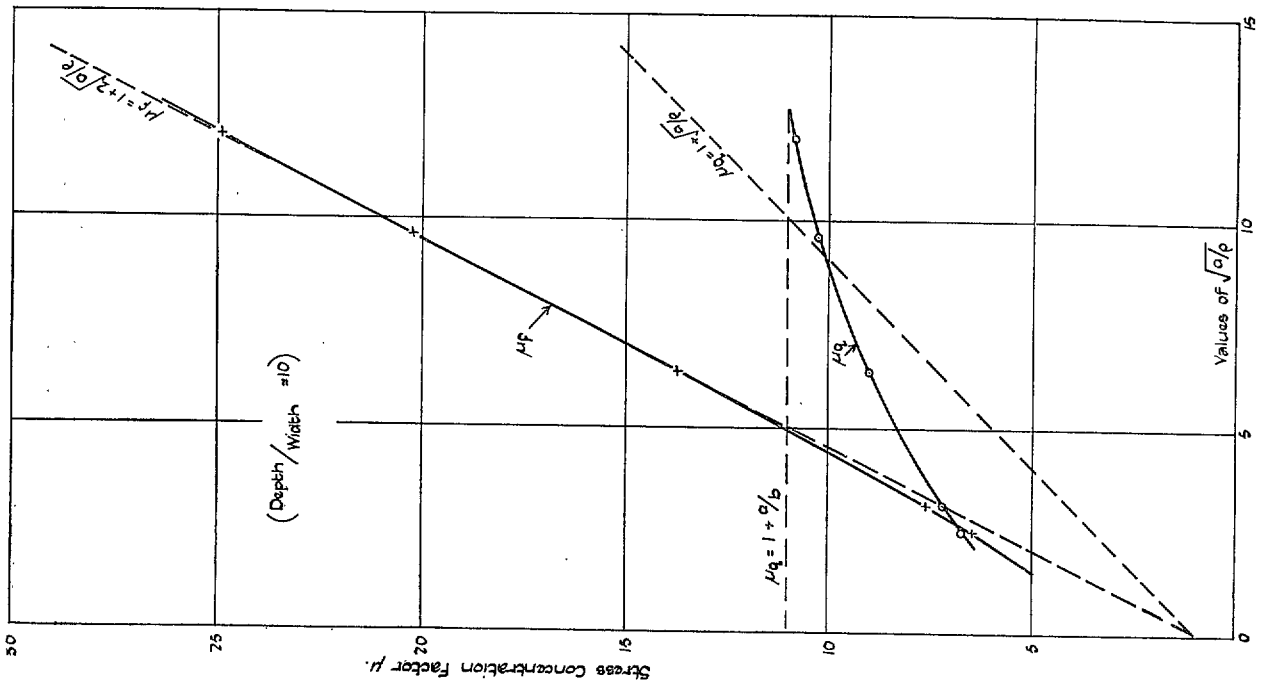

FIG. 14. Stress concentration factors for deep narrow grooves.

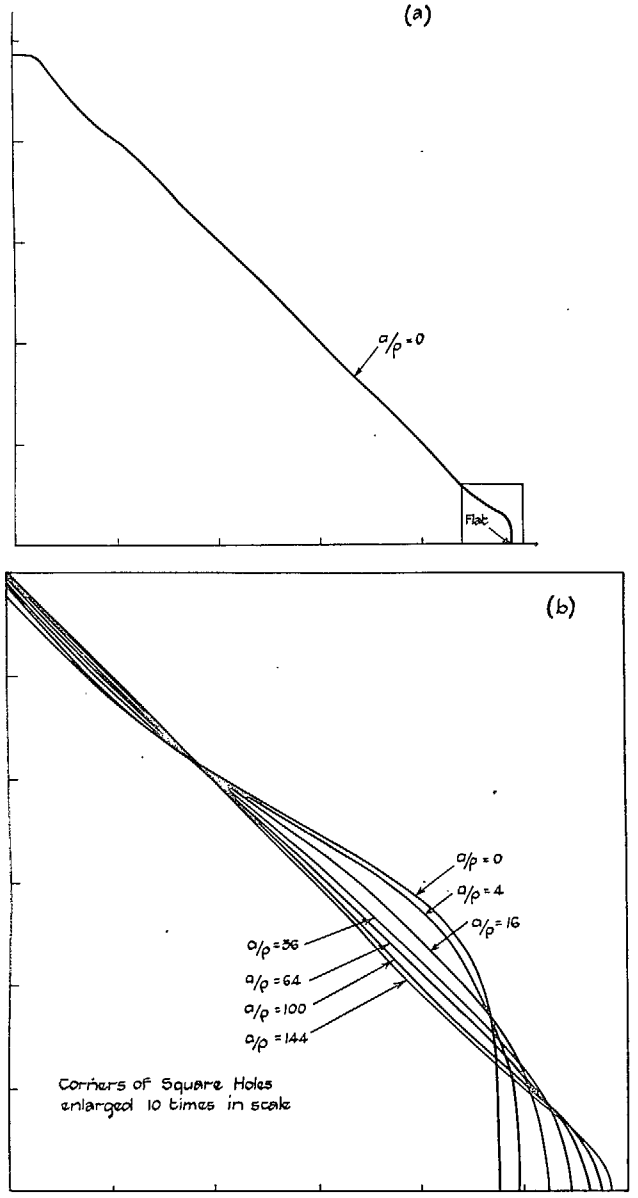

FIG. 15. Approximate representations of square holes with rounded corners.

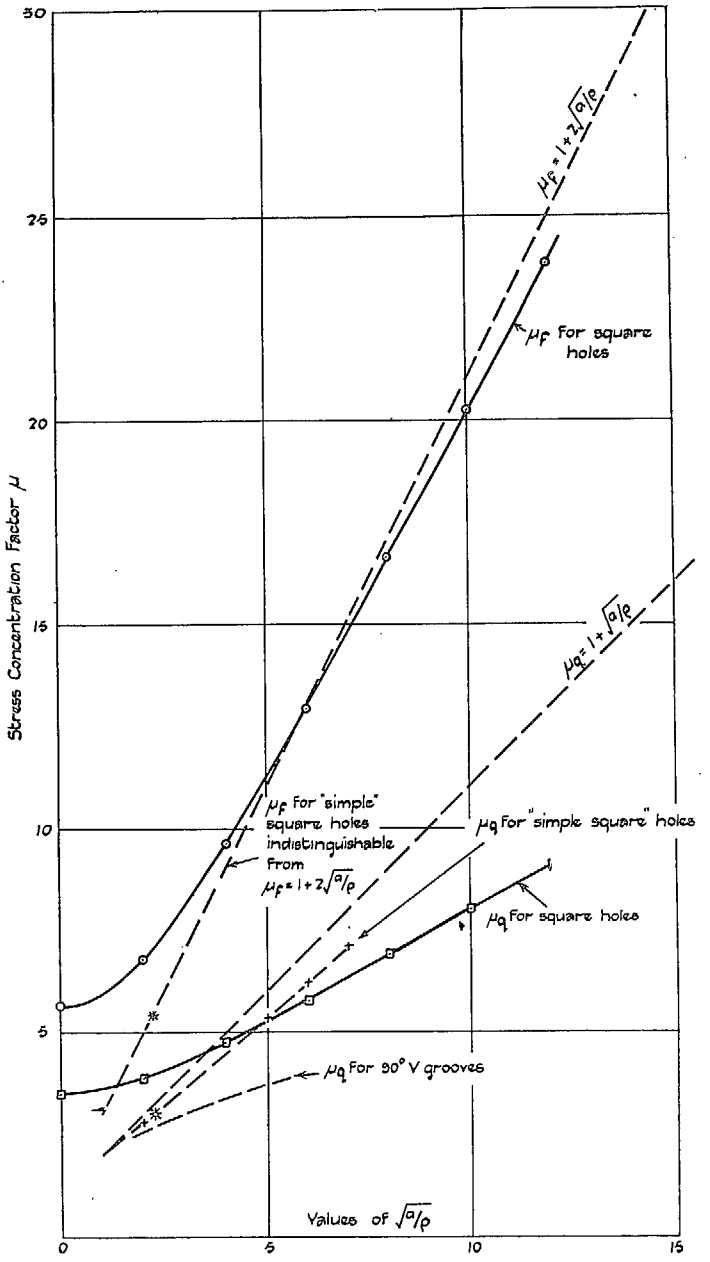

FIG. 16. Stress concentration factors for square holes with rounded corners.

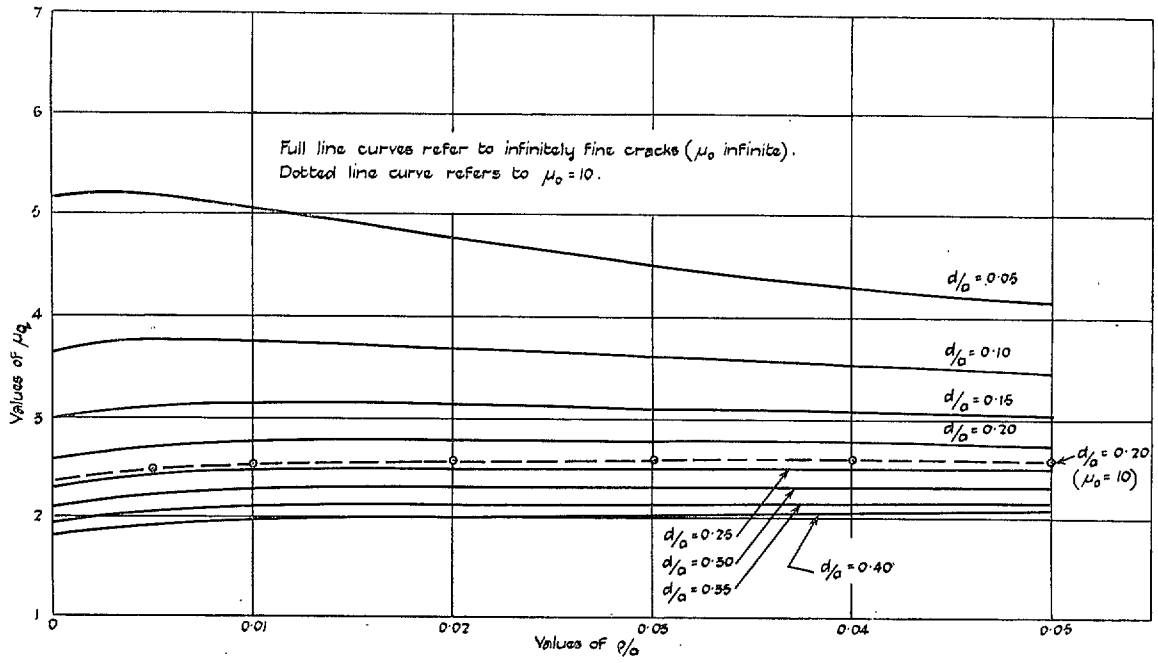

FIG. 17. Apparent values of stress concentration factors in shear as affected by depth of hair cracks.

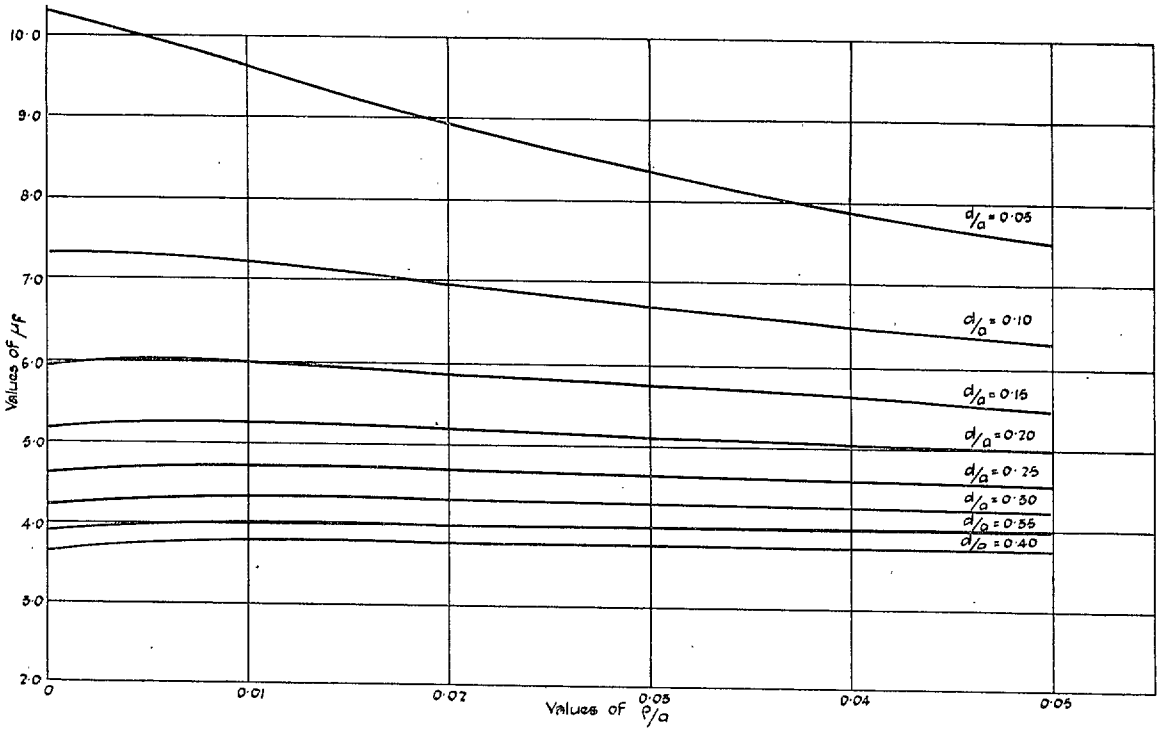

FIG. 18. Apparent values of stress concentration factors in direct stress as affected by depth of hair cracks ($\mu_0 \to \infty$).

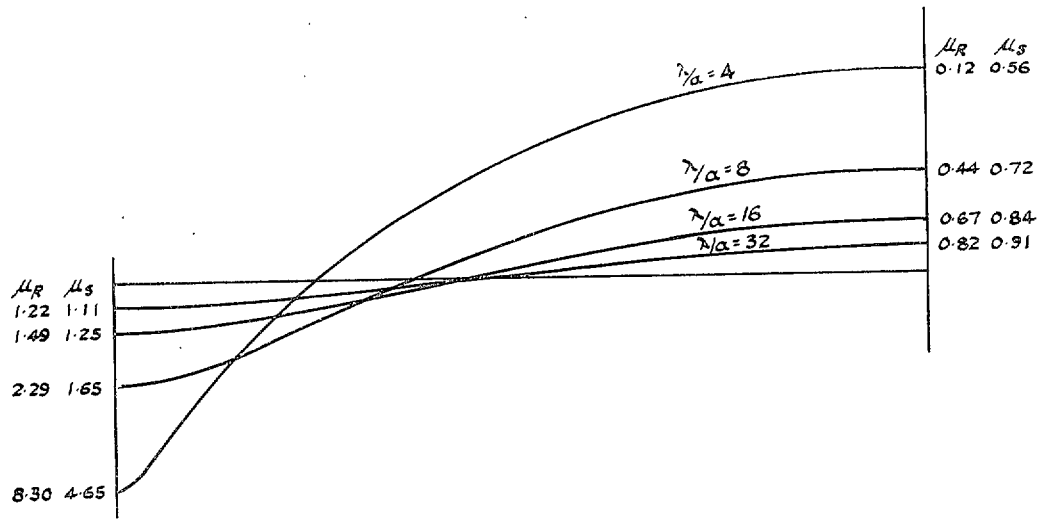

FIG. 19. Forms of continuous undulations to which the basis formulae for stress concentrations are strictly applicable.

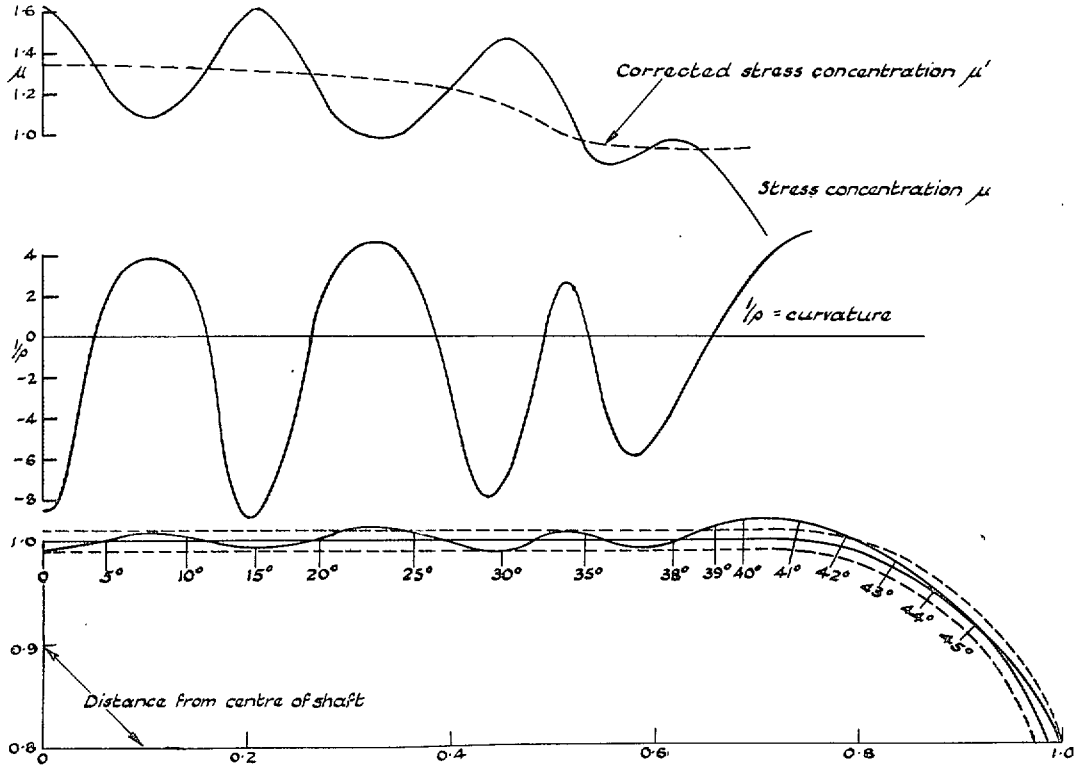

FIG. 20. Stress distribution round square shaft with rounded corners under torsion.

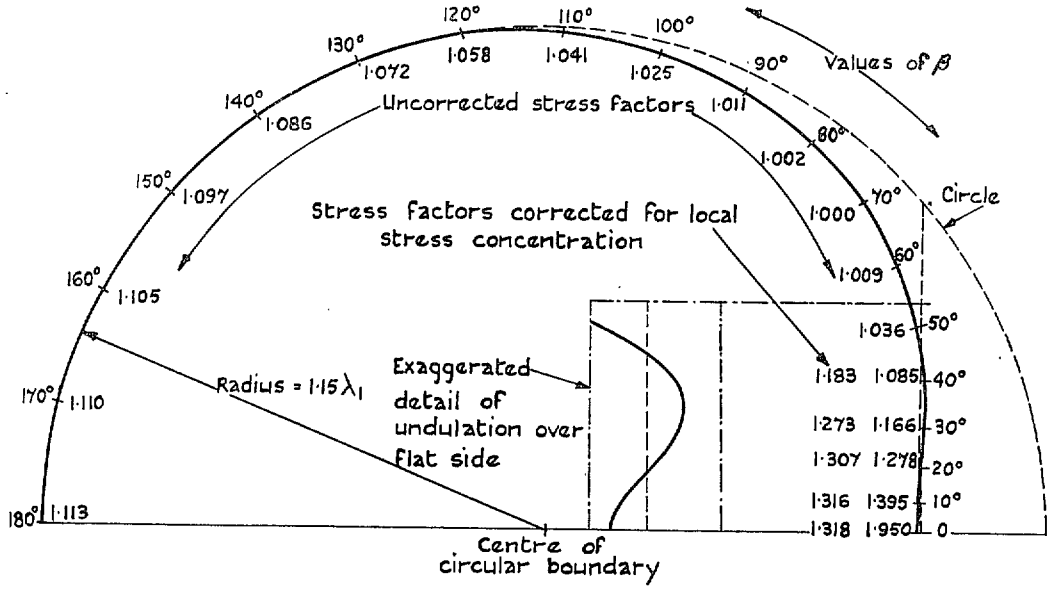

FIG. 21. Distribution of shear stress in a round bar with a flat.

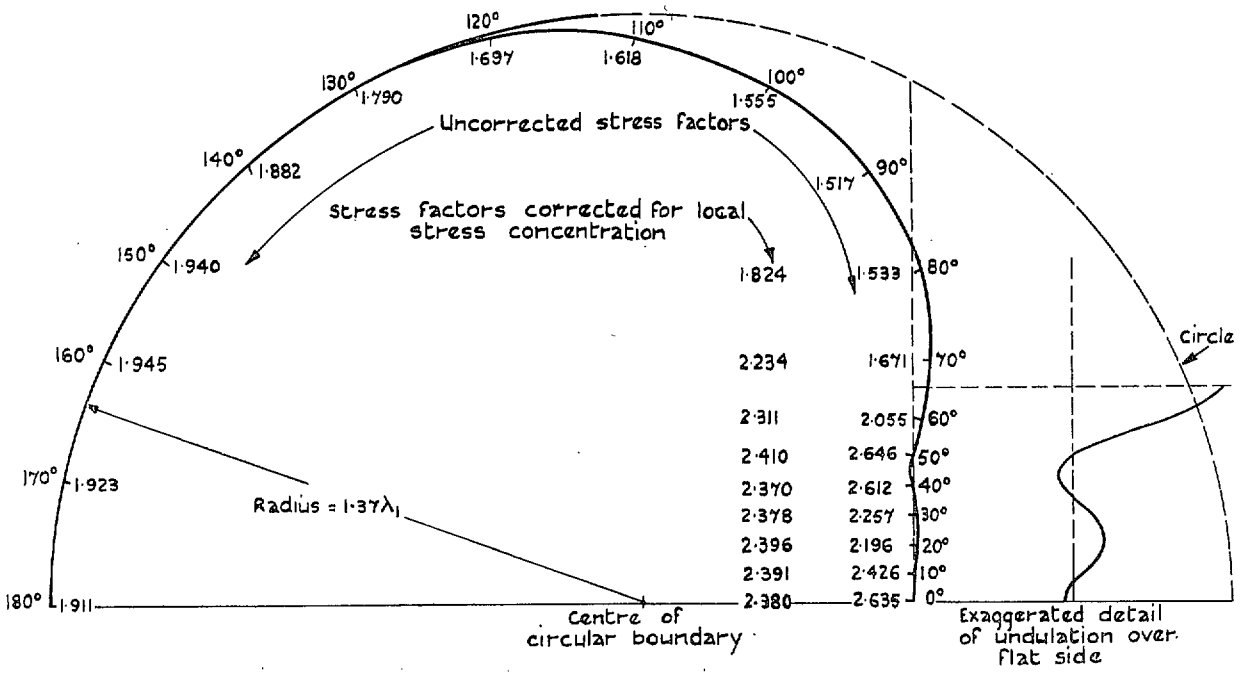

FIG. 22. Distribution of shear stress in a round bar with a flat.

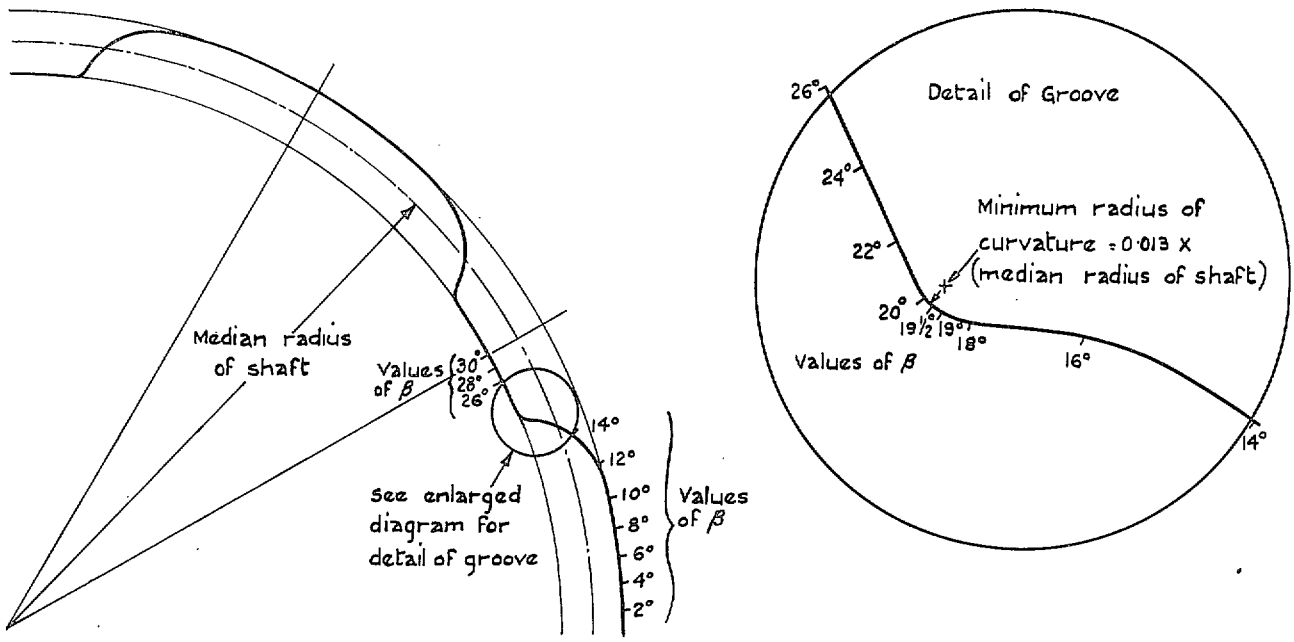

FIG. 23. Form of six-splined shaft.

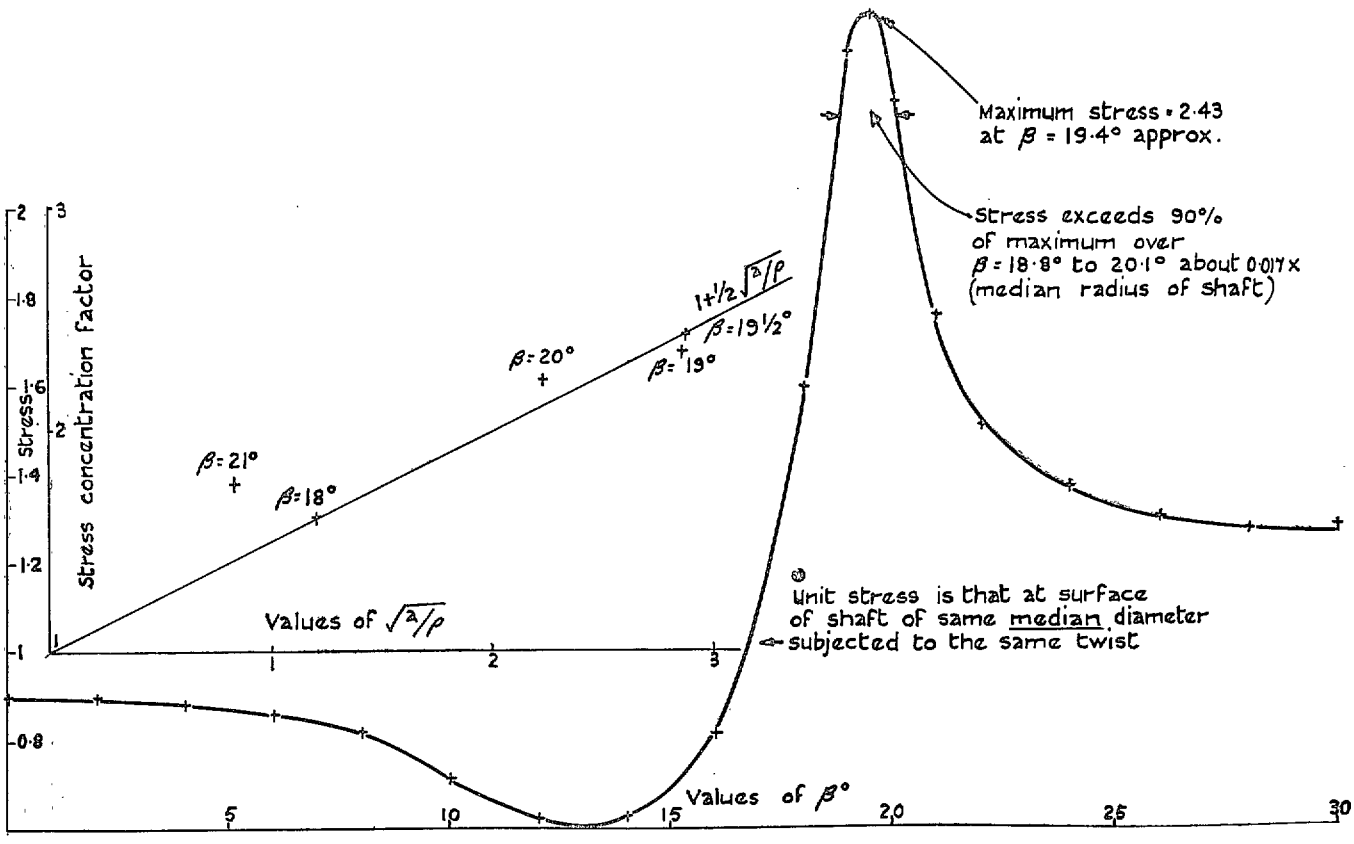

FIG. 24. Distribution of shear stress round the periphery of the six-splined shaft shown in Fig. 23.

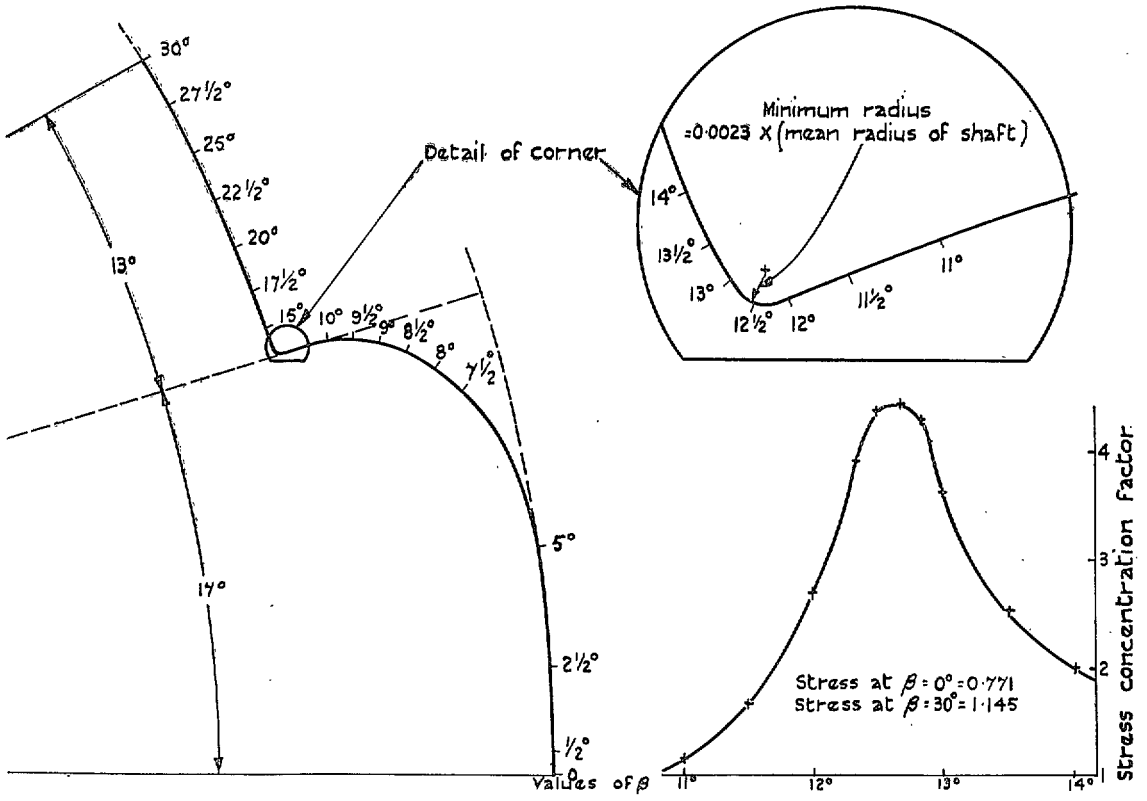

FIG. 25. Stress distribution round a sharp corner in a six-splined shaft.

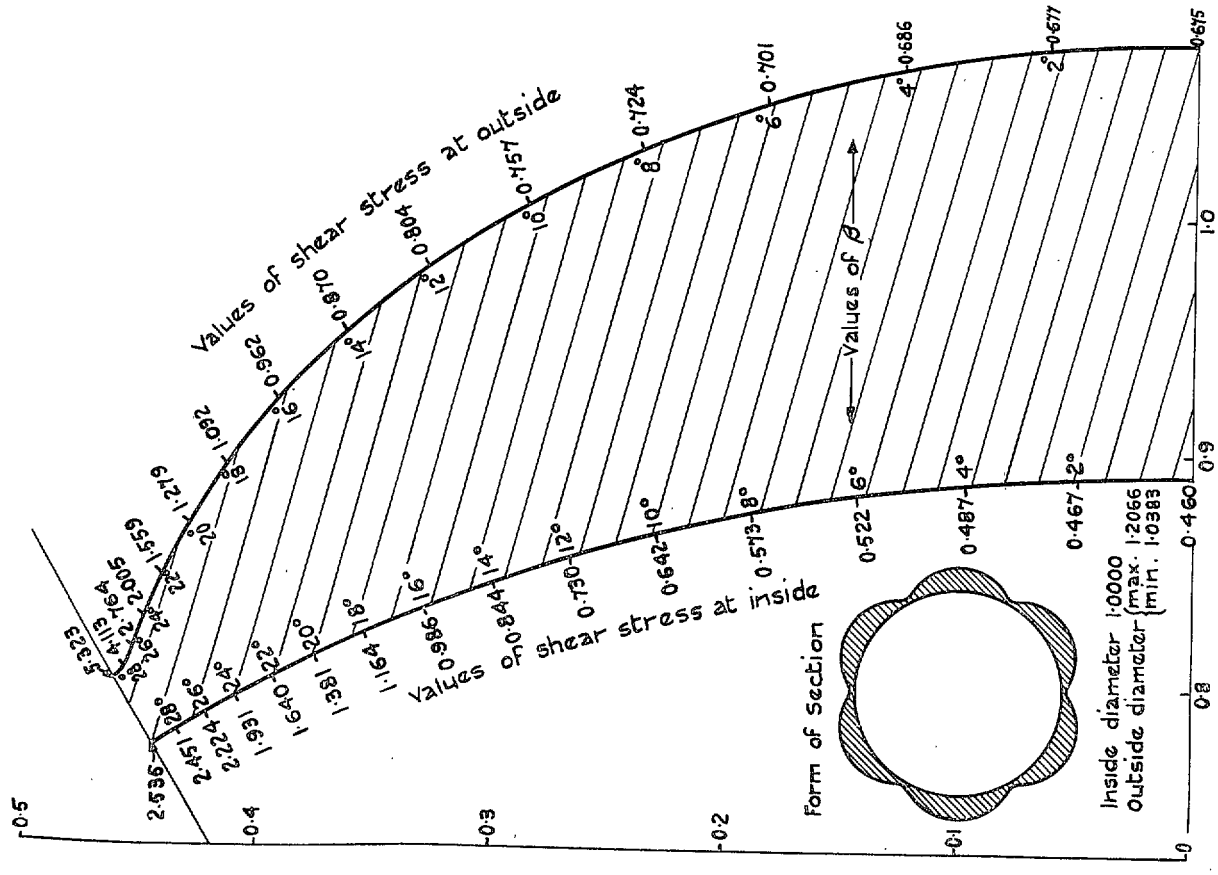

FIG. 26. Distribution of stress in a hollow lobed shaft.

(53510) Wt. 16/680. K.5 10/53 Hw.